

# Virtual Sectorization in Future Mobile Networks: System-Level Assessment and Optimization in a Realistic LTE Network

Master of Science Thesis

A. A. Mendoza Martínez

Technische Universiteit Delft



# VIRTUAL SECTORIZATION IN FUTURE MOBILE NETWORKS: SYSTEM-LEVEL ASSESSMENT AND OPTIMIZATION IN A REALISTIC LTE NETWORK

MASTER OF SCIENCE THESIS

by

**A. A. Mendoza Martínez**

in partial fulfillment of the requirements for the degree of

**Master of Science**

in Electrical Engineering  
Track Telecommunications and Sensing Systems

at the Delft University of Technology,

to be defended publicly on Tuesday October 27, 2015 at 14:00.

Thesis committee: Dr. Ir. G. Janssen, TU Delft  
Dr. . Litjens MSc, TU Delft  
K. Trichias MSc, TNO

*This thesis is confidential and cannot be made public until December 31, 2017.*

An electronic version of this thesis is available at <http://repository.tudelft.nl/>.



# PREFACE

The culmination of this thesis work, and consequently the graduation from the MSc. in Electrical Engineering program at TU Delft, marks the accomplishment of the first goal I set in my mind at the moment I decided to leave Mexico and come to Europe more than two years ago from the moment of this writing. So far it's been a long but pleasant journey full of new friends, experiences and gained knowledge. Now, a new stage of the so-called adventure begins and, as it all appears right now, it is going to be a good ride.

I would like to thank Kostas Trichias and Remco Litjens, my advisors from TNO and TU Delft respectively, for the support, knowledge shared, and confidence given to me in order to reach this point. It has been a great experience to work side by side with you and hopefully we can do it again in the near future.

Additionally, a big word of thanks to Zwi Altman and Abdoulaye Tall, from Orange Research, for their support and ideas during the time we worked together in the AAS use case for the SEMAFOUR project, allowing me to use their contributions for this graduation project.

I also want to thank all the people I had the chance to meet at TNO during my one year stay, with a special mention to Dick van Smirren, Onno Mantel, Adrian Pais and Yohan Toh. In general thanks to everyone from the PoNS and NT departments at TNO for being so welcoming and supportive.

Last but not least, I need to mention that I wouldn't be standing where I am right now if it wasn't because of my family, specially my parents. Both of them have worked hard their entire lives to make sure that everything needed for my development, personal and profesional, was provided and have guided me during my whole life while supporting every decision I've made along the way. I am very proud of you and I hope I have made you proud of me so far. Gracias!

*A. A. Mendoza Martínez  
Delft, October 2015*



# ABSTRACT

Since the first commercial deployment of the Long Term Evolution (LTE) mobile network technology in the last quarter of 2009, mobile data traffic has shown an exponential growth rate driven mainly by the ever growing offer of devices, services and applications available to the mobile subscribers, and by the expansion of cellular network coverage worldwide. It is expected that the total mobile data traffic in 2019-2020 will increase by a factor of ten times the total mobile data traffic reported by the end of 2014. In order to cope with this significant data traffic growth, there is a need to develop and deploy new solutions (e.g. network densification strategies) capable of optimizing network performance, perform dynamic troubleshooting and intelligent resource sharing, and hence, improve the end user experience. Furthermore, these solutions should be able to adapt dynamically to changes in the network in order to optimize performance and minimize operational costs that result from continuously employing people to manually adjust configurations and perform typical troubleshooting tasks.

Virtual Sectorization (ViS) is proposed as a solution to the aforementioned problematic. Through the use of an Active Antenna System (AAS), two vertically separated beams, serving two distinct cells, are created within the original coverage area of a macro-cell. One of these cells, referred to as virtual cell, can be flexibly placed anywhere within the original macro-cell because the large antenna array is capable of producing very narrow beams. The position of the virtual cell is done by choosing an electrical azimuth and downtilt such that the virtual cell's footprint is as much as possible steered towards an area of relatively heavy traffic (a traffic hotspot). The remaining part of the original cell after implementing ViS is denoted as macro-cell.

The involved trade-offs make the deployment of ViS non-trivial. The key advantage of the approach is that, depending on the choice for deployment, either the spectrum or the transmit power is reused in the same geographical region, which provides an increase of traffic handling capacity. With an antenna beam directed to a specific area of high user density, more users can potentially benefit from better antenna gain and hence experience higher Signal-to-Interference-plus-Noise Ratio (SINR) values compared to the non-ViS case. On the other hand, using ViS implies a reduction of either transmit power or bandwidth for the macro-cell, and one additional interferer in the network, both of which can have a negative effect on performance if not addressed correctly.

In order to cope with the complexity of these trade-offs, SON algorithms capable of dynamically share the spectrum or power resources between virtual and macro-cells, as the ones presented in this thesis work, are needed. The key functionality of these algorithms is to find an optimum configuration for the given resource sharing scheme which is able to maximize the network capacity while minimizing the aforementioned negative effects.



# CONTENTS

<b>1</b>	<b>Introduction</b>	<b>1</b>
1.1	Scope and Goals . . . . .	2
<b>2</b>	<b>Theoretical Background</b>	<b>5</b>
2.1	LTE and Future Mobile Networks . . . . .	5
2.2	Self-Organizing Networks . . . . .	9
2.3	Active Antenna Systems . . . . .	12
2.4	Vertical and Virtual Sectorization . . . . .	14
2.4.1	Vertical Sectorization: Literature Overview . . . . .	15
2.4.2	Virtual Sectorization: Literature Overview . . . . .	18
<b>3</b>	<b>Research Questions and Motivation</b>	<b>21</b>
<b>4</b>	<b>System Modelling and Scenarios</b>	<b>23</b>
4.1	System Description . . . . .	23
4.2	Traffic Characteristics . . . . .	29
4.3	Propagation Models . . . . .	31
4.4	Simulation Scenarios . . . . .	32
<b>5</b>	<b>ViS Static Resource Sharing Performance</b>	<b>35</b>
5.1	ViS Deployed in All Cells in the Network . . . . .	36
5.1.1	ViS in All Cells: In-Depth Analysis . . . . .	42
5.2	ViS Deployed in Four Cells with Hotspots . . . . .	44
5.2.1	ViS in Four Cells: In-Depth Analysis . . . . .	46
5.3	ViS Deployed in the Most Loaded Cell . . . . .	46
5.4	Concluding Remarks . . . . .	48
<b>6</b>	<b>ViS SON Algorithm Description</b>	<b>51</b>
6.1	Bandwidth Sharing SON Algorithm . . . . .	51
6.2	Transmit Power Sharing SON Algorithm . . . . .	52
6.3	SON Algorithm Simulation Scenarios . . . . .	52

<b>7 ViS SON Algorithm Performance</b>	<b>55</b>
7.1 SON ViS Deployed in All Cells in the Network . . . . .	55
7.2 SON ViS Deployed in Four Cells with Hotspots . . . . .	57
7.3 SON ViS Deployed in the Most Loaded Cell . . . . .	59
7.4 Concluding Remarks . . . . .	61
<b>8 Conclusions and Future Work</b>	<b>63</b>
<b>Bibliography</b>	<b>65</b>
<b>A Virtual Cells Optimum Configuration</b>	<b>67</b>
<b>B Static Resource Sharing: Additional Results</b>	<b>71</b>
B.1 ViS in Four Cells. . . . .	71
B.2 ViS in One Cell . . . . .	72
<b>C SON Resource Sharing: Additional Results</b>	<b>75</b>
C.1 ViS in All Cells. . . . .	75
C.2 ViS in Four Cells. . . . .	76
C.3 ViS in One Cell . . . . .	77
<b>List of Figures</b>	<b>79</b>
<b>List of Tables</b>	<b>83</b>

# 1

## INTRODUCTION

Since the first commercial deployment of the Long Term Evolution (LTE) mobile network technology in the last quarter of 2009, mobile data traffic has shown an exponential growth rate driven mainly by the ever growing offer of devices, services, and applications available to the mobile subscribers, and by the expansion of cellular network coverage worldwide. According to figures from Ericsson and Cisco, it is expected that the total mobile data traffic in 2019-2020 will increase by a factor of ten times the total mobile data traffic reported by the end of 2014 [1][2]. In order to cope with this significant data traffic growth, there is a need to develop and deploy new solutions (e.g. network densification strategies) capable of optimizing network performance, perform dynamic troubleshooting and dynamic resource sharing, and hence, improve the end user experience. Furthermore, these solutions should be able to adapt dynamically to changes in the network in order to optimize performance and minimize operational costs that result from continuously employing people to manually adjust configurations and perform typical troubleshooting tasks. To this matter, the telecommunications industry has been focusing on the research and development of Self-Organizing Network (SON) features that can automate initial network configuration, operation and maintenance [3].

Within the first 3GPP LTE release, namely Release 8, SON was already considered as a key enabler to exploit network resources at their maximum, seeking to achieve the best performance at the lowest possible cost. The specification for SON included in LTE Release 12 [4] includes several different features aimed to self-configuration, self-healing and self-optimization processes. All these tasks are expected to be controlled by an integrated network management system that is mostly automated and enables the operators to manage and operate their networks with minimal human interaction. The European FP7 SEMAFOUR project is one of the latest research efforts focused on the development of such a unified SON system and of SON functions that provide a closed control loop for the configuration, optimization and failure recovery of the network across different Radio Access Technologies (RATs) and cell layers [5].

One of the most interesting research questions in SEMAFOUR is focused on the usage of Active Antenna Systems (AAS) in combination with SON functions which can lead to increased network capacity. In AAS, the Base Station (BS) is equipped with an antenna array capable of transmitting, simultaneously, independent horizontal or vertical beams that re-use the BS radio resources, e.g. power or bandwidth. The basic principle behind AAS is that every element in the antenna array is capable of adapting its radiation pattern independently in a manner that the gain from the entire array is focused at a particular area. Such property of AAS enables operators to create new cells within an existing one to capture, for instance, a traffic hotspot and maximize capacity, and use them as a cost-effective densification strategy.

Vertical Sectorization (VS) and Virtual Sectorization (ViS) have been proposed as deployment options when using AAS. VS consists of two vertically separated beams, transmitted by a single antenna, serving two distinct cells, close and further away from the BS, denoted respectively as inner and outer cells. The inner cell covers a small portion of the cell's surface before implementing VS, denoted as original cell, and typically has the same azimuth as the outer (and original) cell but a different electrical downtilt. To achieve high capacity gains with VS, a significant part of the cell traffic load should be located near the BS and the original cell's

resources are shared between the inner and outer cell. When high traffic load is located far away from the BS, there is no use of implementing VS. In fact, using such a strategy might lead to a decrease on performance due to the increased interference induced by the new cell and the reduced power of the outer cell, in the case of full bandwidth reuse and egalitarian power sharing. In this case, ViS can be implemented as an alternate solution to increase the cell's capacity. For ViS, the newly created cell, referred to as virtual cell, can be more flexibly placed anywhere within the original cell by using a large antenna array capable of producing very narrow beams and choosing the azimuth and downtilt such that the virtual cell's footprint is as much as possible steered towards an area of relatively heavy traffic (a traffic hotspot). The remaining part of the original cell after ViS is denoted as macro-cell for the rest of this document.

The involved trade-offs make the deployment of VS or ViS non-trivial. The key advantage of these approaches is that, depending on the deployment approach, either the spectrum or the transmit power is reused in the same geographical region which provides an increase of traffic handling capacity. Furthermore, with an antenna beam directed to a specific area of high user density, more users can potentially benefit from better antenna gain and hence experience higher Signal-to-Interference-plus-Noise Ratio (SINR) values compared to the non-VS/ViS case. On the other hand, using VS or ViS implies a reduction of either transmit power or bandwidth for the original cell, and one additional interferer causing inter-cell interference, both of which have a negative effect on performance. In order to cope with the complexity of these trade-offs, SON algorithms capable of dynamically controlling the AAS functionality have to be developed and implemented. The key functionality of these algorithms is to find an optimum activation and deactivation point for VS or ViS, as well as an optimum antenna configuration and resource sharing scheme which is able to maximize the network capacity while minimizing the aforementioned negative effects.

VS and ViS can be considered as technologies that address some of the requirements already set forth regarding new generation mobile network technologies, such as 5G. As the traffic demand in cellular networks is expected to increase exponentially in the coming years, there is a need for solutions that will deliver massive system capacity and very high data rates at a low cost. Network densification is key to achieving these objectives with the addition of new small cells to the system. The use of AAS is expected to be a good densification strategy compared to the deployment of small cells, since the latter require additional backhaul that increases the overall cost of the solution as well as further planning efforts. Energy efficiency is another challenge for future mobile networks that can be addressed by technologies such as VS and ViS. These antenna technologies, together with, for example, massive Multiple-Input-Multiple-Output (MIMO) or multilayer beamforming, are capable of focusing the radiated power towards the user or at a specific area with a high traffic concentration. Finally, next generation mobile networks will become increasingly complex because of the overlay of multiple RATs and small cells, evolving into heterogeneous networks. The planning, operation and troubleshooting of such networks imposes difficulties to the operators and exalts the need for SON functionalities and systems. Using either VS or ViS increases the number of cells in the network, to the double in case they are implemented in every cell, meaning more parameters to configure and optimize by the operators which is traditionally done by teams of people from the operator's engineering departments. With the increase of the number of cells to manage, the network complexity leads to higher probability of human error as well as higher capital and operational costs, hence again, the need of a unified SON entity capable of managing the different features of the network.

## 1.1. SCOPE AND GOALS

At the time of the writing of this thesis, a comprehensive study on VS in a realistic network was ongoing at TNO as part of the SEMAFOUR project via system-level simulations, in collaboration with other partners across Europe. Following on the steps of the work done for VS, a detailed study of ViS will be carried out in order to gain insight into the behavior of ViS and to understand the impact on performance of its different control parameters. To achieve this and to make a relevant contribution to the SEMAFOUR AAS use case, the work has been divided in the following stages:

- Modelling and Implementation: Update the SEMAFOUR simulator with the ViS feature by implementing a new antenna model, new interference and rate modelling, and new SON functionality.
- Optimum ViS Tilt and Azimuth Configuration Study: Done for each cell in the network in order to find

an optimum tilt and azimuth configuration for ViS, based on the traffic density maps available, so that the virtual cell would cover a focused area with a high concentration of users and, consequently, lower the utilization of the macro-cell.

- Resource Sharing Scheme Controllability Study: Simulate several static bandwidth and transmit power sharing fractions between virtual and macro cells for a fully virtually sectorized network in order to assess the sensitivity of the ViS feature.
- SON algorithm assessment: Use a SON algorithm to assess the impact of ViS on the network performance from both bandwidth and power sharing perspectives for different network loads.

Analysis of the impact on coverage and network capacity performance from the deployment of ViS in a realistic environment is the main objective of this thesis, by evaluating the throughput gains achieved by its implementation. A complete LTE network has been modelled for the entire city area of Hannover, Germany. By using real 3D building data, it allows for realistic pathloss predictions and realistic network planning. In addition, sophisticated modelling approaches for macroscopic traffic distribution and generation have been employed, in order to get a realistic simulation of subscribers in the network [5].

The remainder of this project is organized as follows. Chapter 2 provides an overview on the theoretical background behind LTE and the next generation of mobile networks (5G), SON and their functionalities, AAS, and a literature study on prior art for VS and ViS. In Chapter 3, the motivation and research questions that this thesis aims to answer are presented. Chapter 4 gives a thorough description of the system model and simulation scenarios used for this project, e.g. antenna and interference modelling, traffic profiles, etc. In Chapter 5 the results of the bandwidth and transmit power sharing Controllability and Observability (C&O) studies are presented, while Chapter 6 introduces the SON algorithm implemented for efficient resource sharing that maximizes network capacity in combination with ViS. The results and performance analysis of the SON algorithm are presented in Chapter 7. Finally, in Chapter 8, the conclusions drawn from the results obtained in this project are discussed, along with open issues that are left for further research.



# 2

## THEORETICAL BACKGROUND

This chapter presents the theory behind the topic of this thesis along with the findings from prior art work related to VS and ViS. Section 2.1 gives an overview of LTE and introduces the expected requirements and benefits for future mobile networks according to current ongoing research and available literature. In Section 2.2, the concept of SON is analyzed and thoroughly explained, including its relation to network features that will enhance the performance of current and future mobile networks. Active Antenna Systems are described in Section 2.3, focusing on general antenna theory and the advantages of such systems. Finally, in Section 2.4, the findings from the literature survey on VS and ViS is presented, which serves as a foundation for the work presented in this thesis report.

### 2.1. LTE AND FUTURE MOBILE NETWORKS

LTE was designed by the 3GPP as a fourth generation (4G) technology and is known in full as Long-Term Evolution. LTE evolved from the earlier 3GPP system UMTS (Universal Mobile Telecommunication System), a 3G technology, which in turn evolved from the 2G technology Global System for Mobile Communications (GSM). Different from previous systems, LTE is designed and optimized for data traffic delivery and handling. Among the requirements set for LTE by the 3GPP since its first release, Release 8 [4], the most relevant are as follows:

- Higher peak and cell edge data rates, capacity and spectral efficiency as compared to the ones achieved with UMTS.
- Reduced latency in both connection establishment and transmission.
- Flexible spectrum usage by using different bandwidths and frequency bands.
- Interoperability with legacy systems, meaning, seamless mobility among different RATs.

In order to meet the aforementioned requirements, the system architecture from UMTS is modified and simplified. The packet switched core network from UMTS is replaced by an Evolved Packet Core (EPC) network, which is completely based on the Internet Protocol (IP) and is a solution to reduce latency in the network. Unlike UMTS, the core network does not have a circuit switched domain to handle voice calls, which are either handled by the legacy core via a process called circuit switched fallback or they are handled using an external IP Multimedia Subsystem (IMS). This last one includes all the necessary functions to setup voice calls over IP, known as Voice over LTE (VoLTE).

On the Radio Access Network (RAN) side, the architecture is also simplified by integrating the functionalities of the Radio Network Controller (RNC) from UMTS into the base station, known as evolved NodeB

(eNodeB), which is the only node in the RAN. Additionally, the entirely new radio interface is based on Orthogonal Frequency Division Multiple Access (OFDMA) and Single Carrier Frequency Division Multiple Access (SC-FDMA) in the downlink and uplink, respectively. In order to tackle the requirements on data rates, LTE supports different transmission modes, including the use of Multiple-Input-Multiple-Output antennas (MIMO) techniques such as beamforming. Since LTE is an evolution from UMTS, the radio interface is formally named Evolved UMTS Terrestrial Radio Access Network (E-UTRAN).

Enough documentation has been available on LTE architecture and performance for the past fifteen years, therefore the rest of this section will approach exclusively the latest LTE releases and the expected benefits from these standards.

It is expected that data traffic through mobile networks will grow almost ten times by 2020 when compared to the current traffic reported by major vendors such as Ericsson or Cisco in 2014 [1][2]. This accelerated growth will be driven by new use cases for mobile networks that will start operating in the upcoming years, and the number of users they will target. Among these use cases we can find vehicular communication, terrestrial TV, cloud-based services, public transport automation, and machine-to-machine and device-to-device communications [6][7]. 3GPP Release 9 introduced LTE-Advanced as the first attempt to standardize new technologies that will cope with the challenges foreseen for future mobile networks by the International Telecommunication Union (ITU) [8], which key performance requirements are:

- Peak data rates of 100 Mbps for high mobility users and 1 Gbps for low mobility users
- Scalable bandwidths up to 100MHz for the downlink
- Control plane latency of less than 100 ms and user plane latency of less than 10 ms
- High quality mobile services
- Capability of interworking with other radio access systems

In order to meet these requirements, the 3GPP has focused its efforts on different technological improvements for the network e.g. Carrier Aggregation (CA), high order MIMO for both downlink and uplink, Coordinated Multipoint (CoMP) transmission/reception, Enhanced Inter-Cell Interference Coordination (eICIC) and the concepts of heterogeneous networks (HetNets) and Self-Organizing Networks (SON).

HetNets, same as VS and ViS, can be considered as a densification strategy to improve network coverage and capacity because they consist on adding more cells to the network. The 3GPP has introduced repeaters and relays as low-power devices that extend the coverage area of a cell. They are useful in sparsely populated areas in which the performance of a network is limited by coverage rather than capacity. They can also increase the data rate at the edge of a cell, by improving the signal-to-interference plus noise ratio there [9]. Repeaters work by receiving a signal, amplifying and rebroadcasting it. The main problem with repeaters is that they also amplify noise and interference, limiting their performance. Relays have also been standardized and the difference with a repeater is that before amplifying and rebroadcasting the signal, a relay decodes it, thus removing noise and interference. In addition to the aforementioned, low power cells with full eNodeB functionality, which receive the name of Home eNodeB (HeNB), can be deployed to create cells of different sizes i.e. macro, micro, pico and femto cells. These low-power small cells will increase capacity in traffic hotspots with high user demand and fill areas not covered by the macro network. The advantages of using HeNBs are the added extra capacity and that site acquisition and deployment are easier because the hardware is smaller when compared to a regular eNodeB. The main disadvantages are deployment costs and the increase of interference when the new cells are deployed in the same frequency band as the macro-cell as shown in Figure 2.1. In this case the interference of a high power eNodeB reduces the SINR experienced by the UE served by the small cell, limiting its performance.

The idea of Self-Organizing Networks (SON) was first specified by the 3GPP since Release 8, focusing more on eNodeB self-configuration. In later LTE releases, new procedures focusing on self-optimization were introduced e.g. handover optimization, load balancing, coverage and capacity self-optimization, enhanced Inter-Cell Interference Coordination (eICIC), self-healing functions and minimization of drive tests [10]. These procedures allow the network to detect changes, make intelligent decisions based upon these

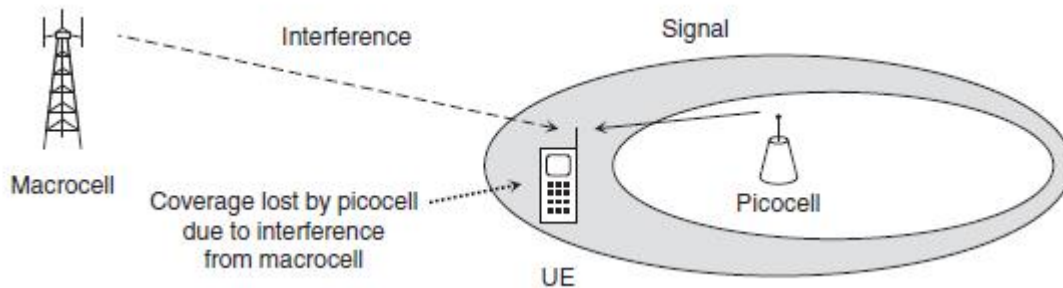


Figure 2.1: Small cell inter-cell interference problem. [9]

inputs and then implement the appropriate action. Since SON is one of the key concepts of this thesis work, a more detailed overview is given in Section 1.2.

With 3GPP Release 12 and the upcoming further releases, 3GPP is laying the grounds for 5G, the next generation of mobile networks. First deployments for 5G are expected by 2020, with the premise of connecting everything to everything in the so called Internet of Things (IoT). This means that future mobile networks will not be only about connecting people but rather focus on providing connectivity to any device and application that may benefit from being connected [11]. Among the new uses envisioned for future mobile networks, the most relevant are:

- **Massive Machine-type-Communications (MTC):** Machine-type-Communication (MTC) refers to the connection through the network between devices without the need for human interaction. This will have a large scale impact on capacity and coverage because the deployment of billions of wirelessly connected sensors, actuators, vehicles and similar equipment will increase the number of devices in the network from 10 to a 100 times more of what we see today [7].
- **Device to Device (D2D) Communication:** Refers to the direct communication between devices without any user data traffic going through the network infrastructure. Under normal conditions the network controls the radio resource usage of the direct links to minimize the resulting interference. The goals are to increase coverage, reduce backhaul utilization, provide fallback connectivity, and increase spectrum utilization and capacity per unit area [12].
- **Mobile Broadband Evolution:** Data is growing at a rate between 25% and 50% annually and is expected to continue towards 2030 [13]. This growth can be attributed at the increase in content size and the number of applications requiring higher bit rates, such as mobile devices with high resolution cameras e.g. 4K resolution, and the developments in 3D video. Additionally, streaming services, mobile internet connectivity and interactive video will continue to be used more as more devices connect to the internet.
- **Cloud Based Services:** Cloud storage and applications are rapidly increasing for mobile communication platforms and is one particular use case driving the growth of uplink data rates. 5G will be used for remote work in the cloud which, when done with tactile interfaces, requires much lower end-to-end latencies in order to maintain a good user experience. Entertainment, for example cloud gaming, is another key driver for the increasing need for mobile broadband capacity and fast mobility [13].

The main challenges and requirements these applications and services impose on 5G networks are higher bit rates, virtually zero latency, massive capacity, efficient energy consumption, fast mobility, and high reliability. A brief summary of the expected requirements for 5G and typical applications is given in [12] by the European FP7 METIS project and shown in Figure 2.2.

New technologies are currently under research and development in order to comply with the above mentioned requirements. The main 5G enabler technologies in ongoing research found in recent literature, can be summarized as follows:

Requirements	Desired value	Application example
Data rate	1 to 10 Gb/s	Virtual reality office
Data volume	9 Gbytes/h in busy period 500 Gbytes/mo/subscriber	Stadium Dense urban information society
Latency	Less than 1 ms	Traffic efficiency and safety
Battery life	One decade	Massive deployment of sensors and actuators
Connected devices	300,000 devices per AP	Massive deployment of sensors and actuators
Reliability	99.999%	Teleprotection in smart grid network Traffic efficiency and safety

Figure 2.2: Key requirements for 5G and its typical applications. [12]

- Network Densification Enhancements:** Since the 5G network will be a dense heterogeneous network consisting of macro-cells along with a large number of low power nodes and with D2D and MTC capabilities, there is a need to develop solutions that will be robust against new interference and mobility schemes. The idea of ultra-lean RAN design is introduced in [11] and refers to the minimization of signals related to synchronization, channel estimation, and in general control signals that are not dedicated to deliver user data. This concept aims to reduce interference from non-user-data related signaling and increase data rates, while improving the network energy efficiency by enabling network nodes to enter low energy (stand by) states. On the same line as ultra-lean RAN design is the concept of user/control plane separation. The control plane in the core network can be separated from the user plane in order to alleviate the increase of signaling traffic that will come as a consequence of the deployment of dense small cells networks. A proposal to implement this separation is, for example, that the user data may be delivered by the dense layer of nodes while control information is provided by the overlaying macro-cell. This solution will also help with the deployment of device-centric optimizing solutions such as those relying on beamforming for data transmission. In this case the user plane radio links can be optimized in real time while maintaining the control plane signals static in the overlaying macro-cell. Additionally, alternative densification strategies can be considered such as VS and ViS. The advantage of them compared to small cell deployment is that there is no need for additional backhaul deployment, only a larger antenna array has to be implemented to create a narrow beam towards a traffic hotspot.
- Efficient Spectrum Usage:** In order to achieve higher data rates and spectrum efficiency, 5G networks will use frequency ranges going up to 100 GHz or more, as stated in [12]. New frequency bands for mobile communications are expected to be allocated below 6 GHz at the World Radio Conference (WRC) 2015, while spectrum in higher bands is suggested for allocation in the WRC 2019. Higher bands will be used as a complement to an underlying RAT operating below 6 GHz because of propagation restrictions at higher frequencies. Those frequencies will be used to provide additional capacity and wide transmission bandwidths for very dense deployments. In addition to the new frequency bands, Full-Duplex (FD) transmission is a technology that has the potential to significantly increase the spectral efficiency at the physical layer through the removal of a separate frequency band/time slot for both uplink and downlink transmission [14]. This was not possible for previous generations of mobile networks because of the internal interference between the transmitter and receiver, an issue that can be overcome nowadays by recent developments in antennas and digital baseband technologies in combination with advanced RF interference cancellation techniques. A final approach is flexible spectrum usage and management. Under this scheme, spectrum resources can be shared among a limited set of operators and by using unlicensed bands following initiatives such as the Limited Assisted Access (LAA)

[6], mainly for frequencies beyond 10 GHz. The availability of higher frequency bands is beneficial for ViS and AAS in general. If the goal is to cover a smaller area, then higher antenna gains are needed which means that the number of radiating elements of the antenna array will considerably increase and there will be a need for higher operating frequencies.

- **Network Virtualization and Cloud-based RAN (C-RAN):** Wireless Network Virtualization (WNV) aims to reduce operational and capital expenditure (OPEX and CAPEX) for service providers and operators. The virtualization mechanism transforms the physical resources (e.g. network infrastructure, backhaul, spectrum, core network and RAN, etc.) to a number of virtual resources which are shared by different consumers. The main advantages of WNV are high resource utilization, improved system performance, reduced CAPEX and OPEX, better QoS for the end users, and easier migration to newer technologies [14]. C-RAN can be seen as a first approach towards WNV that consists on separating the baseband processing from the base station and moving it to a cloud where a pool of Baseband processing Units (BBUs) perform centralized signal processing and management for an area with a larger number of Radio Remote Heads (RRHs) and hence base stations.
- **Multiple Antennas Techniques and AAS:** By increasing the number of transmit and receive antennas at the base stations to eight or more (massive MIMO), a significant gain in network capacity and spectral efficiency can be achieved. This gain can be further enhanced by using advanced receiver schemes based on dedicated demodulation reference signals [6]. Especially for operation at higher frequencies, the use of multiple antennas for beam-forming at the transmitter and/or receiver is a critical component to counter the worse propagation conditions. On top of this, beam-forming will also be an important component for lower frequencies to improve coverage and provide higher data rates. Using AAS where the RF components are integrated into the antenna and performing vertical or virtual sectorization can give significant improvements in cell capacity compared to a single beam system. In both techniques, the AAS is capable of creating separate beams creating two cells that share the same resources. These topics are further explained in 2.3 and 2.4..

Since the main objective of this thesis project is to focus on the SON aspects and performance of AAS, especially on ViS, the next sections will focus on the specifics of these technologies. The final section is a literature study summarizing prior-art work available for VS and ViS.

## 2.2. SELF-ORGANIZING NETWORKS

Achieving and maintaining optimal performance in future cellular systems will become increasingly difficult with manual configuration, optimization, and maintenance due to their ever increasing degree of densification, which involves a rise of the number of configurable parameters involved. As a consequence, the mobile network industry has taken the approach of developing SON features that will automate the above mentioned tasks in order to reduce OPEX and CAPEX while boosting network performance. The first SON features were introduced by the 3GPP with LTE Release 8, based on the set of requirements defined by the Next Generation Mobile Networks (NGMN) alliance in [15]. This specification was focused on self-configuration (e.g. automatic initial radio parameter configuration, automatic neighbor relationships) and self-optimization mechanisms (e.g. mobility robustness optimization, load balancing, interference management, coverage and capacity optimization, energy savings). Further releases focus on new features that enable network self-planning. Eventually, the combination of self-configuration, self-optimizing and self-planning functions will result in increased operational efficiency, as shown in Figure 2.3.

The LTE network is maintained and supervised by a Network Management (NM) system which interacts with diverse Network Elements (NE), e.g. eNodeBs, for configuration and optimization purposes. SON functions can be categorized in three different classes, according to how they are mapped onto the NM architecture [3].

- **Centralized SON Functions:** Operate based on centralized policies defined in the network's Operation, Administration and Maintenance (OAM) system. This type of SON functions involve feedback from a large number of NEs to the NM system and require many of these NEs to be treated simultaneously. The

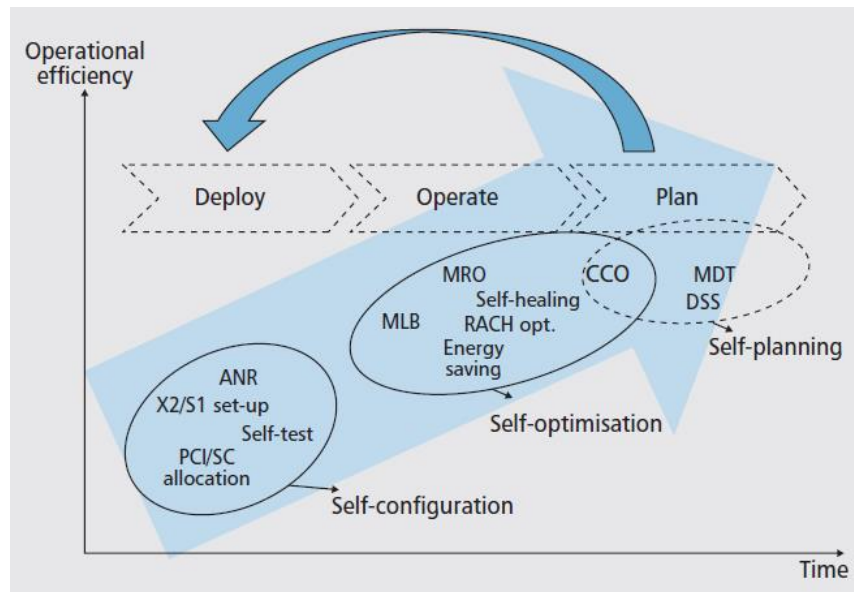


Figure 2.3: Evolution of SON features. [3]

functions are executed across different vendor equipment, RATs and technologies, eliminating compatibility issues and the need to have separate systems per technology or RAT. Because of the large number of NEs involved, the response from the system can be too slow for certain SON functions. Centralized functions can be more robust against network failures caused by the operation of other SON functions with conflicting objectives because control is centralized.

- **Distributed SON Functions:** These functions are implemented directly in the NEs and apply to at most a few of them, since their impact is usually more localized. Since these functionalities are embedded directly in the NEs, they are designed for near real-time response in seconds or milliseconds and therefore support more frequent and more localized changes than centralized functions. Each NE can start a SON process and provide optimization decisions independently or in coordination with other NEs, since there exists information exchange between neighbors.
- **Hybrid SON Functions:** As expected from the naming, hybrid SON functions are essentially a combination between centralized and distributed SON functions.

Examples of these SON functions, for which requirements have been specified up to LTE Release 12, are network self-configuration, automatic neighbor relations (ANR), automatic cell identity management, mobility robustness optimization (MRO), mobility load balancing (MLB), energy savings and minimization of drive tests (MDT) [5][3].

The desired quality of experience requirements and vision of 5G, and the associated scale of complexity and cost, demand a significantly different approach toward SONs in order to make 5G technically as well as financially feasible [16]. One take on the challenges that future mobile networks represent for SON functionality is the work done by the EU FP7 SEMAFOUR research project that aims at a unified self-management system. SEMAFOUR addresses the operation of the SON system by ensuring the conflict-free execution of a multitude of SON functions by run-time coordination, but also the management of the SON system itself through policies and rules. This would enable network operators to holistically manage and operate their complex heterogeneous mobile networks [5]. The SON system proposed by SEMAFOUR is shown in Figure 2.4.

The general network-oriented objectives are defined by the network operator and later translated into policies by a process called policy transformation. The transformed objectives are then fed into the different parts of the SON system. The multi-RAT and multi-layer SON functions provide a closed loop for configuring and optimizing a selected set of network configuration parameters in order to achieve the network-oriented objectives. The operational SON coordination has the roles of supervising the functioning of the multitude of

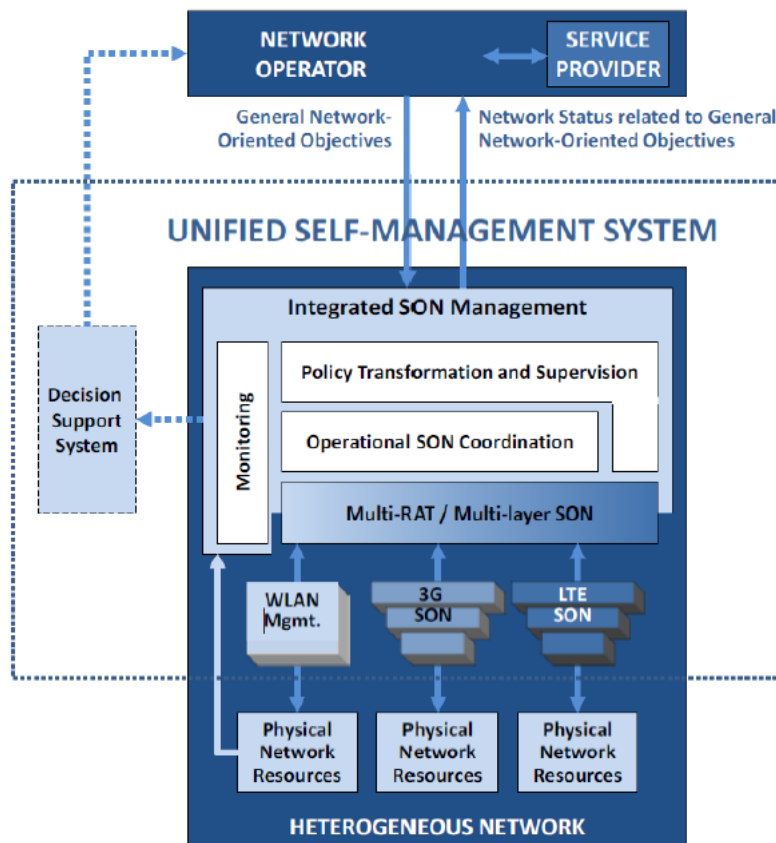


Figure 2.4: Proposed SON system from SEMAFOUR. [5]

SON functions. It detects and resolves conflicts, system instabilities and undesired behavior occurring due to the independent operation of individual SON functions. The monitoring functionality acquires performance data from network elements (NEs) and mobile terminals and is responsible for processing this data such that feedback can be given towards the mobile network operator regarding the actual network status and performance according to the network-oriented objectives. When the objectives can't be achieved by means of the SON system, a decision support provides recommendations towards the operator about possible additional network deployment and enhancement actions needed to meet them.

Within the SEMAFOUR project, a selection of SON functions that will be relevant for operators in the short and midterm have been defined and are presented hereafter [5]:

- **Dynamic Spectrum Allocation (DSA):** DSA is one of the SON functions thought for future multi-RAT networks. The scope of multi-RAT dynamic spectrum allocation is that existing spectrum from legacy systems may be dynamically allocated to LTE or 5G. The purpose is to adapt the available spectrum resources to the spatial and temporal requirements by automatically assigning carriers to base stations based on usage and/or estimated load. This function also helps to reduce interference while optimizing coverage, capacity and the quality of service in the network. To avoid overload or underutilization of carriers a new or lightly-utilized carrier frequency could be assigned to a base station that is in or near overload and is requesting an additional carrier.
- **Performance Optimization for High Mobility Users:** This use case focuses on mitigating frequent handovers that occur when users travel at high velocities through a dense network and the negative impact that is caused by them both on the users and the core network. The SON function proposed for this case will try to predict the future mobility behavior of users based on the trajectory that they follow through a cell.
- **Multi-layer LTE/Wi-Fi Traffic Steering:** Most smart phones today are dual mode phones supporting

both cellular and Wi-Fi interfaces. However, the network selection between the cellular and Wi-Fi networks is usually manually controlled by users and set as connecting to Wi-Fi when available. With high user expectations in terms of service availability and quality, there is a trend in the telecommunication industry to enable Wi-Fi as an integrated piece of the operators' networks. Intelligent traffic steering between the two access networks is a key technology component to fulfil the target, which can be done through a set of SON solutions investigated within SEMAFOUR.

- **SON mechanisms for AAS:** AAS are one way to increase the capacity of existing networks since they are considered to be a densification technique. Currently, one use of these systems is to create a new static cell close to the base station by means of VS. There is the possibility of a more dynamic use when AAS are used in combination with SON algorithms that will enable user specific or area specific beamforming, with cell shaping and splitting (e.g. ViS) or by simply turning on and off the new cell based on traffic conditions. Since AAS is a part of the core subject of this thesis, a more elaborate description of the topic is given in Section 2.3.

It is clear that the implementation of a SON unified management system in combination with a wide range of SON functionalities is one of the key technologies, if not the most important, that will drive the success of future mobile networks. In the context of this thesis work, SON algorithms have been developed and used to control the sharing of resources between virtual and macro-cells when using ViS and they are presented in Chapter 6.

### 2.3. ACTIVE ANTENNA SYSTEMS

Unlike traditional passive antenna systems, an active antenna is a MIMO antenna array that has active electronic components that allow radiation pattern flexibility. This means that the AAS is created by integrating several Radio Frequency (RF) components (low power amplifiers and transceivers) with the antenna's radiating elements as depicted in Figure 2.5. This enables the phase and amplitude of the signals from each radiating element inside the antenna to be electronically controlled, using signal processing to shape and steer the direction of the radiated beam vertically and horizontally.

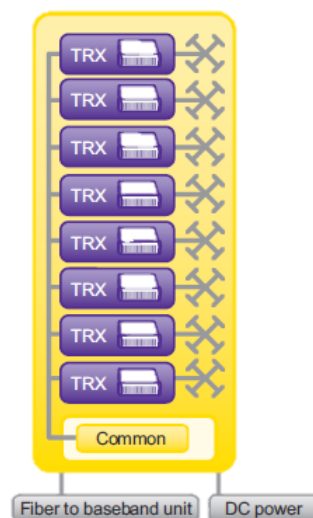


Figure 2.5: Active Antenna System. [17]

The main advantages of using AAS can be summarized in the following:

- **Reduced Footprint:** In legacy mobile networks all the analog and digital radio functions were incorporated directly in the radio base station, which implied the use of long coaxial cables connecting the

antenna (usually at the top of a mast or rooftop) to the base station (located at the bottom). This configuration is costly to the operator and introduces losses to the radio link that translate into poorer performance. For LTE the concept of Remote Radio Units (RRU) or Remote Radio Heads (RRH) was introduced. In this case the base station is responsible for the base band processing by means of the Base Band Unit (BBU) which is connected through optical fiber to the digital RRU, reducing link budget losses and resulting in improved performance. With the integration of the radio within the antenna there is the benefit of elimination of several components like cables, connectors, and mounting hardware and an overall reduction in the physical tower space required. The evolution of the cell architecture throughout time can be observed in Figure 2.6.

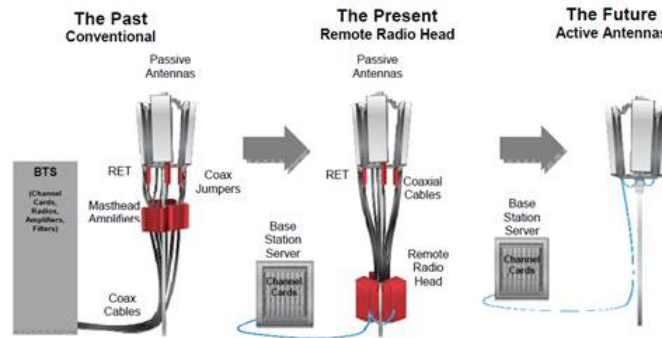


Figure 2.6: Cell Architecture Evolution. [18]

- Failure resilience and Self-Healing:** Since every antenna element is equipped with its own transceiver, the failure of one of them doesn't cripple the entire system performance. Even more, when a transceiver fails, the rest of the elements can be reconfigured to automatically adjust the radiation pattern and minimize the impact on coverage performance as illustrated in Figure 2.7. In this case when one of the transceivers fails, the amplitude and phases on the remaining elements are automatically adjusted digitally to compensate for the elevation beam distortion and the reduction of Effective Isotropic Radiated Power (EIRP) on the horizon. This characteristic of AAS results also in lower OPEX for the operators, since an antenna with a faulty transceiver can be scheduled for maintenance and repair after a longer period of time without affecting normal network operations too much.

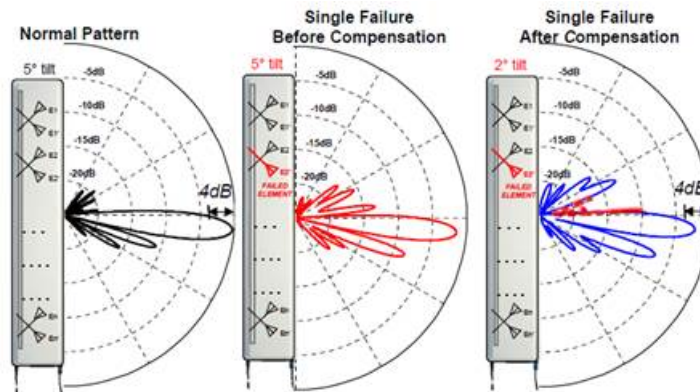


Figure 2.7: AAS Radiation Pattern Self-healing. [18]

- Advanced Antenna Tilt Features:** A principal advantage of active antennas is their ability to create and steer beams within the cell by changing the phase delay of individual carriers and amplitude of the signal emitted from each radiating element, to create constructive or destructive interference and provide electronic beam control in both horizontal and vertical domains. An AAS is capable of creating beams for different frequency bands, RATs, downlink, uplink or dedicated users. Typically a new tilt configuration may be needed when a new cell is deployed in a separate frequency carrier, in this case, the AAS is capable of creating separate cells with tilts on a per-carrier basis. The same goes for multiple

RATs and for link direction (downlink and uplink) because the link budget can be different, hence requiring different tilt configurations, e.g. GSM and LTE. Furthermore, the AAS is able to form multiple cells in the vertical and/or horizontal domain by establishing multiple static beamforming vectors in a vertical array. This type of cell splitting doubles available radio resources by separating user equipment (UE) or cells in the vertical and/or horizontal domain, increasing the system capacity [18]. All the aforementioned AAS applications are exemplified in Figure 2.8.



Figure 2.8: AAS Advanced Tilt Features. [17]

- **Improved Thermal Margin:** Because of the elimination of coaxial cables, jumpers and RF connectors, a substantial part of the power losses is eliminated. Additionally, with the radios integrated directly into the antenna housing, and by replacing a small number of large amplifiers with many small amplifiers, the heat is spread over the larger antenna structure as opposed to the smaller RRH [18].

The work presented in this thesis is focused in the case shown in Figure 2.8-f, where VS and ViS are made possible through the use of an AAS in combination with SON functionalities.

## 2.4. VERTICAL AND VIRTUAL SECTORIZATION

In this section the capabilities and potential of AAS for performance capacity enhancement of a cellular network are surveyed based on prior existing work. The focus is on the application of VS and ViS, where the former can be regarded as a special case of the latter. The basic principle is that the antenna resources in an AAS are exploited to create a secondary cell which is shaped by the effective antenna pattern in the vertical and/or horizontal plane as explained in Section 2.3. VS corresponds to the scenario where the original macro-cell (before VS) is split into a relatively small cell (inner cell) near the antenna and a larger outer cell covering the rest of the area of the original cell. The inner cell is configured with typically the same azimuth as the original cell but with an increased electrical downtilt. The larger outer cell continues to serve users that are not absorbed by the inner cell. In the case of ViS the newly created cell, which for the remainder of this thesis will be referred as virtual cell, can be more flexibly placed anywhere within the coverage area of the original cell (before implementing ViS) by choosing an azimuth and downtilt such that the virtual cell's footprint is as much as possible steered towards an area of relatively heavy traffic. The rest of the coverage area from the original cell that is not served by the virtual cell is referred for the remainder of this thesis as macro-cell, and it inherits the same parameters as the original cell i.e. azimuth, tilt, transmit power. Both applications are visualized in Figure 2.9.

When implementing either option, the resources available at the macro-cell need to be shared with the newly created cell. This sharing can be done either in the power or the frequency domain. The involved trade-offs make the deployment of VS or ViS non-trivial. The key advantage of VS/ViS is that, considering the assumed deployment approach, either the spectrum or the transmit power is reused in the same geograph-

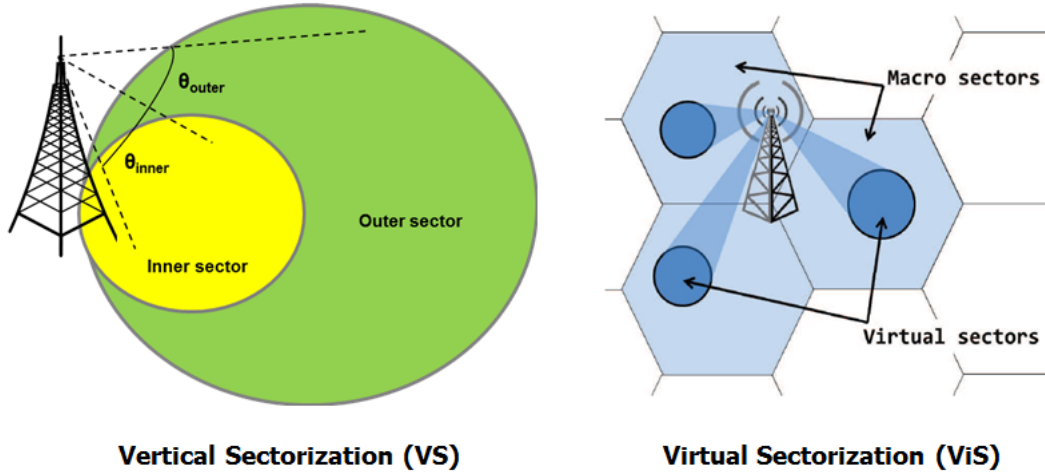


Figure 2.9: VS and ViS Representation. [19][20]

ical region which provides an increase of traffic handling capacity per km<sup>2</sup>. Furthermore, with an antenna beam directed to a specific area of high user density, more users could possibly have better antenna gain and hence a stronger signal compared to the case without VS or ViS. On the other hand, the application of these techniques implies a reduction of either transmit power or bandwidth of the original cell, both of which could have a negative effect on the performance if the resource sharing schemes are not properly configured. Most of the available literature on these topics is focused on VS, with the exception of the work presented in [19] which addresses ViS extensively and constitutes the foundation for the results presented in the SEMAFOR [5] project and consequently this thesis project. Section 2.4.1 will present prior-art work related exclusively to VS, emphasizing on the system model and performance results. In Section 2.4.2 the expected benefits from ViS reported in available literature are explored.

### 2.4.1. VERTICAL SECTORIZATION: LITERATURE OVERVIEW

In VS the original macro-cell is split into an inner cell (close to the base station) and an outer cell (covering the rest of the cell) as previously shown in Figure 2.1.4 1. From the studied literature available for VS, the most common way to implement this technique is through a transmit power sharing scheme with an equal power split between cells, i.e.  $P_{inner} = P_{outer} = \frac{P_{Total}}{2}$ , and make full reuse of the total available bandwidth (bandwidth reuse one). A better power split of the transmit power between the inner and outer cells is challenging because of the complex dependencies between the transmit powers and the average data rates of the users [21].

Although the work presented in [22] is based on an ideal antenna pattern and an ideal hexagonal network scenario, it shows the potential benefits that VS has over a typical cellular network deployment. This study tested two different Inter-site Distances (ISD), i.e. 3GPP Case 1 and Case 3, as well as the impact of Remote Electrical Tilt (RET) and half-power antenna beamwidth (HPBW) for scenarios with VS and without VS. The results for the capacity gains of VS show a clear improvement in cell throughput, beyond 50%, compared to the scenarios without VS.

In [23] the authors focused on the performance gains from VS in an HSPA network as well as its impact on network outage level as a consequence of the increased interference conditions when more cells are added to the network. The work proposes a new scheduling scheme that will mitigate the network outage levels while still yielding gains from VS. Their results from the study show that VS can achieve a gain of up to 59% in mean network throughput over the reference case when the scheduling scheme is not used and hence the outage levels are always higher than the reference. When the new scheduler is used, the gain from VS is 18% and the outage levels are even lower than the reference scenario, which was one of the objectives from the authors. Therefore, the proposed scheme can still provide an important capacity gain, along with the enhancement in network outage performance.

The work by Vook et. al. in [24] explores the use of two elevation beamforming methods, i.e. VS and Vertical Beamforming (VBF), under line of sight (LOS), non-line of sight (NLOS) and mixed propagation conditions for an LTE network. The results show similar gains, of around 17%, for both methods for cell edge user throughput, except for the case when VBF uses a more advanced MIMO technology such as Multi-User MIMO.

The work published in [25] concentrates on the development of a computationally efficient algorithm to find the optimum tilt angles for the inner and outer cells to achieve maximum performance with VS. The algorithm, named closed-form based vertical sectorization (CVS) is compared to the performance of an existing exhaustive search based vertical sectorization (EVS) algorithm, and to the performance of an implementation of VS with a fixed set of tilt angles. The study concluded that VS gives rise to a significant performance improvement over the reference scenario without VS and the CVS algorithm performs the same as the EVS but is computationally less demanding. The study shows that VS can achieve gains higher than 50% in cell-edge throughput over the case without vertical sectorization.

The results from the mathematical model derived for VS by Kifle et. al. in [26] demonstrate the impact of the inner and outer cell's tilt difference on the system performance. This approach was taken by the authors mainly due to the fact that when the inner sector is introduced the SINR is degraded and it is shown in the paper that the SINR performance depends on the tilt difference between the cells.. In the study they found out that, against the premise of the study, the tilt difference between the inner and outer cells doesn't return a maximum aggregate cell throughput rather there should be a reasonable setting that balances the inner and outer cells performance to maximize overall performance when compared to the performance of the original cell. The model presented in this work is valid only when the outer cell's tilt is already optimized and remains unchanged when VS is active. The authors found that a gain of more than 50% is achieved in user average throughput once VS is implemented with an optimum tilt balance.

In [27] the authors evaluate the performance of VS in LTE when combined with the use of advanced receivers such as a Symbol Level Interference Cancellation (SLIC) receiver and compare it to the performance of a non VS scenario with a minimum mean square error (MMSE) receiver. As in the previous findings already presented in this section, VS shows a clear and significant gain in performance over the reference case without VS, achieving higher gains when a SLIC receiver is implemented.

A field test using VS on a HSPA network was conducted and documented in [28]. The main focus of the field study was to assess the performance of VS in a real environment and how this performance is impacted by UE mobility. Two fundamental scenarios were tested. The first one involved a user moving between two vertically sectorized sites, the position of the inner and outer cells were kept static during the whole study. The second scenario focused on two static users residing in the inner and outer cells of one of the original cells, respectively. Ten measurement results were collected using VS and two measurements results collected without VS. The study concluded that there is no benefit for a moving user when VS is enabled because the UE experiences more handovers while moving which impacts on performance. On the other hand, the stationary user experiences higher average throughputs that lead to a gain of more than 100% in the best cases.

The work done in [20] for VS, an outcome of the SEMAFOUR project, presents a thorough system-level evaluation on the impact of tilt and power sharing on performance of a realistic LTE network using real three-dimensional building data, a realistic traffic distribution, and applying an advanced ray tracing modelling with a pixel size of 10 x 10 m<sup>2</sup>. Additionally, the authors present a framework for the design of a SON controller enabling the smart (de)activation of the feature based on the estimated traffic distribution. The average and 10th percentile user throughput results obtained when VS is used in all the cells of the network using different combinations of tilts and power settings are presented in Figure 2.10.

The results show that VS is always beneficial for the parameter configurations tested. The gains in average UE throughput go up to 33% while the cell-edge UE throughput gains are beyond 95% compared to the no VS scenario. The development of the SON controller and the performance results after its implementation are published in [29] and shown in Figure 2.11. For the evaluation of the performance of VS in combination with a SON functionality, the case labeled as *Full VS* uses an optimal combination of tilt and power split for all the cells in the network and VS is on during the entire simulation time. The case *SON VS* refers to the use of the SON algorithm capable of switching the VS feature on or off every time a call arrives and also capable of dynamically adapt the transmit power split. From Figure 2.11 it is clear that in all the cases VS performs

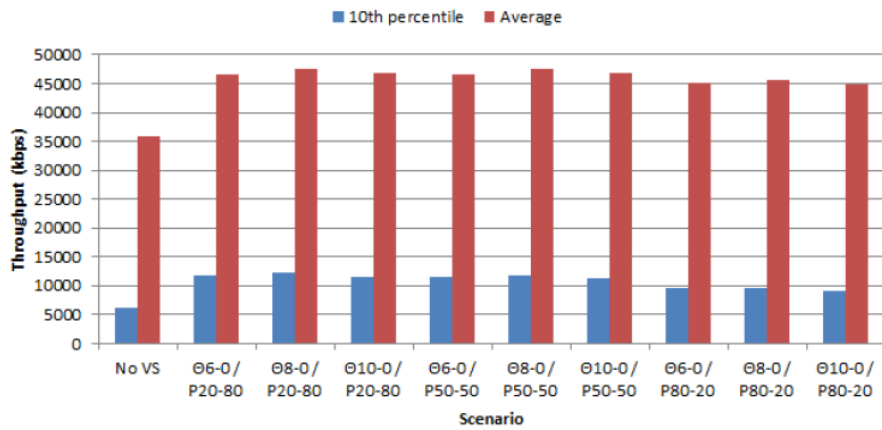


Figure 2.10: Network-wide average user throughput and 10th user throughput percentile (VS in all cells) [20]

better than the baseline scenario without VS. It is also noted that by implementing a SON algorithm capable of making a decision every time a new call arrives or departs to the system the performance gains are higher than the case when VS is always active, achieving gains up to 45% in average user throughput and 140% for cell edge user throughput when compared to the reference case without VS. The corresponding throughput gains of the *SON VS* scenario compared to the *Full VS* case are 9.5% and 26%, respectively.

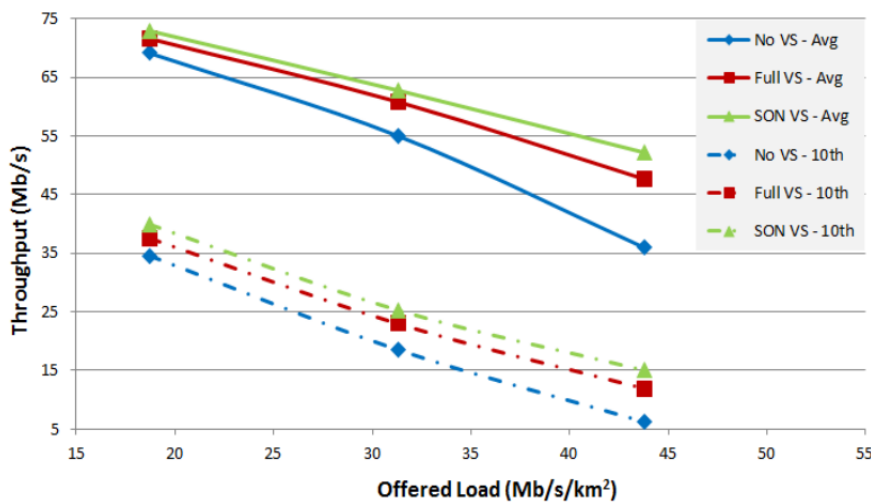


Figure 2.11: Network wide throughput using a SON controller (VS in all cells) [29]

The impact of resource sharing and cell load for VS is approached in [21]. In previous work, the total transmit power was split between the two cells and the frequency bandwidth was fully reused, creating additional interference between the two cells. For low traffic demand, VS with power sharing ('VS reuse one') may lead to performance degradation, while for high traffic demand in both cells, VS is likely to bring about important capacity gains. The authors propose a load threshold-based SON controller using a dynamic bandwidth sharing scheme for low and medium loads that automatically switches to power sharing when the load surpasses a certain threshold. They present results showing the performance of the three solutions and compare them to the baseline scenario without VS. The mean user throughput values as a function of arrival rates are presented in the study are displayed in Figure 2.12. In the figure it is clear that VS with BW sharing always performs better than the baseline scenario and that at higher loads it is preferred to switch to a power sharing scheme in order to obtain higher gains, which is exactly what the SON controller does automatically and hence it has the higher throughputs in the whole load range.

In summary, from the study of the literature available on this topic, it is expected that using AAS to perform VS would yield to capacity gains of 50% or more compared to a non VS deployment. It is important

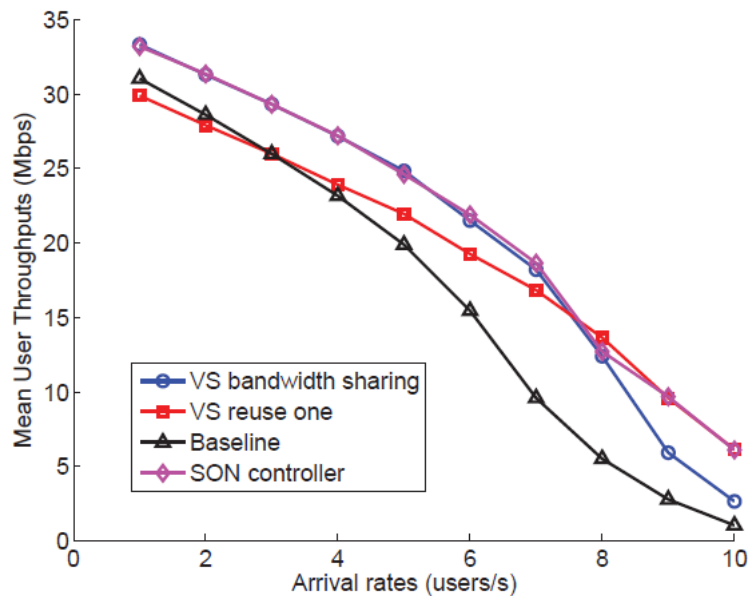


Figure 2.12: VS Mean User Throughputs for Increasing Arrival Rates [21]

to highlight that the gains are highly dependent on the optimum configuration of critical parameters such as vertical downtilt, the choice of an adequate resource sharing scheme that would help minimize interference while boosting performance, and on the network's traffic distribution. In addition, the combination of SON functionality with VS capable AAS enhances even further the network performance and yields to greater gains, but it also introduces a new level of complexity to the system which has to employ efficient algorithms in order to make fast and accurate decisions.

#### 2.4.2. VIRTUAL SECTORIZATION: LITERATURE OVERVIEW

Virtual Sectorization can be seen as a natural evolution of VS, but unlike VS, the new cell (virtual cell) can be located anywhere in the original cell's coverage area by setting a particular vertical (downtilt) and horizontal (azimuth) tilt. It is important to remark that no available literature on previous work related to ViS was found except for the results presented in [19] which were partially drawn from work carried out within the SEMAFOUR project and therefore constitute a basis for this thesis project.

In [19] the authors developed the ViS model and provide the guidelines for the design of a ViS capable AAS using a frequency bandwidth based resource sharing scheme. In order to mitigate interference between the virtual cell and the macro-cell, a Dynamic Spectrum Allocation (DSA) algorithm that self-optimizes the frequency bandwidth split between the two cells is also proposed. Similarly as in [21], they also explore the option of power sharing with full bandwidth reuse (bandwidth reuse one) and compare it to the performance of the bandwidth sharing scheme and the baseline scenario without ViS. The research was conducted by system level simulation of an ideal hexagonal LTE network consisting of three macro-cells, each with its corresponding virtual cell as shown in Figure 2.13, along with two rings of macro-cell interferers.

Two layers of traffic were superposed in this study. The first layer corresponds to the entire coverage area of the macro-cell and has a uniform arrival rate  $\lambda$  of users/s. The second layer is a traffic hotspot with a different arrival rate  $\lambda_h$  of users/s, located in the virtual cell coverage area. The antenna design and system modelling will be introduced in Chapter 4 of this document. The mean and cell-edge user throughput results as a function of time obtained in [19] are shown in Figure 2.14.

Deploying the ViS with bandwidth sharing is shown to provide the best performance during the whole simulation period for different load conditions as shown by both KPIs. Moreover, the bandwidth sharing enables the two cells (macro-cell and virtual cell) to serve their traffic without mutual interference and a better SINR compared to a ViS deployed with full bandwidth reuse. It is noted that the bandwidth reuse of

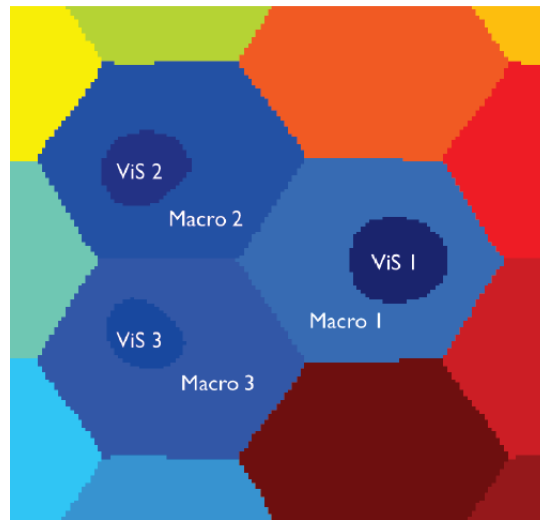


Figure 2.13: ViS Best Server Coverage Map [19]

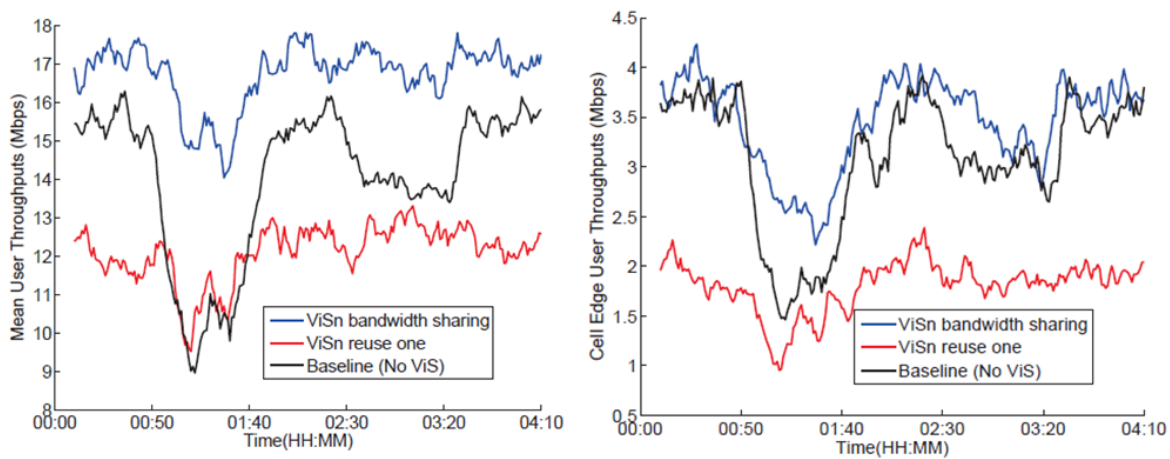


Figure 2.14: ViS Mean and Cell-edge UE Throughput Over Time [19]

one is expected to provide better performance when the loads approach 100% [19] as already demonstrated in [21]. During the time of higher traffic load (between 00:50 and 01:40) there is a gain of more than 50% in mean UE throughput between ViS with bandwidth sharing and the baseline scenario, which is an indication of the values that can be expected for the system level simulation of ViS under realistic network conditions.

ViS can be considered as a special case of VS because it employs the same approach of capturing a large number of users from an original cell by creating a new cell, hence, the literature study for both techniques serves as a basis to evaluate the expected gains and challenges for ViS. It is expected that ViS will have similar or larger gains than VS given the flexibility of positioning the virtual cell at any location within the original cell original coverage area, giving the possibility to attract a higher number of UEs and provide higher throughputs. Additionally, the performance of ViS is also dependent on the configuration of the virtual cell, i.e. vertical and horizontal tilt, resource sharing scheme and traffic profile.

The outcome from the literature study shows that ViS yields to substantial gains when deployed in a typical hexagonal network scenario using standard propagation models as defined by the 3GPP, but no prior work has been found on the performance analysis of ViS in a realistic network as the one modelled for the SEMAFOUR project and used to derive the results present in this thesis work.



# 3

## RESEARCH QUESTIONS AND MOTIVATION

The main motivation for the work on this thesis is to discover whether and to what degree an AAS technique such as ViS, in combination with a SON resource sharing algorithm, is a suitable solution to improve the capacity and performance of a realistic LTE network and therefore can be chosen as a densification strategy for operators.

This thesis will expand on the work done in [19] by implementing ViS in a realistic LTE network using real three-dimensional building data, a realistic traffic distribution, and applying advanced ray tracing modelling. An optimum tilt and azimuth configuration for the virtual cell will be found based on the realistic traffic profile in order for it to serve as many users as possible. Additionally, the impact of transmit power and bandwidth sharing will be thoroughly investigated at cell and network level when ViS is implemented in all the eNodeBs in the network with the presence of traffic hotspots in some selected cells. The resource sharing schemes will be tested using static bandwidth or transmit power allocations for the virtual cell and macro-cell and also using SON algorithms capable of updating the resource proportions dynamically as new calls arrive and depart from the network.

In order to guide the work of this thesis project, the goals presented in 1.1 have been redefined as a list of specific research questions. After answering these questions, the potential of self-optimized ViS for LTE and future mobile networks will become clear and its performance will be better assessed and understood.

The research questions formulated for this project are outlined as follows:

1. What is the impact on performance related to the configuration parameters of ViS?
  - (a) How do azimuth and tilt values of the virtual cell affect the performance of ViS?
  - (b) What are the performance effects of using a static transmit power or bandwidth sharing scheme between the virtual and macro-cell, compared to the case when ViS is not used?
  - (c) What is the impact on performance of the deployment strategy for ViS, e.g. ViS implemented in all cells, only the most loaded cells and only the most loaded single cell?
2. What is the impact on performance from ViS related to the deployment environment?
  - (a) How does the location of a traffic hotspot within a cell affect the performance of ViS?
  - (b) How does network load affect the performance of ViS?
3. What are the gains in capacity and performance when using ViS in combination with SON resource sharing algorithms?

- (a) What are the performance effects of using an adaptive transmit power- or bandwidth-based resource sharing SON scheme between the virtual and macro-cell, compared to the case when ViS is not used and to static resource sharing?
- (b) Which is the most suitable SON resource sharing algorithm for ViS, bandwidth sharing or transmit power sharing?

Answering these questions will give a comprehensive overview of the capabilities of ViS as a function of all the different control parameters (tilt, azimuth, transmit power and frequency bandwidth allocation) and network related parameters (deployment strategy, traffic distribution), as well as the performance of ViS when combined with a SON function. It is expected that ViS will improve performance in terms of capacity for LTE and future mobile networks and the results from this thesis will lay the grounds for new AAS-related research in the future.

# 4

## SYSTEM MODELLING AND SCENARIOS

This section presents the key modelling aspects for the downlink performance assessment of ViS in a realistic LTE network, as well as the traffic characteristics, propagation environment, and various simulation scenarios with their respective parameter configuration.

### 4.1. SYSTEM DESCRIPTION

A realistic network layout of outdoor sectorized LTE sites covering a  $5 \times 7 \text{ km}^2$  area in the city of Hannover, Germany is considered, as depicted in Figure 4.1.

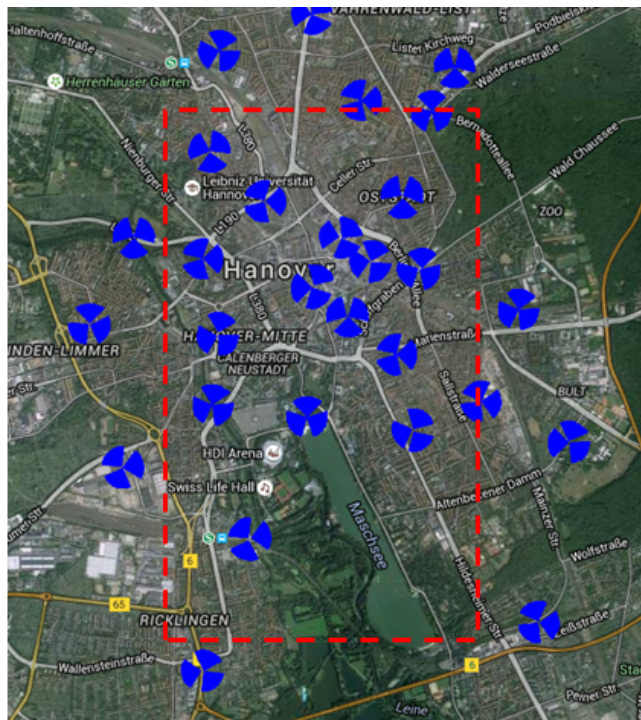


Figure 4.1: Hannover Realistic LTE Network Layout. (Background image: Google Maps)

The area covers both urban and a suburban areas. Although the entire network area (63 sites, 84 cells) is analyzed in the dynamic event driven system-level simulations, the performance statistics are collected only

in the indicated central area of  $3 \times 5 \text{ km}^2$  (36 sites, 51 cells) in order to minimize the impact of border effects in the simulation and to focus specifically in the central part of Hannover. From Figure 4.1 it is clear that most sites are tri-sectorized, however that is not the case since most of them are simply located very close to each other (e.g., at 3 edges of a rooftop). Each cell in the entire network area is equipped with an active antenna operating in the 1800 MHz frequency band using a 20 MHz bandwidth, with a maximum transmit power of 40 W (46 dBm) and capable of Virtual Sectorization.

The antenna model developed in [19] was used for the implementation of ViS in the system-level simulator. The antenna comprises a two-dimensional array with  $N_x \times N_z$  elementary vertical dipoles in front of a metallic planar rectangular reflector. The  $N_x$  and  $N_z$  elements in each row and column respectively are equally spaced with distances  $dx$  and  $dz$  as seen in Figure 4.2. For the purposes of the AAS use case, the ViS antenna array is set to have  $N_x=10$  and  $N_z=40$  elements, with dipole separations of  $dx=0.5\lambda$  and  $dz=0.6\lambda$  respectively,  $\lambda$  being the wavelength.

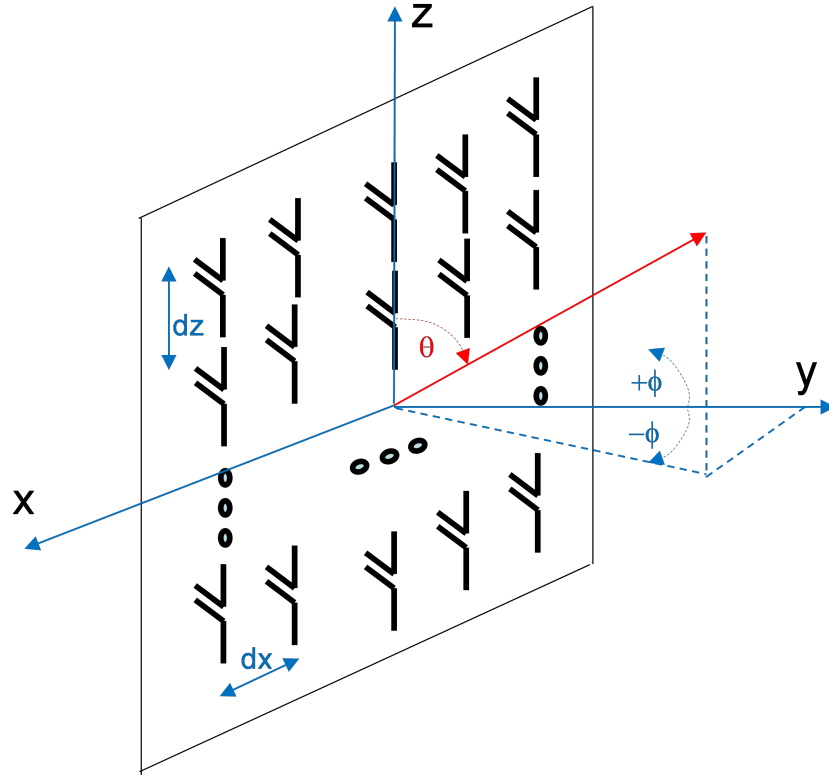


Figure 4.2: ViS antenna design [19]

$L_x$  and  $L_z$  denote the array size in the  $x$  and  $z$  directions respectively, with  $L_x = (N_x - 1)d_x$  and  $L_z = (N_z - 1)d_z$ . In order to generate a beam with a desired diagram, each antenna element is excited, e.g. by an amplifier, with a given complex amplitude. For example, the complex amplitude for a linear array of  $N_z$  vertical dipoles with maximum gain pattern pointing at  $\theta = \theta_e$  is given by [30]

$$\exp\left(j2\pi(n-1)\frac{d_z}{\lambda}\cos(\theta_e)\right); n = 1, \dots, N_z$$

To reduce the side lobe level, and consequently, the undesired interference, the dipole's excitation is tapered using Gaussian functions  $v_m$  and  $w_n$  for the  $m$ -th and  $n$ -th elements in a row and a column respectively:

$$w_m = \exp\left(-\left(\frac{(m-1)L_x - \frac{L_x}{2}}{\sigma_x}\right)^2\right)$$

$$v_n = \exp\left(-\left(\frac{(n-1)L_z - \frac{L_z}{2}}{\sigma_z}\right)^2\right)$$

The Gaussian tapering used for both the  $x$  and  $z$  axes is often used in signal processing to filter out high frequencies of a signal. In the case of antenna array, the middle (center) element of the array receives the maximum value of the Gaussian amplitude and the edge dipoles receive the minimum value. The values of  $\sigma_{x,z}$  are configured by fixing the ratio of the extreme and center dipole amplitude respectively to the value of  $\alpha_{x,z}$  (both of them set to 0.2 for the work in this thesis) so that

$$\sigma_s^2 = -\frac{L_s}{2\log(\alpha_s)}; s = x, z$$

Given these tapering functions, the antenna factor in the  $x$  direction is defined as:

$$AF_x(\theta, \theta_e, \phi, \phi_e) = \frac{1}{\sum_{m=1}^{N_x} w_m} \sum_{m=1}^{N_x} w_m \cdot a_m$$

with

$$a_m = \exp\left(-j2\pi(m-1)\frac{d_x}{\lambda}(\sin(\theta)\sin(\phi) - \sin(\theta_e)\sin(\phi_e))\right)$$

$\theta_e$  and  $\phi_e$  denote, for the remainder of this document, the electrical tilt angles pointing from the antenna array to the virtual cell as shown in Figure 4.2.

The antenna factor in the  $z$  direction is defined as:

$$AF_z(\theta, \theta_e) = \frac{1}{\sum_{n=1}^{N_z} v_n} \sum_{n=1}^{N_z} v_n \cdot b_n$$

with

$$b_n = \exp\left(-j2\pi(n-1)\frac{d_z}{\lambda}(\cos(\theta) - \cos(\theta_e))\right)$$

$a_m$  and  $b_n$  provide the phase contributions of an isotropic radiating element located at  $(m-1)d_x$  and  $(n-1)d_z$  in wavelengths, respectively, with a linear phase shift that generates a maximum beam in the direction of  $(\theta_e, \phi_e)$ . The antenna factor in the  $y$  direction, which accounts for the impact of the metallic reflector modelled as an infinite perfect electric conductor, is given by:

$$AF_y(\theta, \phi) = \sin\left(\frac{\pi}{2}\sin(\theta)\cos(\phi)\right)$$

The accuracy of the model for  $AF_y$ , namely of the image quality produced by the finite reflector size, has not been analyzed and is left for future studies. Since large reflector sizes (in terms of wavelengths) are considered, one could expect an impact of the finite reflector size mainly at edge elements. Combining the above expressions, the normalized antenna gain is given by

$$f(\theta, \phi) = \left| AF_x^2(\theta, \theta_e, \phi, \phi_e) \cdot AF_y^2(\theta, \phi) \cdot AF_z^2(\theta, \theta_e) \right| G_d(\theta)$$

Where  $G_d(\theta) = \sin(\theta)^3$  is the gain pattern normalized to one of a single dipole proposed by Kathrein [31]. One can expect coupling between adjacent dipoles. It is noted that in a practical antenna array, coupling

effects can be considerably reduced by introducing separators between the radiating elements [32], which makes the proposed model relevant. Finally, the antenna gain can be written as  $G(\theta, \phi) = G_0 f(\theta, \phi)$ , where the term  $G_0$  is obtained from the power conservation equation:

$$G_0 = \frac{4\pi}{\int_{-\pi/2}^{\pi/2} \int_0^\pi f(\theta, \phi) \sin(\theta) d\theta d\phi}$$

Figure 4.3 depicts the vertical (E-Plane) and horizontal (H-Plane) radiation patterns for the ViS antenna model with  $\theta_e = 110^\circ$  and  $\phi_e = 20^\circ$ .

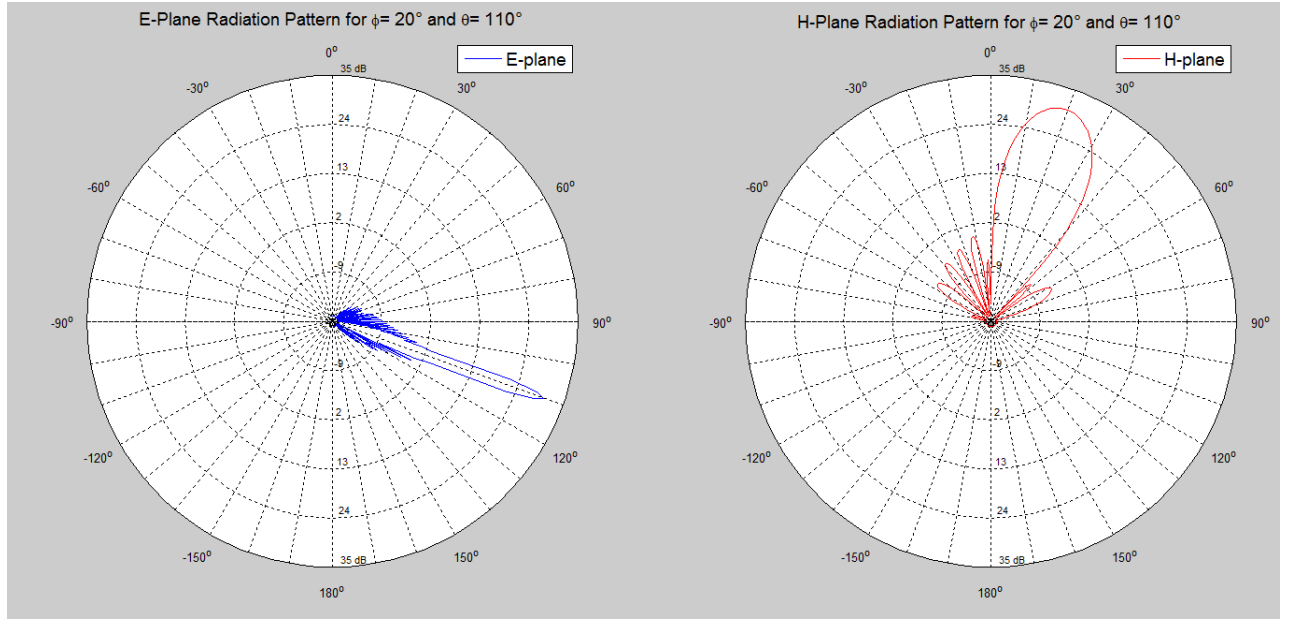


Figure 4.3: ViS antenna vertical plane (left) and horizontal plane (right) patterns

There are four main control parameters to configure ViS. These parameters have been chosen based on results presented in prior art [19] and are outlined as follows:

- **Virtual cell tilt:** It is expected that tilt will play a major role in performance optimization since it is one of the parameters that control the position of the virtual cell within the coverage area of the macro-cell. For the rest of this report the notation  $\theta_e$  will refer to the vertical tilt for the virtual cell in the spherical coordinate  $\theta$ , measured with reference to the sky's zenith. The values for this parameter are constrained to  $\theta_e < 120^\circ$  [19]. Finally, the electrical tilt of the virtual cell can be defined as  $\theta_{ViS} = \theta_e - 90^\circ$ , which is referenced to the horizon.
- **Virtual cell azimuth:** The second parameter that controls the location of the virtual cell within the coverage area of the macro-cell is the azimuth. The notation  $\phi_e$  will refer to the horizontal tilt of the virtual cell in the spherical coordinate  $\phi$ , measured relative to the original cell's azimuth denoted as  $\phi_o$ . The values for this parameter are constrained to  $|\phi_e| \leq 45^\circ$  [19]. For consistency, the rest of the document will refer to  $\phi_{ViS} = \phi_e$ . Note that the cell's tilt is expressed relative to the horizon while the cell's azimuth is relative to the macro-cell's azimuth.
- **Power per cell:** Power sharing is one of the resource sharing mechanisms proposed for using in combination with ViS. The total available transmit power  $P_T$  is shared between the macro-cell and the virtual cell, hence

$$P_T = P_m + P_v$$

With  $P_m$  and  $P_v$  being the power assigned to the macro-cell and the virtual cell respectively. Additionally, if the parameter  $\delta_{P_v}$  represents the fraction of the power that is assigned to the virtual cell, it is

derived that

$$P_v = \delta_{P_v} P_T$$

$$P_m = (1 - \delta_{P_v}) P_T$$

The parameter  $\delta_{P_v}$  can be configured as a fixed value in the simulations for all the cells in the network or can be controlled by a SON algorithm.

- **Bandwidth per cell:** Bandwidth sharing, similar to power sharing, has also been selected as a one of the resource allocation schemes for the evaluation of the performance of ViS. A similar approach as the one taken for power allocation can be taken to split the total available bandwidth,  $W$ , between the macro and the virtual cell, yielding to

$$W_v = \delta_{W_v} W$$

$$W_m = (1 - \delta_{W_v}) W$$

With  $\delta_{W_v}$  representing the fraction of the total bandwidth allocated to the virtual cell. Assuming a fixed and uniform, power density over the given bandwidth, the fraction of the bandwidth for the virtual cell is the same as the fraction of the power allocated to it, so that

$$\frac{P_v}{W_v} = \frac{\delta_{W_v} P_T}{W_v} = \frac{P_T}{W}$$

Hence

$$\frac{P_v}{P_T} = \frac{W_v}{W}$$

Meaning that not only the cells do not interfere with each other, but also the transmit power per Hertz remains unchanged, yielding to an improved SINR but impacting the data rate due to the reduced bandwidth.

The SINR of each user is modelled in the system-level simulator on a PRB level. This is useful specially for the case when bandwidth sharing is used, because it allows to easily take into account the interference from all the cells when each one has a different bandwidth allocation. Effective SINR Mapping (ESM) is used to translate the set of individual  $p$  SINRs per PRB into an effective SINR, denoted  $SINR_{eff}$ , as shown in Figure 4.4 and described in [33].

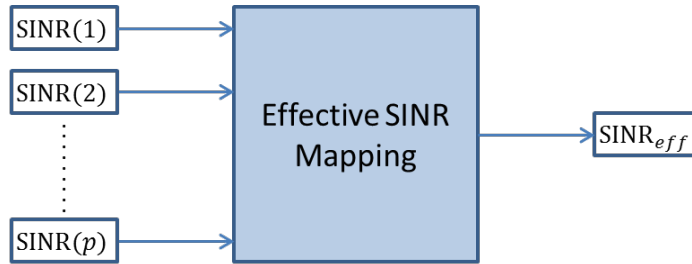


Figure 4.4: Effective SINR Mapping Schematic Flow-chart

Out of the proposed ESM functions in [33], Mutual Information Effective SINR Mapping (MI-ESM) is used to calculate the SINReff for each user in the system-level simulations. Mutual information is commonly used in information theory to describe the relationship between two variables that are sampled simultaneously. In particular, it indicates how much information is communicated in one variable about the other. In the context of MI-ESM, this should be seen as to what extent a received symbol provides information about the transmitted symbol. For high SINR (ideal channel) the mutual information is maximum and equal to the number of bits per symbol. For low SINR (no data transfer possible) the mutual information reduces to zero, i.e., the received symbol provides no information about the transmitted symbol. The  $SINR_{eff}$  is then given by:

$$SINR_{eff} = I_k^{-1} \left( \frac{1}{N} \sum_{i=1}^N I_k(SINR_i) \right)$$

where  $SINR_i$  is the SINR of PRB  $i$  and  $N$  is the number of assigned PRBs to the user in the considered bandwidth.  $I_k$  is the Bit-Interleaved Coded Modulation (BICM) capacity for the considered modulation order  $k$ . The function  $I_k$  translates each  $SINR_i$  into a mutual information measure as described thoroughly in [33] and depends on the modulation scheme used for transmission. For this thesis, the MI-ESM curve for the modulation order of 6 bits/symbol (64QAM) is used in the system-level simulations to calculate the  $SINR_{eff}$ , and the graph of  $I_k$  as a function of SINR is shown in Figure 4.5.

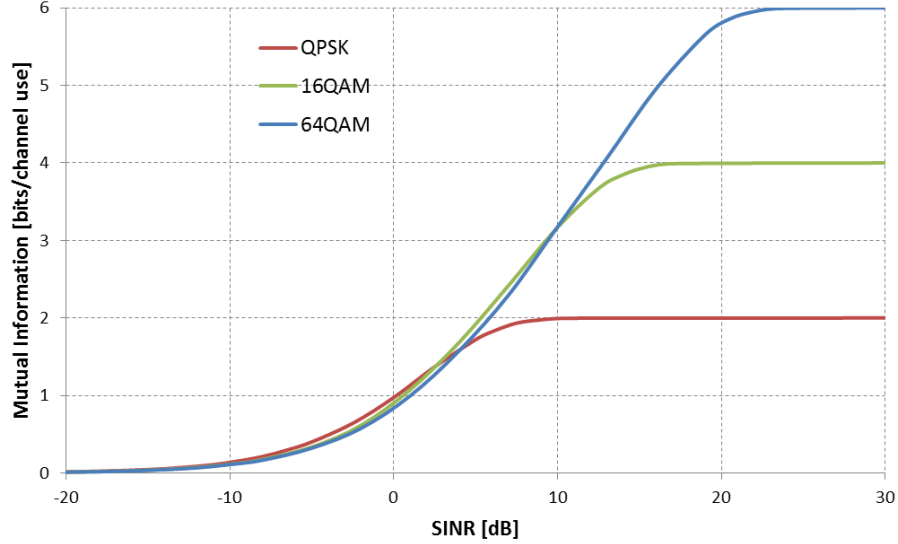


Figure 4.5: Mutual information as a function of SINR for 64QAM modulation in LTE

Thus, the MI-ESM function works as follows:

- The mutual information is computed per PRB, depending on the SINR for that PRB. For low SINR, the mutual information is zero, meaning that no useful information can be extracted for that PRB. For high SINR, the mutual information is equal to the number of bits per symbol for the given modulation order. This means that all the information in the symbol can be successfully transferred.
- The average mutual information is determined from all the PRBs assigned to the user.
- The  $SINR_{eff}$  is determined as the SINR that would yield the average mutual information calculated in the previous step, as if it was the mutual information applied on all PRBs.

When power sharing is used, the data rate  $R_u$  for a given user can be calculated, using the  $SINR_{eff}$ , with a modified Shannon capacity formula [21] given by

$$R_u = \eta W \min(4.4, 0.6 \log_2(1 + SINR_{eff}))$$

where  $W$  is the total available bandwidth and  $\eta$  is the proportion of the time that the user is scheduled by the eNodeB. The simulator uses a resource fair scheduler to allocate resources, hence, each user in the cell is scheduled with the same amount of time and resources. This proportion is updated in the simulator every time a new call arrives to the cell.

In the case of bandwidth sharing, the data rate  $R_u$  is given by

$$R_u = \delta_{Wv} \eta W \min(4.4, 0.6 \log_2(1 + SINR_{eff}))$$

As stated before, using the bandwidth sharing scheme yields to higher SINR experienced by the users but the reduced bandwidth allocated has its impact on the user data rate.

## 4.2. TRAFFIC CHARACTERISTICS

In order to realistically simulate large networks on a system level, appropriate knowledge on the distributions of user terminals and their requested or generated traffic is of importance. Moreover, these distributions tend to vary over time. A modified version of the traffic intensity map from the SEMAFOUR project as described in [5] was used. In concrete, two distinct traffic maps were generated, each one containing four artificially created hotspot zones in four cells located in Hannover's downtown. The traffic intensity in each hotspot is a scaled version of the total traffic in the hotspot area from the input traffic map. The scaling factor is uniform in the whole area of the hotspot and is denoted by the parameter  $\alpha$ . The hotspot traffic is added to the original traffic intensity map to generate a new modified traffic map as shown in Figure 4.6.

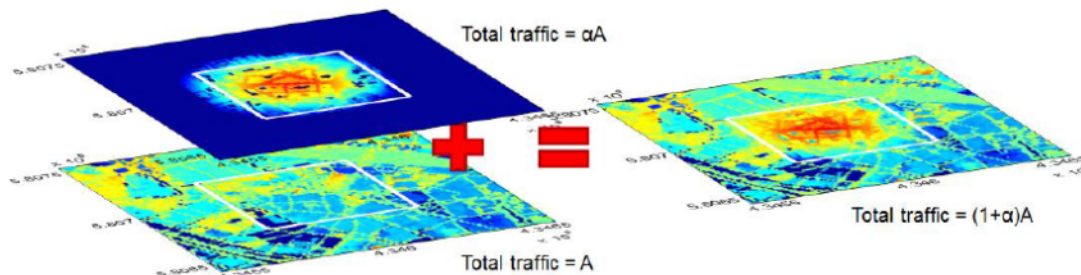


Figure 4.6: Traffic intensity map generation [5]

Locations close to and far from the eNodeBs were chosen for each of the four spots, yielding two traffic intensity maps. Hence, one traffic map with all four hotspots close to the eNodeBs and the other one with all four hotspots far from the eNodeBs. The location, size and shape of the four hotspots for each traffic intensity map is shown in the Hannover baseline (No ViS) Best Server Area (BSA) coverage plots from Figure 4.7 as white rectangles along with the cell ID for each cell where they are located.

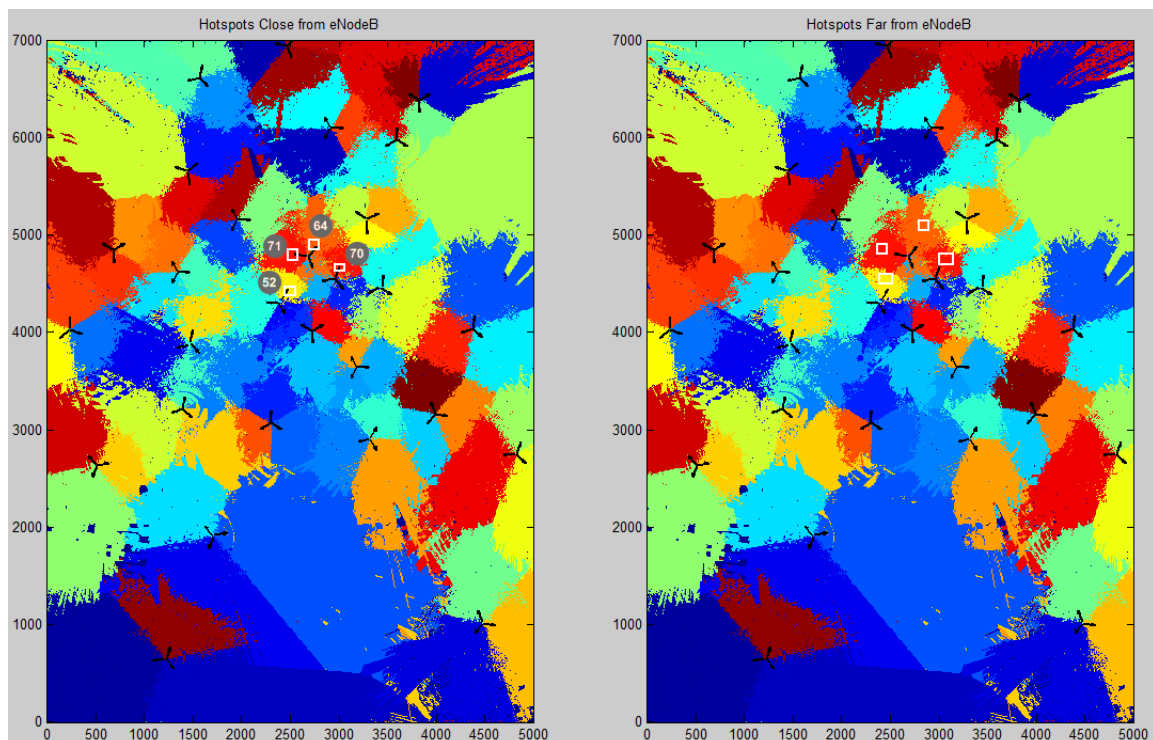


Figure 4.7: Hannover BSA with hotspot locations

Each color in the BSA map corresponds to the predicted coverage area of a cell in the network and any UE in that area will be served by the corresponding cell. These maps can be overlapped to the Hannover map

shown in Figure 4.1 to predict which areas of the city are covered by any given cell.

The values used for the traffic scaling factor  $\alpha$  for all the hotspots (close and far from the eNodeBs) are listed in Table 4.1. The values of  $\alpha$  were chosen by testing different values in simulations in order to achieve a high utilization (cell load) in the cell where the hotspot is present, since it is known from available literature that ViS performs best under these load conditions.

Table 4.1: Hotspot traffic intensity factor  $\alpha$

	Close to eNodeB	Far from eNodeB
Cell ID	$\alpha$	$\alpha$
52	1.2	1.2
64	7	6
70	8	7
71	14	13

The four aforementioned cells were selected because they are located in the downtown area of Hannover, the zone with highest traffic intensity in the city. Finally, the resultant traffic intensity map for the area of the selected cells, including hotspots, are depicted in Figure 4.8. These traffic maps are used for all the simulation scenarios and results analysis of this thesis work.

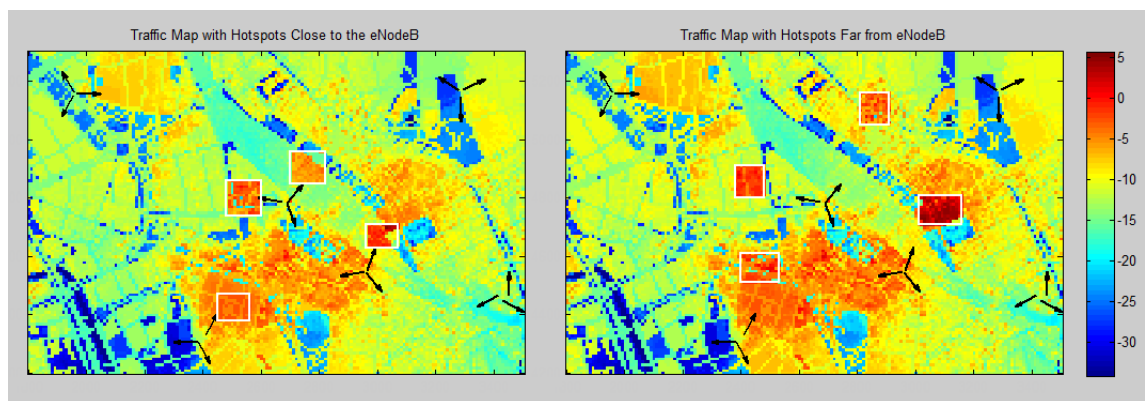


Figure 4.8: Traffic intensity maps with different hotspot locations

The traffic generation process generates calls throughout the simulation using an exponential distribution and ensures that the traffic concentration is according to the modified traffic intensity map. The call arrival process in the simulator is based on the probability of calls arriving at a specific location in the simulated area, which is calculated from the traffic intensity map. The traffic simulated is data traffic and the file size of each data call to be completed is selected, for this thesis, in a deterministic way with a fixed file size of 16 MB. The modified traffic intensity map corresponds to a relative weight value per pixel per hour for the selected Hannover area. Every hour the corresponding intensity map is read in and from that, a call arrival rate per hour, denoted as  $\lambda(h)$ , value is generated which is used as input to the exponential distribution that the call arrival process is using. The call arrival rate is given by

$$\lambda(h) = \lambda \sum w_{ij}$$

where  $\lambda$  is a lambda scaling factor used in the simulator to vary the arrival rate and hence the load in the network, and  $w_{ij}$  is

$$T_i = -\frac{1}{\lambda(h)} \times \ln(1 - \text{random})$$

Meaning that the higher the arrival rate, the smaller will be the call inter-arrival time ( $T_i$ ) and the system will experience higher loads. Finally, the probability  $P_{ij}$  that a call will be generated in a pixel with coordinates  $(i, j)$  is

$$P_{ij} = \frac{w_{ij}}{\sum w_{ij}}$$

These equations imply that the call generation process depends on the total traffic intensity and that each pixel gets calls assigned according to its individual traffic weight. Once a call has been generated in the system, a serving eNodeB is assigned to it based on the best Reference Signal Received Power (RSRP) and admission control is performed for that call in that eNodeB based on the number of concurrent calls already being served by that eNodeB.

### 4.3. PROPAGATION MODELS

The propagation models used for the simulations are the same as previously used for the SEMAFOUR project and are fully described in [5]. Since three-dimensional building information has been accessible for the city of Hannover, a ray tracing model has been used to predict the outdoor coverage of the cells in this scenario. This predictor looks for the ray optical propagation paths between the transmitter and the receiver antennas by employing a Vertical Plane Model (VPM) and a Multi-Path Model (MPM) [34]. This means that each pixel in the grid will have a set of rays coming from the transmitter antenna with a corresponding individual pathloss. The visual representation of the model is shown in Figure 4.9.

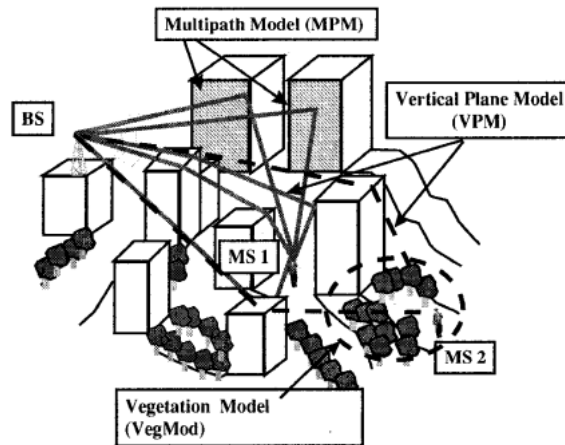


Figure 4.9: Propagation model representation [34]

The VPM is used to calculate the pathloss for both Line-of-Sight (LOS) and non-LOS (NLOS) cases. It uses a combination of free-space propagation loss and Okumura-Hata model depending on the distance between transmitter and receiver. The MPM is used to account for the different paths from transmitter to receiver. It considers reflected paths up to the second reflection, and scattered paths up to a maximum distance of 500 m between transmitter and receiver.

To predict the path loss for indoor areas, i.e. inside buildings, a “Ground Outdoor-to-Indoor” approach [35] has been used. It is assumed that the path loss inside a building is directly related to the path loss outside of it. The outdoor coverage outside the building and at ground level (1.5 m) is predicted and used as a reference. An outer wall attenuation is then considered when going from outdoor to indoor coverage. A value of 10 dB was chosen as the outer wall attenuation, as used for the SEMAFOUR project. Coverage for upper floors is calculated by adding a floor gain as described in [35]. Afterwards, a linear attenuation of 0.8 dB/m is added to the pathloss to account for the distance between the indoor position and the outer wall, i.e. outdoor reference points. For each indoor position there are different propagation paths coming from the reference outdoor points. The set of received signal levels from all the paths is compared and the one with

the maximum value is selected as the indoor signal strength.

#### 4.4. SIMULATION SCENARIOS

ViS is implemented in each site of the network to evaluate its impact on performance. The baseline network layout used is the original configuration of the sites in Hannover in which all cells have an electrical tilt of  $0^\circ$  and mechanical tilt of  $4^\circ$ . After ViS the virtual cell will inherit attributes from the macro-cell except for the electrical and mechanical tilts, azimuth, antenna model, and Cell ID. The mechanical tilt for the virtual cell is, in all cases,  $0^\circ$  because at this time we consider that the virtual cell is created by a separate antenna array.

Bandwidth and transmit power sharing schemes are implemented in the network separately and for each traffic map when ViS is used in each site of the network. Different fixed proportions of bandwidth or transmit power are allocated to the virtual cell in order to evaluate the network-wide gains coming from ViS when compared to the case with no ViS. Additionally, as stated in 4.2 and shown in Figure 4.7, four traffic hotspots are created in four different cells in the Hannover downtown area. The performance of these cells is further analyzed to investigate the cell-level gains of ViS when a hotspot is present. The details of the selected cells are presented in Table 4.2.

Table 4.2: Cells with traffic hotspots

Cell ID	X Coordinate	Y Coordinate	Azimuth
52	2409	4333	$30^\circ$
64	2690	4784	$40^\circ$
70	2964	4553	$20^\circ$
71	2675	4787	$280^\circ$

The electrical downtilt  $\theta_{ViS}$  and azimuth  $\phi_{ViS}$  for each virtual cell are configured based on the total traffic intensity per pixel that would be captured by the cell's coverage area. The possible values for  $\theta_{ViS}$  and  $\phi_{ViS}$  considered for this work are outlined in Table 4.3, out of which a configuration pair  $\{\theta_{ViS}, \phi_{ViS}\}$  is selected for each virtual cell.

Table 4.3: Possible values for configuration parameters

Parameter	Values
$\theta_{ViS}$	$[0, 1, 2, 3, \dots, 11]^\circ$
$\phi_{ViS}$	$[-45, -40, \dots, 0, \dots, 40, 45]^\circ$

A BSA coverage map was created for each possible configuration pair, yielding to 228 different coverage maps. Using a MATLAB script, each coverage map was overlaid on each traffic map and the total traffic intensity per pixel for all virtual cells was calculated. For each individual virtual cell the configuration pair yielding to the highest total traffic intensity per pixel was then selected as its optimum configuration. From the literature available there is an indication that the benefits of ViS (and VS) are greater when more users are served by the virtual cell, hence the decision for finding the optimum configuration through this method. Figure 4.10 shows the results obtained for the virtual cell with ID 148 after using the procedure on the traffic map with hotspots located far from the eNodeB. This cell was selected for this example because its corresponding macro-cell is cell 52, one of the cells where a hotspot is located. For this particular virtual cell, the optimum configuration pair is  $\{\theta_{ViS}, \phi_{ViS}\} = \{6^\circ, -10^\circ\}$ .

The final virtual cell configuration for all the cells and for each traffic map can be found in Appendix A.

In order to test the impact on performance of the frequency sharing scheme and transmit power sharing scheme, the network is simulated when ViS is implemented in: all the cells in the network, only the four cells with hotspots (most loaded cells in the network) and a single cell in the network (the most loaded cell). The

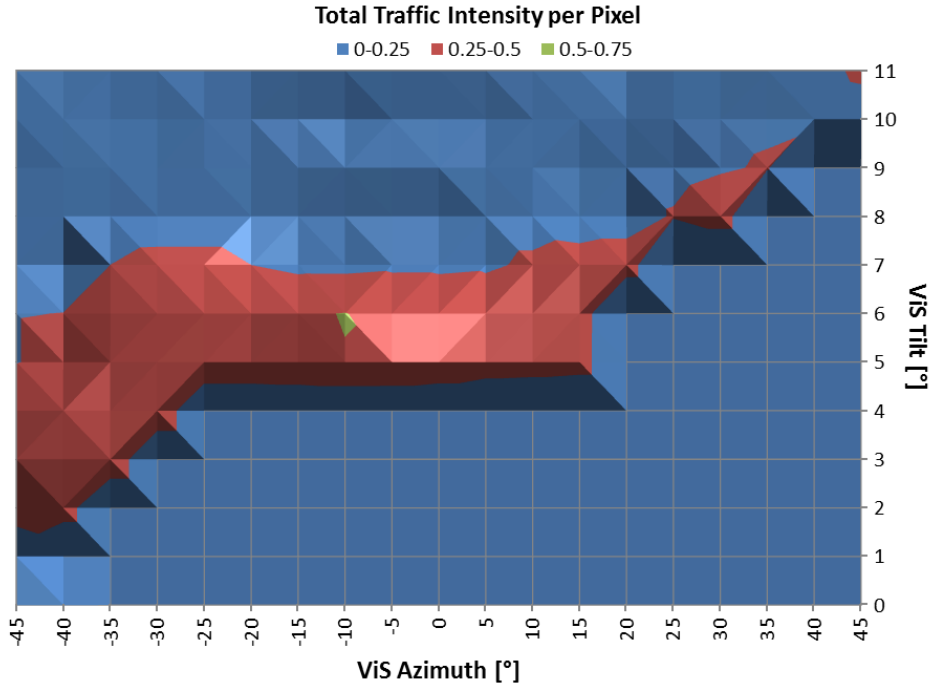


Figure 4.10: Optimum ViS configuration for cell 148

optimum tilt and azimuth configuration for each cell is used for simulations with fixed values of  $\delta_{Wv}$  and  $\delta_{Pv}$  and for each traffic map. The values used for the  $\delta_{Wv}$  and  $\delta_{Pv}$  control parameters are shown in Table 4.4.

Table 4.4:  $\delta_{Wv}$  and  $\delta_{Pv}$  fixed values for simulations

Parameter	Values
$\delta_{Wv}$	[10%, 20%, 30%, ..., 90%]
$\delta_{Pv}$	[10%, 20%, 30%, ..., 90%]

The combination of resource sharing schemes and hotspot locations yields to a total of four simulation scenarios, as shown in Table 4.5, per deployment strategy. This amounts to a total of twelve distinct scenarios, each of which contains nine simulations (one per each fixed resource allocated fraction). An offered load of  $45.6 \text{ Mbps}/\text{km}^2$  was used for the simulations with hotspots close to the eNodeB and  $47.8 \text{ Mbps}/\text{km}^2$  for the scenario with hotspots far from the eNodeB because these load values bring the network close to its maximum capacity.

Table 4.5: ViS simulation scenarios

Hotspots Close to eNodeB	Hotspots Far from eNodeB
BW Sharing	BW Sharing
Transmit Power Sharing	Transmit Power Sharing

The average user throughput and 10th percentile user throughput are the main KPIs used to measure the performance gain of ViS and are collected for all the users within the statistics area (network-wide) presented in 4.1 and also at aggregate cell-specific (macro-cell plus virtual cell) level.



# 5

## VIS STATIC RESOURCE SHARING PERFORMANCE

The goal of this chapter is to present the results of the C&O study on the impact on the performance and capacity of ViS at network-wide level and area-specific level when using frequency bandwidth and transmit power sharing schemes. By modifying  $\delta_{Wv}$  or  $\delta_{Pv}$ , the system resources are shared between the virtual cell and the macro-cell in different proportions. The purpose of the C&O study presented in this chapter is to assess whether using static resource allocations yields to gains in performance and capacity when compared to the case when ViS is not used and, if so, what is the static value for  $\delta_{Wv}$  or  $\delta_{Pv}$  that will maximize the gain on network and area-specific level. The simulation scenarios for this study were previously outlined in 4.4.

As described in 4.1, a virtual cell is created for each cell in the baseline Hannover network. The optimum configuration pair  $\{\theta_{Vis}, \phi_{Vis}\}$  for each virtual cell is selected by choosing a pair for which the virtual cell captures the maximum total traffic intensity for a given traffic map. Hence, an optimal configuration is found specifically for each traffic map. The procedure to find the optimum configuration was presented in 4.4 and consists of testing a wide range of possible combinations of azimuth and electrical tilt for each virtual cell in order to find a configuration that captures as much traffic as possible. The final BSA map for the downtown area of Hannover when using the optimum ViS configuration for all the cells in the network is shown in Figure 5.1.

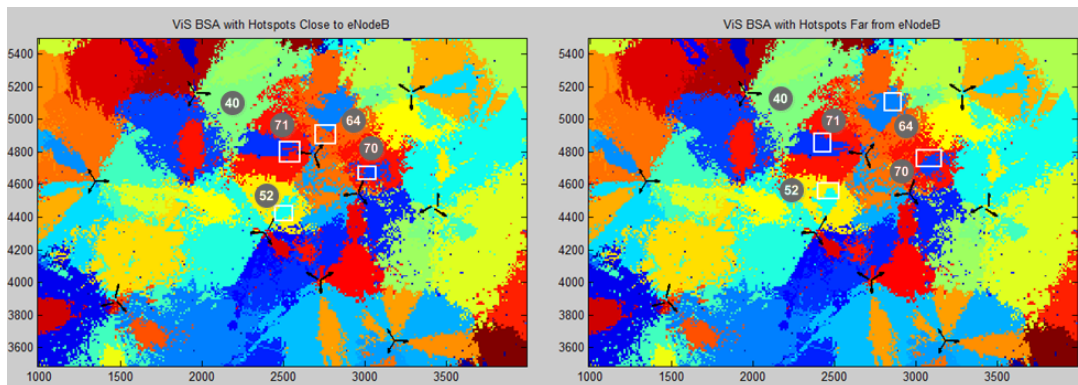


Figure 5.1: Downtown Hannover BSA maps with ViS configuration optimized for each cell according to hotspot location

The main KPIs used to evaluate the impact on throughput performance of ViS are the network-wide level (aggregated user statistics over all the cells of the network) and cell-specific level (aggregated user statistics of a specific cell, including the users of both the macro-cell and the associated virtual cell, when deployed) average throughput and 10th user throughput percentile. The cell-specific throughput results presented throughout this Chapter when analyzing the impact of different static resource allocations correspond to the *most*

*loaded cell* of the network, i.e. the cell with highest utilization, before ViS was implemented. This most loaded cell was cell 52 for all the scenarios and its location is shown in Figure 5.1. In order to test the impact of the different percentages of resources allocated to the virtual cell, simulations were performed using a high load in the network. For all the scenarios with the hotspots close to the eNodeB the average offered load in the system was  $45.6 \text{ Mbps/km}^2$ , while the offered load in all the simulations with hotspots far from the eNodeB was  $47.8 \text{ Mbps/km}^2$ .

Taking the results from the static resource allocation studies under high loading conditions as a starting point, a *best static resource allocation configuration* for each scenario is determined by looking at the 10th user throughput percentile performance (cell-edge performance) of the *bottleneck cell* in the network. This cell is defined as the cell with the lowest 10th user throughput percentile in the entire network for each static resource allocation, hence separately for bandwidth (BW) and power (PW) sharing and specifically for each considered resource split. Once the bottleneck cell is determined for each resource allocation, the best static resource allocation configuration is the one with the maximum 10th user throughput percentile in the bottleneck cell. This best static resource allocation is used then to simulate each of the scenarios under different loading conditions to investigate the capacity gains of ViS and to observe the behavior of each resource sharing scheme as a function of offered load. The capacity of the network is defined as the maximum offered load that can be served by the bottleneck cell before its 10th user throughput percentile drops below a threshold of 2 Mbps, a typical value used by mobile operators. It is important to highlight, for clarity, that the *most loaded cell* is the cell that is busy with transmissions most of the time during the entire simulation time, while the *bottleneck cell* is the cell with the lowest 10th user throughput percentile throughput in the entire network. These two are not necessarily the same cell because the most loaded cell is the one that remains busiest during the entire simulation (e.g. always serving users) while the bottleneck cell could be a different cell with the worst 10th user throughput percentile throughput, which can be a consequence of bad propagation conditions for instance.

This Chapter is divided in three main sections corresponding to the ViS deployment strategies mentioned in the scenarios description in 4.4. First the results of implementing ViS in all the cells in the network for both traffic maps and for both fixed resource allocation schemes are presented, followed by the results for the case when ViS is implemented in the four cells containing hotspots and moving on to the case when only the most loaded cell in the network is virtually sectorized. All the results for the traffic map with hotspots located near the eNodeBs are presented in this chapter, while results for the traffic map with hotspots far from the eNodeBs are only presented in the case when ViS is implemented in all the cells in the network and for the other two cases the results can be found in Appendix B.

## 5.1. ViS DEPLOYED IN ALL CELLS IN THE NETWORK

The performance of ViS has been evaluated for the case when all the cells in the network are virtually sectorized with the optimum configuration corresponding to the traffic density map with hotspots close and far from the eNodeB. In the following figures, the graphs on the left hand side of the page show the network-wide performance for each resource sharing scheme while the graphs on the right hand side present the cell-specific (most loaded cell in the network) performance results for each resource scheme. The graphs on the top of the figure correspond to the results of using the BW sharing scheme while the graphs on the bottom present the PW sharing scheme simulation results. The  $x$  axes in each graph represents the static resource percentage allocated to the virtual cell while the primary (left)  $y$  axes is used for throughput in Mbps and the secondary (right)  $y$  axes is used to represent the gain of using ViS over the case without ViS, labelled as No ViS in all the plots and represented by a horizontal line for each throughput KPI.

The results for the baseline scenario without ViS and for the cases when ViS is active with different static bandwidth and transmit power allocations for the traffic map with hotspots close to the eNodeB are shown in Figure 5.2. From the top-left graph it can be observed that using ViS with *static BW* is never beneficial based on the network-wide KPIs and always leads to performance degradation when compared to the No ViS case. When all the cells in the network are virtually sectorized using static BW sharing, all the virtual cells will interfere with each other in their allocated bandwidth and the same happens for the macro cells, so, for each cell the number of interferer cells is the same as for the No ViS scenario but the number of served users per cell will be lower, hence the number of interferer users is lower, and an improvement in SINR is

expected. In addition, the users in the virtual cell experience higher signal strengths as a result of the focused beam produced by the proposed antenna array. When more bandwidth is allocated to the macro users (small  $\delta_{Wv}$ ) the aggregated statistics never reach or exceed the baseline performance because the users in the virtual cells are being served with very little bandwidth and they amount to a high number (since every cell in the network is virtually sectorized). When more bandwidth is assigned to the virtual cells (large  $\delta_{Wv}$ ), the users in the virtual cells experience very high throughputs while the users in the macro-cells are starved in bandwidth resources. This increases the average user throughput but gives a clear poor performance on the 10th user throughput percentile. When the bandwidth allocated to the virtual cell is  $\delta_{Wv}=30\%$  (low-medium range of  $\delta_{Wv}$ ), the users in both macro and virtual cells are starved in bandwidth resources. The BW allocated to either cell is not sufficient to serve its users with good performance, resulting in a dip in average throughput. The combination of the effects described for the three aforementioned cases (small, medium and large  $\delta_{Wv}$ ) yields a V-shaped average throughput curve.

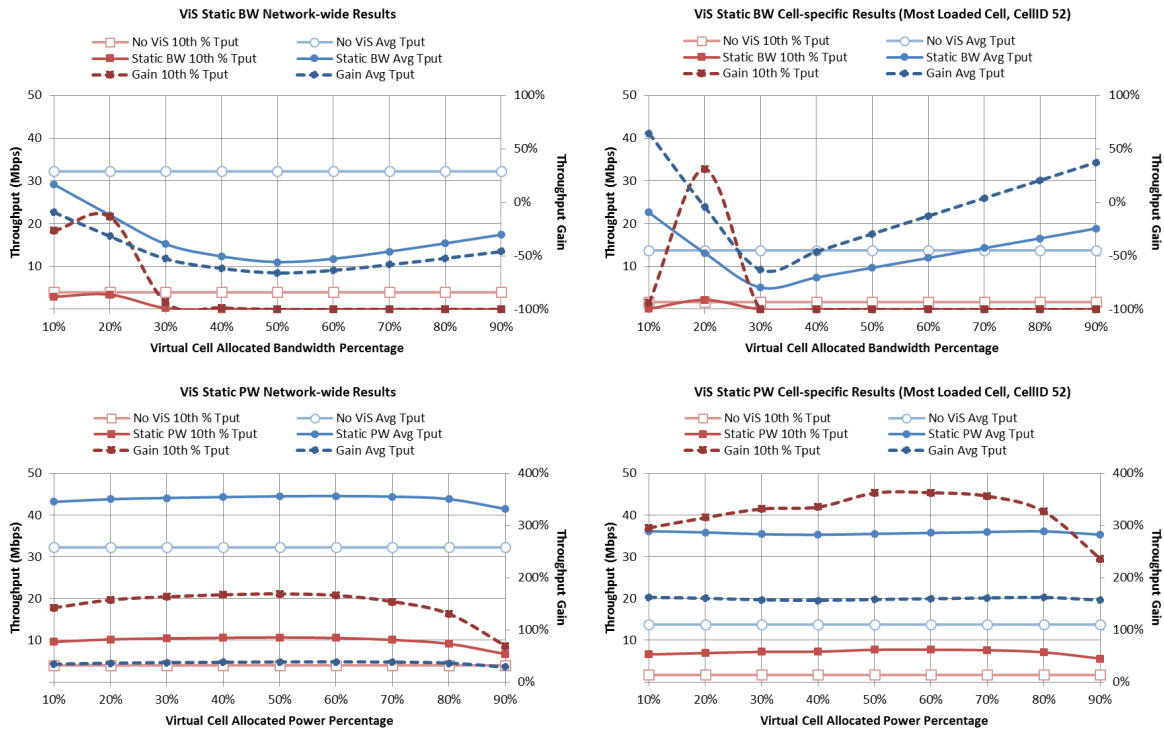


Figure 5.2: ViS in all cells: average throughput and 10th user throughput percentile results with hotspots close to the eNodeBs

On a cell-specific level (top-right graph), it can be observed that the most loaded cell follows the same behavior as the network performance. In this case it is important to notice how the cell average throughput is the highest with  $\delta_{Wv}=10\%$ , meaning that in this case the users in the macro-cell experience medium to high throughputs, however, the users on the virtual cell experience low throughputs and the number of these users is enough to lower the 10th user throughput percentile. When  $\delta_{Wv}=20\%$  the users in the virtual cell are served with enough bandwidth and they benefit from the gain of the antenna array, this leads to the 10th user throughput percentile gains. However, this allocation means that the bandwidth resources of the macro-cell are lowered, which leads to losses in the aggregated average throughput of the cell. From the top-right graph it is observed that there is a crossing point between the two dotted lines before  $\delta_{Wv}=20\%$  in which both KPIs are improved for this specific cell, meaning that there is a value for  $\delta_{Wv}$  that creates a good balance between the bandwidth allocated to the virtual and macro-cells and the number of users that benefit from the allocation in each cell.

Moving to the bottom part of Figure 5.2, it is easily observed that using *static PW* allocations always leads to performance gains for both network-wide and cell-specific KPIs compared to the No ViS baseline. It is noted that in the range  $\delta_{Pv}=[10\%-70\%]$  the overall performance does not change much for different alloca-

tions of transmission power per cell. The larger the amount of power assigned to the macro-cells (small to medium  $\delta_{pv}$ ), the lower the interference between neighboring cells. The majority of the cells will be transmitting at a slightly reduced power when compared with the No ViS case (macro-cells) and the users in the virtual cells will be served with a very low power such that the interference from these users to the neighboring cells is almost negligible, the combination of these effects leads to a slight improvement in SINR. When assigning more power to the virtual cells (large  $\delta_{pv}$ ) most of the users in the network are served with very low power (users in macro-cells) and the overall interference is very small, however, so is the overall Received Signal Strength (RSS). This effect, as for the cases with smaller, returns a slight improvement in SINR, but the gains are visibly smaller. In addition to the aforementioned SINR improvements, *using static PW split means that the bandwidth resources are doubled and fewer users share the same amount of bandwidth than in the No ViS case, which is the main reason for the high gains observed when using in this resource scheme over the static BW split.* An in-depth analysis of the effects of extreme PW allocations is shown in 5.1.1 to further understand the mechanisms behind this resource allocation scheme. It is important to highlight that the high gains observed in this scenario come primarily from the fact that the performance of the No ViS case is very poor at a high load (the network was already in a congested state) and the throughputs achieved with ViS are then compared to very small throughputs.

As already stated in the introduction to this chapter, a best configuration for each static resource allocation scheme is determined based on the 10th user throughput percentile results of the bottleneck cells for the simulations at high load. Table 5.1 shows the results for the bottleneck cells for each resource allocation scheme.

Table 5.1: ViS in All Cells: Bottleneck cells for each static resource allocation for the case with hotspots close to eNodeBs

Resource Allocation	Static BW		Static PW	
	Cell ID	10th User Throughput [Mbps]	Cell ID	10th User Throughput [Mbps]
No ViS	40	680	40	680
10%	70	70	40	4550
20%	<b>40</b>	<b>1300</b>	40	5400
30%	40	0	40	5960
40%	31	0	<b>40</b>	<b>6250</b>
50%	12	0	62	6100
60%	11	0	40	5910
70%	8	0	40	5580
80%	8	0	40	4950
90%	8	0	40	3310

For the case of static BW sharing the best allocation is  $\delta_{Wv}=20\%$  and for PW sharing is  $\delta_{pv}=40\%$ , in both cases the bottleneck cell is cell 40, same cell as for the No ViS case. The location of the cell can be seen in the BSA map shown in Figure 5.1. The impact of offered load in the network and in the bottleneck cell is addressed by simulating the best static configurations using the loads presented in Table 5.2. These offered loads will be used in all the subsequent sections of this chapter for all the simulations related to the scenario with hotspots close to the eNodeB.

Table 5.2: Load values for the case with hotspots close to the eNodeB

Offered Load [ $Mbps/km^2$ ]
[26, 33, 39, 46, 52, 59]

In Figure 5.3 the graphs on the left hand side of the page show the network-wide performance for each best static resource sharing allocation while the graphs on the right hand side present the cell-specific (cell 40, the bottleneck cell) performance results for each resource scheme. The graphs on the top of the figure correspond to the results of using the BW sharing scheme while the graphs on the bottom present the PW

sharing scheme simulation results. The x axes in each graph represents offered load in  $Mbps/km^2$  while the y axes is used for throughput in Mbps.

From the top-left part of Figure 5.3 it can be seen that there are no *network-wide* gains from using an *static* BW sharing allocation of  $\delta_{WV}=20$  in all the cells of the network. The static configuration performs the worst at lower loads, where the difference to the No ViS scenario is greater. At low loads less users benefit from the percentage allocated to the virtual cell and most of the users (served by the macro-cells) have less bandwidth resources. As the offered load increases the throughput in both curves decreases due to the high interference and the resource sharing between more users. At higher loads more users will benefit from the resources allocated to the virtual cell, which is the reason why the ViS curves slowly tend to the No ViS scenario. The behavior of the *bottleneck cell* follows the same trend as the network-wide performance, however, in this case there is a crossing point in the average throughput curve in which using ViS with the static BW configuration returns some visible gains. This crossing point suggests that the performance of ViS using BW sharing is dependent on the number of users benefited by the virtual cell and the fact that some gains have been observed at higher loads with the static allocation indicate that even higher gains can be obtained when the BW of the virtual cell is dynamically matched with the proportion of users it is serving. The capacity of the No ViS case is  $43.6 Mbps/km^2$  when the bottleneck cell's 10th user throughput percentile reaches the 2 Mbps threshold, as described in the introduction to this chapter. For the scenario with ViS using the best static BW allocation the capacity is  $45 Mbps/km^2$ , which represents a 3% capacity gain over the reference scenario. Although there is a small capacity gain for this case, it is important to highlight that deploying this configuration in a low load situation will harm the overall performance of the cell and the network. This result highlights the potential of using SON able to adapt the resource sharing according to the cell load.

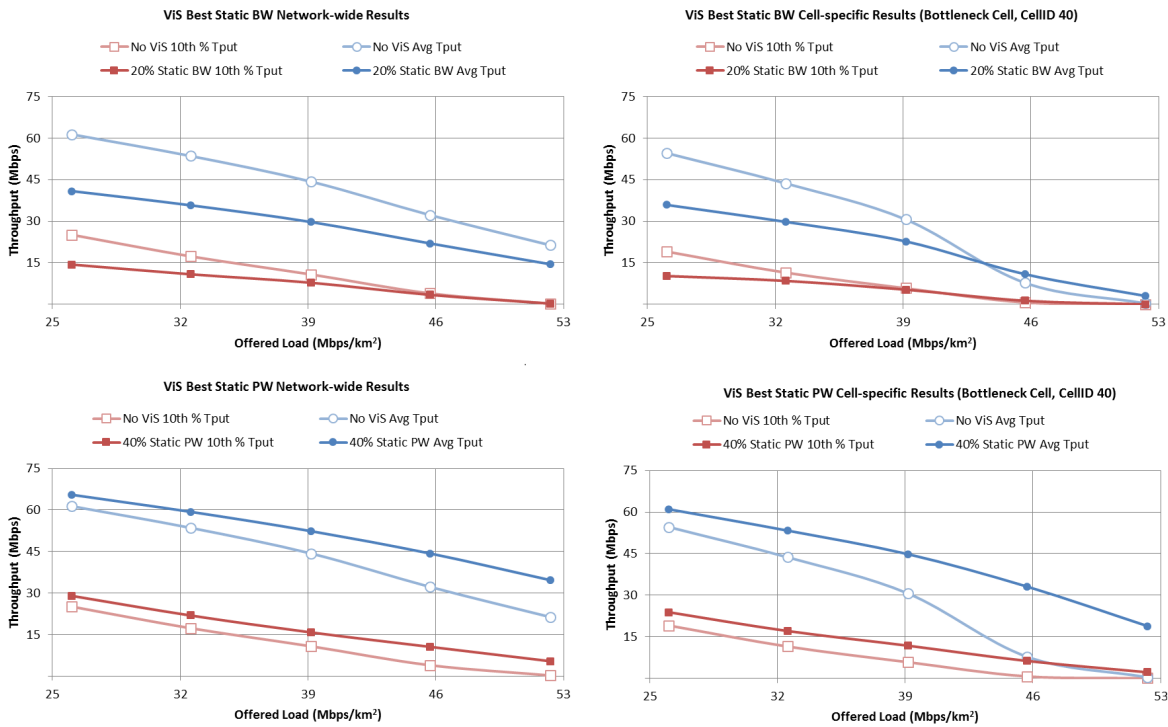


Figure 5.3: ViS in all cells: Bottleneck cell results with hotspots close to the eNodeBs

From the top-left part of Figure 5.3 it can be seen that there are no *network-wide* gains from using an *static* BW sharing allocation of  $\delta_{WV}=20$  in all the cells of the network. The static configuration performs the worst at lower loads, where the difference to the No ViS scenario is greater. At low loads less users benefit from the percentage allocated to the virtual cell and most of the users (served by the macro-cells) have less bandwidth resources. As the offered load increases the throughput in both curves decreases due to the high interference and the resource sharing between more users. At higher loads more users will benefit from the resources allocated to the virtual cell, which is the reason why the ViS curves slowly tend to the No ViS scenario. The

behavior of the *bottleneck cell* follows the same trend as the network-wide performance, however, in this case there is a crossing point in the average throughput curve in which using ViS with the static BW configuration returns some visible gains. This crossing point suggests that the performance of ViS using BW sharing is dependent on the number of users benefited by the virtual cell and the fact that some gains have been observed at higher loads with the static allocation indicate that even higher gains can be obtained when the BW of the virtual cell is dynamically matched with the proportion of users it is serving. The capacity of the No ViS case is  $43.6 \text{ Mbps/km}^2$  when the bottleneck cell's 10th user throughput percentile reaches the 2 Mbps threshold, as described in the introduction to this chapter. For the scenario with ViS using the best static BW allocation the capacity is  $45 \text{ Mbps/km}^2$ , which represents a 3% capacity gain over the reference scenario. Although there is a small capacity gain for this case, it is important to highlight that deploying this configuration in a low load situation will harm the overall performance of the cell and the network. This result highlights the potential of using SON able to adapt the resource sharing according to the cell load.

The bottom graphs in Figure 5.3 show that using  $\delta_{P_V}=40\%$  as the *static PW* allocation in this scenario yields throughput gains in the whole offered load range, with the gains increasing for higher loads, especially in the bottleneck cell. By focusing in the bottleneck cell it is observed that as the offered load increases the No ViS curve reaches a congestion state faster and both throughput KPIs decay to low levels, while the ViS scenario with static PW sharing congests only with a very high load. This is because at high loads, the users in the bottleneck cell experience better interference conditions when compared to the No ViS case because the majority of the users in the neighboring cells (macro-cell users) are being served with 60% of the total available power and the interference from the virtual cell users is even smaller because of the  $\delta_{P_V}=40\%$  allocated to them. Although the RSS of each cell is also reduced, a slight improvement in SINR is achieved, which is combined with the bigger impact from the fact that less users are now sharing the entire available bandwidth because of the doubling of resources. The capacity when using ViS with the static PW allocation is  $53.2 \text{ Mbps/km}^2$ , this implies a 22% capacity gain over the reference scenario without ViS.

The results obtained for the traffic map with hotspots far from the eNodeB are shown in Figure 5.4.

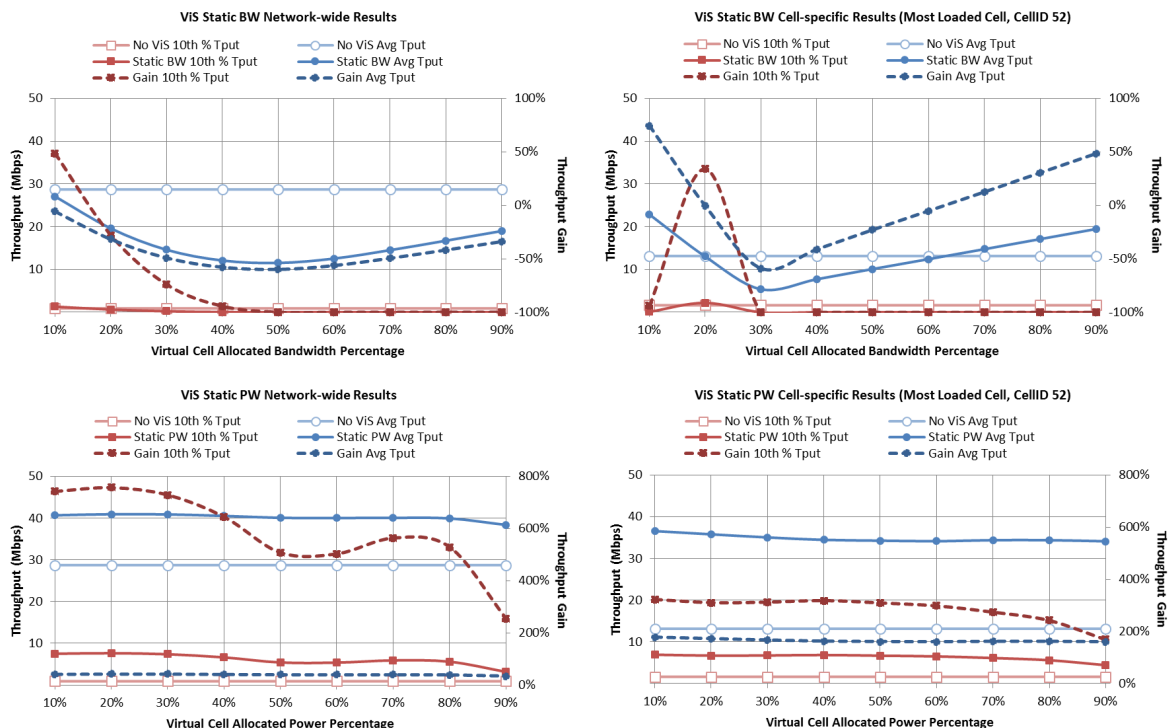


Figure 5.4: ViS in all cells: average throughput and 10th user throughput percentile results with hotspots far from the eNodeBs

In general it can be observed that the graphs shown in Figure 5.4 show a similar behavior as in the case when the hotspots were located close to the eNodeBs. In the case of *static BW* sharing using  $\delta_{W_V}=10\%$  the

network-wide 10th user throughput percentile benefits from the fact that the virtual cells in the cells with hotspots are optimized to provide coverage to the users near the cell edge. In principle this means that these users will be served with very little bandwidth and their performance is bad (as can be seen in the top-right graph for cell 52), however, these users are no longer interfering with the macro-cell users residing in the edge of neighboring cells (they transmit in a separate frequency bandwidth), which translates into network-wide gains. This effect also gives a comparable average throughput from the case with static BW allocation to the No ViS case, however, the very low throughput of the users in the virtual cells prevent it to achieve higher values than the reference scenario.

Using *static PW* allocations, as it was in the case with the location of the hotspots close to the eNodeB, leads to performance gains for both network-wide and cell-specific KPIs in the whole range of transmit power percentages, especially very high gains in the 10th user throughput percentile which are mostly due to the very poor performance of the No ViS case. Since in this scenario a large number of users is located near the cell edge of the four cells with hotspots, and these hotspots are being served by the virtual cells, when the power allocated to the virtual cells is small the users in the cell edge of neighboring macro-cells experience a reduction on interference which leads to improved SINR values. As already described in the scenario with hotspots close to the eNodeBs, on top of the improved SINR for these users, they also benefit from the doubling of the bandwidth resources. Assigning more power to the virtual cells reduces the overall interference on the network at the cost of lower RSS. This tradeoff leads to small improvements of SINR which, together with the additional BW resources, boost the performance. The bottom-right graph for cell 52 shows that it follows the same trend as the behavior described for the network-wide performance. The users in the hotspot (served by the virtual cell) benefit from the added gain coming from the focused beam created by the ViS antenna array, which helps to boost the performance even when little power is assigned to it.

As it was done for the case when the hotspots are located near the eNodeB, a best static resource allocation is chosen based on the results of the bottleneck cell for each resource fraction. For the case of static BW sharing the best allocation is  $\delta_{Wv}=20\%$  and  $\delta_{Pv}=80\%$  for PW sharing, in both cases the bottleneck cell is cell 70, same cell as for the No ViS case. The location of the cell can be seen in the BSA map shown in Figure 5.1, this cell is also one of the cells where one of the hotspots is created. The impact of offered load in the network and in the bottleneck cell is studied by simulating the best static resource configurations for ViS using the loads presented in Table 5.3.

Table 5.3: Load values for the case with hotspots far from the eNodeB

Offered Load [ $Mbps/km^2$ ]
[27, 34, 41, 48, 55, 61]

These offered loads will be used for all the simulations related to the scenario with hotspots far from the eNodeB which results are show in Figure 5.5.

In Figure 5.5 the graphs on the left-hand side of the page show the network-wide performance for each best static resource allocation while the graphs on the right-hand side present the cell-specific (cell 70, the bottleneck cell) performance results for each resource scheme. The graphs on the top of the page correspond to the results of using the BW sharing scheme while the graphs on the bottom present the PW sharing scheme simulation results. The  $x$  axes in each graph represents offered load in  $Mbps/km^2$  while the  $y$  axes is used for throughput in Mbps.

In general, it can be noted that the behavior of the throughput curves is similar between the scenarios with the hotspots far and close, therefore the explanation for the curves presented in Figure 5.5 is the same as for the curves in Figure 5.3. From the graphs on the top it is observed that there is no benefit of using an *static BW* allocation in the whole range of offered loads for neither the network or the bottleneck cell. With the bottleneck cell (cell 70) having a capacity of  $40.5 Mbps/km^2$  when ViS is not implemented and a capacity of  $31.2 Mbps/km^2$  with ViS using the static BW sharing, it is clear that this implementation leads to a loss in capacity of 23% and shouldn't be employed. On the other hand, it is observed that the use of ViS with a *static PW* allocation of  $\delta_{Pv}=80\%$  yields a capacity of  $44.9 Mbps/km^2$ , a gain of 11% over the reference scenario. The use of such a high power allocation to the virtual cells reduces the interference experienced by

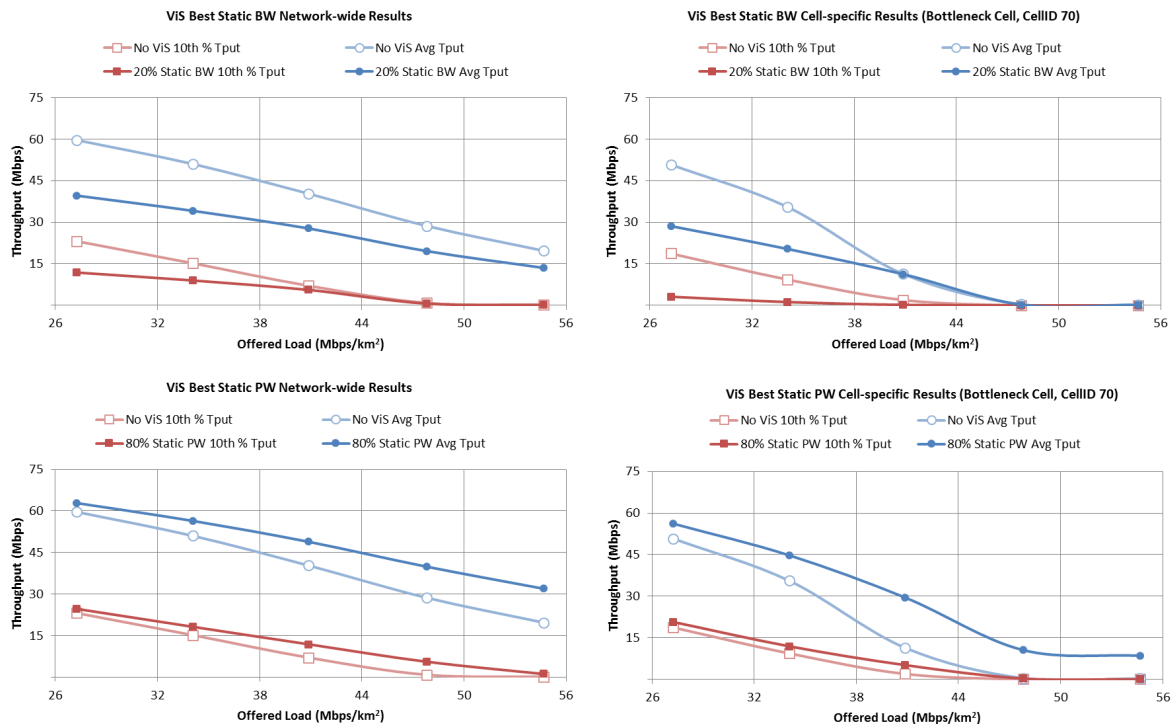


Figure 5.5: ViS in all cells: Bottleneck cell results with hotspots far from the eNodeBs

the bottleneck cell coming from neighboring macro-cell users while serving the users close to the cell edge with high power, because this cell is serving one of the hotspots created. Although it is seen in Figure 5.4 that this configuration doesn't provide the highest throughput gains, it has to be pointed out that it achieves the best balance between performance and capacity gains.

### 5.1.1. ViS IN ALL CELLS: IN-DEPTH ANALYSIS

The results observed above indicate that when using ViS in all the cells in the network, regardless of the location of a traffic hotspot, using fixed transmit power allocations is always better than using fixed bandwidth allocations. This effect can be explained by looking at the relations between power and bandwidth with the Shannon-Hartley channel capacity theorem

$$C = W \log_2(1 + SINR)$$

where  $C$  is the channel capacity and  $W$  represents the channel bandwidth. In the case when *static power* split is used the power for the virtual and macro cells is reduced compared to the case where ViS is not implemented, which creates a lower interference level in the network at the cost of a weaker transmitting signal strength. In the simulations this tradeoff proved to always return a slightly improved SINR and on top of it the bandwidth resources for each cell are doubled ( $2 \times W$ ) and the bandwidth in each cell is shared by fewer users. In the case of *static bandwidth* split the interference is reduced when compared to the fixed transmit power scheme because the macro and virtual cells do not interfere each other anymore and the useful signal is increased because the transmit power is not shared. This SINR improvement comes at the loss of bandwidth. Since the effect of changes in SINR in the Shannon-Hartley capacity theorem is logarithmic (and in many cases less than linear), the positive impact on performance is relatively small when the SINR goes from lower to higher values, compared to the linear loss that is incurred in terms of the available bandwidth. Hence, even though both resource allocation schemes improve the SINR, static PW split is better than static BW split because it uses more bandwidth resources for all the served users.

The fact that some cell-specific gains have been observed when using the fixed bandwidth resource sharing scheme indicate that this resource scheme can be beneficial when an appropriate value for  $\delta_{WV}$  is chosen on a per cell basis, which is a strong motivation for a self-optimizing algorithm for this parameter.

For the case of static PW sharing it was observed that gains were always achieved even when using extreme power allocations. Figure 5.6 shows that for a power allocation of 90% to the virtual cells, the interference levels experienced by the users are lower than in the reference case because all the neighboring cells are transmitting with reduced power, but this implies that also the RSS of all the users is also reduced. When using  $\delta_{Pv}=10\%$  the majority of the users experience a small reduction in interference, as a result of the neighboring cells with reduced power, while their RSS is almost the same as in the reference case because the reduction in power is very small.

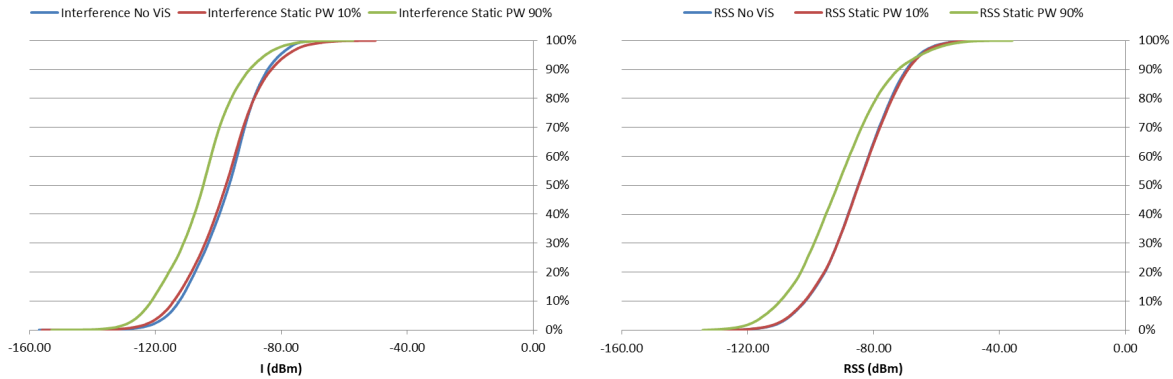


Figure 5.6: Static PW sharing, network-wide CDF of user experienced interference (left) and RSS (right)

The result of combining these two effects is that in both cases the users experience better SINR than in the reference scenario, as can be observed in the left side of Figure 5.7, with the case with 10% having the highest SINR, except at very high SINRs (the top percentiles) which don't impact performance because the rate calculation in the simulator is done with a truncated Shannon formula [21]. Additionally, it is observed that in the case with 10% static PW split the total available bandwidth is shared better among the users in the network because the users finish their transmissions faster and the bandwidth is shared by fewer users at the same time (from the total number of users in the cell before ViS, now a smaller number is served by the virtual cell and the rest by the macro cell) as shown in the right-hand side of Figure 5.7.

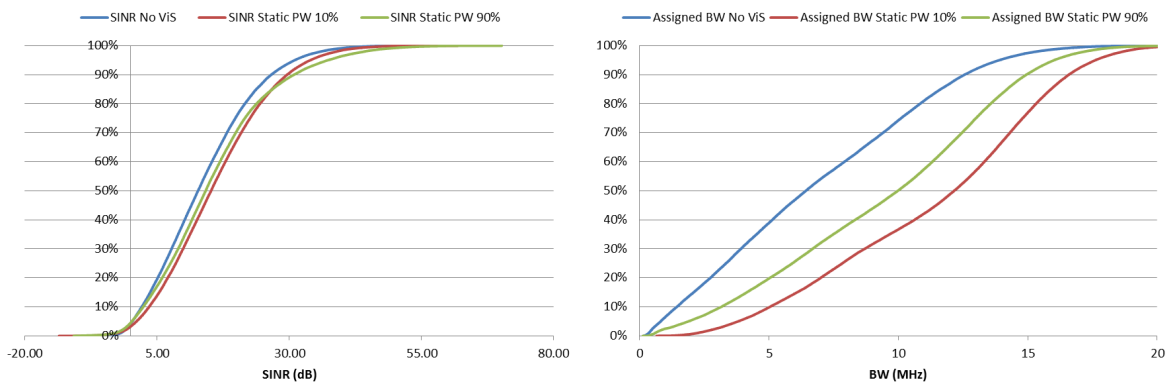


Figure 5.7: Static PW sharing, network-wide CDF of user experienced SINR (left) and average assigned BW (right)

From the right-hand side of Figure 5.7 it is observed that in the case of No ViS 10% of the users or more are assigned, on average, 1 Mhz of bandwidth. Using an static PW split, on the other hand, returns an average bandwidth assignment of 2.5 MHz and 5 Mhz for 90% and 10% of the power allocated to the virtual cell, respectively. This reinforces the conclusion that the good performance of static PW split comes mainly from doubling the bandwidth resources.

## 5.2. VIS DEPLOYED IN FOUR CELLS WITH HOTSPOTS

In this section, the results obtained when ViS was implemented in the four cells with hotspots in the downtown area of Hannover are presented. The layout of the graphs with the results is the same as explained in 5.1 and the plots show the throughput values and gains at network-wide and cell-specific levels.

Figure 5.8 presents the results for the baseline scenario without ViS and for the cases when ViS is active with different static bandwidth and transmit power allocations for the traffic map with hotspots close to the eNodeB.

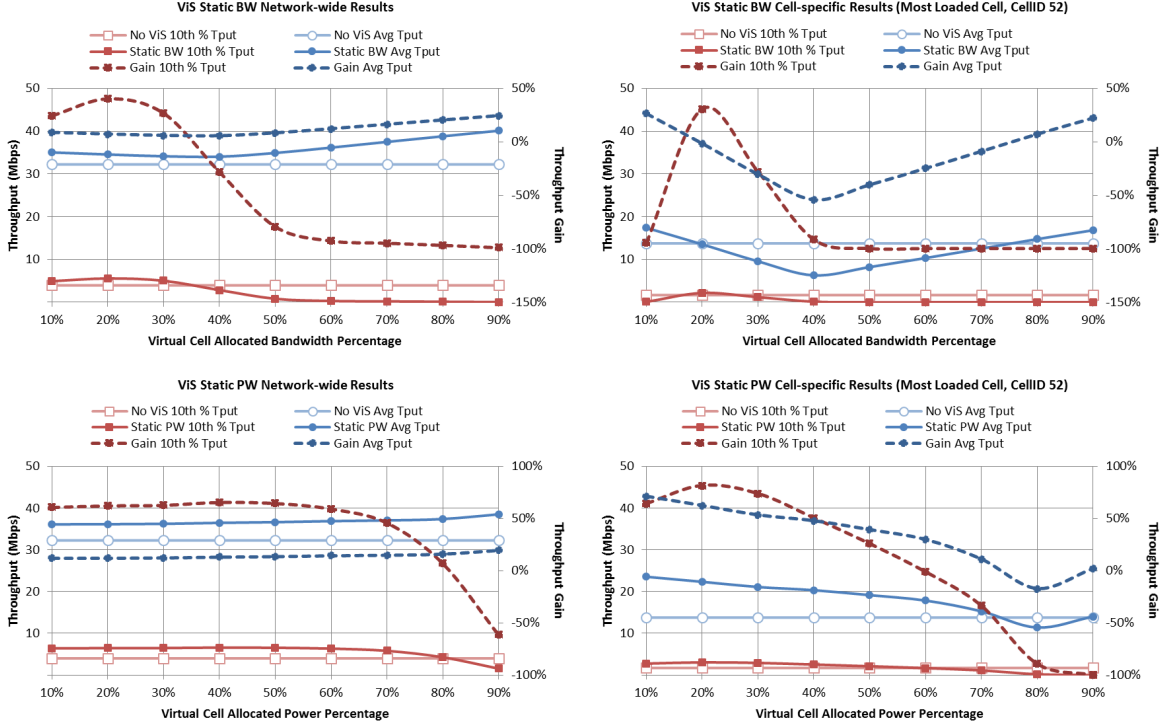


Figure 5.8: ViS in four cells: average throughput and 10th user throughput percentile results with hotspots close to the eNodeBs

From the top-left graph it is observed that, in contrast to what was seen in Figure 5.2 for the case when all the cells are virtually sectorized, a *static BW* allocation with small  $\delta_{Wv}$  in this scenario leads to improved throughput performance in both average Tput and 10th user throughput percentile at a network-wide level. Since in this scenario only the four cells containing hotspots are virtually sectorized and the virtual cells are focused on the hotspots, the performance of the neighboring cells is only affected by any change in the new virtual or macro-cells. When  $\delta_{Wv}$  is small the macro-cells interfere in a smaller percentage of the bandwidth of the neighboring cells, which improves their performance and contributes to the gains observed. This is also observed on the performance of the most loaded cell (cell 52) in the top-right graph. Since the four cells with hotspots are located next to each other (they are all 1st tier neighbors), the macro-cell users benefit from the fact that the users being served by the neighbor virtual cells no longer interfere with them. Additionally it can be observed that at  $\delta_{Wv}=20\%$  the average throughput of cell 52 is the same as it was on the reference scenario, but the 10th user throughput percentile shows a gain. This indicates that with this allocation there is a good balance between the BW assigned to the virtual and macro-cell and also that the users served by the virtual cells benefit from the enhanced signal strength from the beam produced by the antenna array. This effect on the virtually sectorized cells plus the reduced interference in the neighboring cells account for the gains observed in network-wide performance, which are described more in depth in 5.2.1.

As can be seen from network-wide results for the *static PW* allocation scheme (bottom-left graph), the performance on network-wide and cell-specific levels is the same as it was observed in Figure 5.2. The only observed difference is that the resulting gains are lower when compared to the case when all the cells are

virtually sectorized (which leads to performance losses when more power is assigned to the virtual cells), meaning that the interference and bandwidth sharing mechanisms already described for Figure 26 still occur but on a smaller scale because less cells are virtually sectorized. The explanation of these mechanisms can be found in section 5.1.

As it was done for the results presented in 5.1, a *best configuration* for each static resource allocation scheme is determined based on the 10th user throughput percentile results of the bottleneck cells for the simulations of the different BW and PW allocations at high load. For the current scenario under study, when only four cells in the network are virtually sectorized and their hotspots are located close to the eNodeBs, the *best static BW* split is  $\delta_{W_V}=20\%$  and the *best static PW* split is  $\delta_{P_V}=30\%$ . In both cases the bottleneck cell is cell 40.

The impact of offered load in the network and in the bottleneck cell is studied by simulating the best static resource configurations for ViS using the loads previously presented in Table 5.2. The results from this study are presented in Figure 5.9, where the top graphs correspond to the BW sharing scheme and the bottom graphs to the bottleneck cell results.

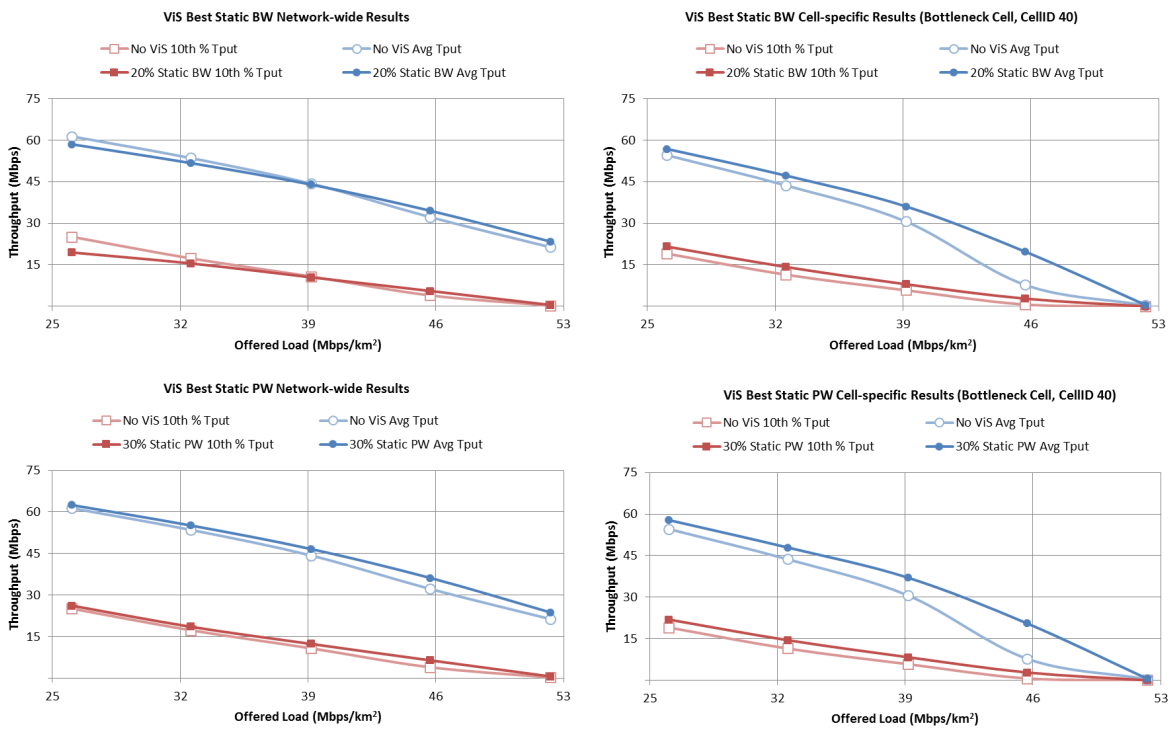


Figure 5.9: ViS in four cells: Bottleneck cell results with hotspots close to the eNodeBs

From the top-left hand side graph of Figure 5.9 it is observed that at higher loads the *static BW* allocation of 20% leads to network-wide and cell-specific performance gains in both throughput KPIs. As already explained for Figure 5.8, this comes a consequence of the balance achieved between the number of users served by the virtual and macro-cells and the corresponding allocated BW. When the offered load is lower, the balance is lost and the network performance is affected. For the case of the bottleneck cell there are clear gains in the whole offered load range. This happens because cell 40, the bottleneck cell, is not virtually sectorized but it is a 1st tier neighbor to the sectorized cells in the downtown of Hannover and its performance is improved by the reduction on interference from the large number of users residing in the macro-cells who now affect only 80% of the total bandwidth. The capacity of the bottleneck cell for the No ViS case is  $43.6 \text{ Mbps}/\text{km}^2$  and  $47.7 \text{ Mbps}/\text{km}^2$  after ViS is implemented, yielding a gain of 9.4%.

The case of *static PW* allocation (shown in the bottom part of Figure 5.9) shows performance gains in the whole offered load range, as it was also the case with the results obtained when all the cells are virtually sec-

torized. With this configuration the capacity is  $47.8 \text{ Mbps/km}^2$  for a gain of 9.4% over the reference scenario without ViS.

The results obtained for the traffic map with hotspots far from the eNodeB show the same behavior as the results already presented in 5.1 and the results obtained for the traffic map with the hotspots close to the eNodeBs, therefore the results of these simulations are not presented in this section and can be found in Appendix B.

### 5.2.1. VIS IN FOUR CELLS: IN-DEPTH ANALYSIS

Figure 5.8 showed that network-wide average throughput gains are achieved with extreme static BW allocations and, additionally, 10th user throughput percentile gains are observed when  $\delta_{Wv}$  is small. This is better observed in the graphs presented in Figure 5.10. On the left hand side it can be observed that when using  $\delta_{Wv}=10\%$  (red curve) a small percentage of the users in the whole network experience very poor throughput performance but are not enough to reach the 10th user throughput percentile. These users are the ones served by the virtual cells, which have poor performance. When going to  $\delta_{Wv}=90\%$  (green curve), the number of users in the network with very poor performance increases until the point that they reach more than 10% of the total users in the network. This is a consequence of the macro-cells users being served with very little available bandwidth. By looking at the right-hand side of Figure 5.10, it is clear that the users in all other cells in the network besides the four with ViS (neighbor cells) are benefited from the reduced interference in a large part of the bandwidth. The user throughput is higher for every user percentile. The same effect happens when  $\delta_{Wv}=10\%$  but the throughput gain for the neighbors is smaller because there are more users interfering in the same portion of the bandwidth. The higher throughputs experienced by the neighboring cells are the drivers for the observed network-wide average throughput gains.

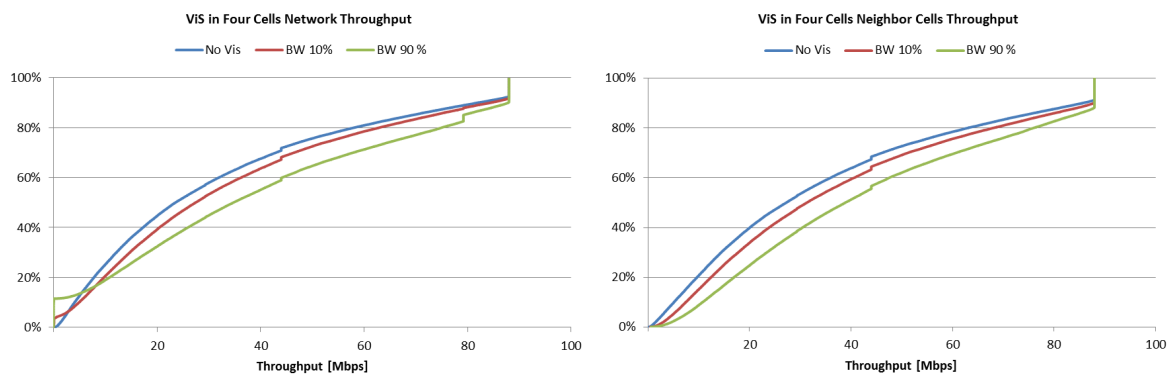


Figure 5.10: Static BW sharing, network-wide (left) and neighboring cells (right) CDF of user experienced throughput

### 5.3. VIS DEPLOYED IN THE MOST LOADED CELL

The results obtained when ViS was implemented in the most loaded cell, which also contains a hotspot, in the network are presented in Figure 5.11. On the network-wide KPIs when *static BW* allocation is used (top-left graph) it is observed that the maximum throughput gains in both KPIs are achieved when  $\delta_{Wv}=90\%$ . This can be explained with a similar approach as the one described in 5.2.1. When such a large part of the bandwidth is allocated to the virtual cells, the users served by the macro-cell interfere in only 10% of the bandwidth to the neighboring cells, improving their performance and the average network-wide throughput. This benefit to the neighbor cells comes at a cost of very poor performance for the macro-cell users, since the number of users in this cell is not enough to reflect on the network-wide 10th user throughput percentile, the high gains seen in this KPI are also an effect of the neighbor cells and the very poor performance of the reference scenario. At a cell-specific level (most loaded cell, cell 52) the same behavior as in the cases presented in 5.1 and 5.2 is observed but the throughput gains are smaller because, since cell 52 is the one virtually sectorized, the effect of the interference from the neighboring cells is bigger. With large  $\delta_{Wv}$  the users in the virtual cell experience very high throughputs, which improves the cell's average throughput, but since the majority of

the users are served by the macro-cell with very little bandwidth the 10th user throughput percentile is very low. With small  $\delta_{WV}$  the number of users in the virtual cell and the BW allocated to them is more proportional, which leads to small improvement in the 10th user throughput percentile but the average throughput is always worse than the reference case because the neighbor cells interfere in the whole bandwidth with the users in the virtually sectorized cell and the aggregated cell throughput deteriorates.

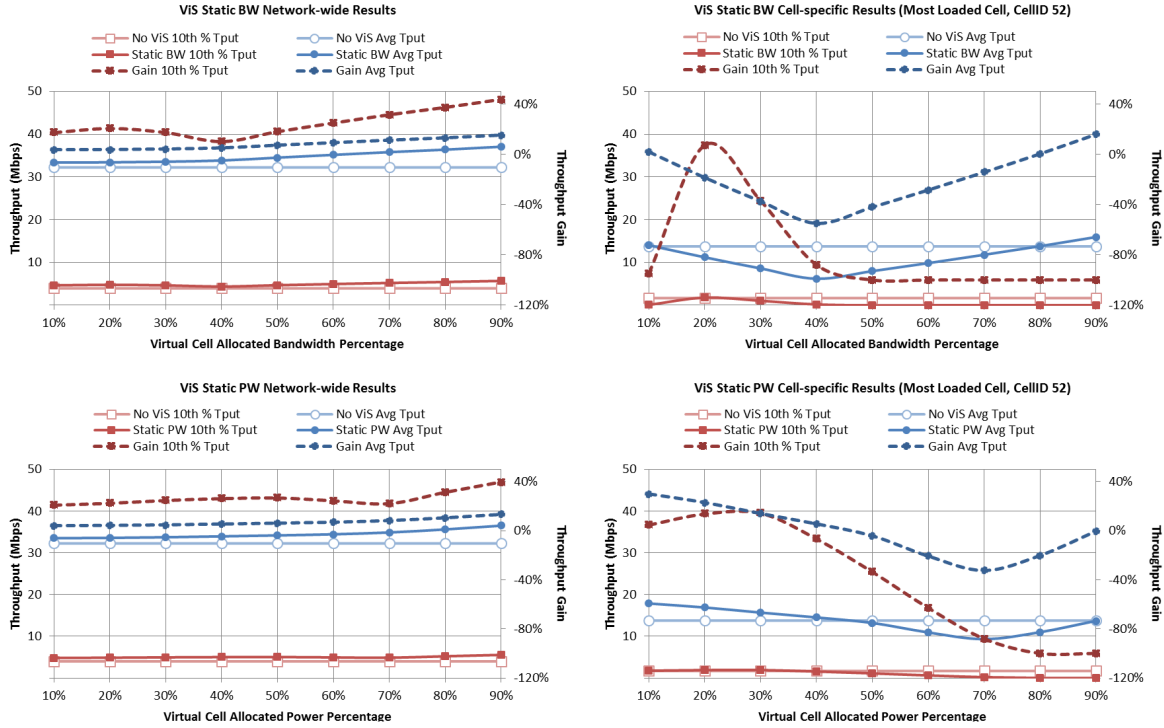


Figure 5.11: ViS in most loaded cell: average throughput and 10th user throughput percentile results with hotspot close to the eNodeB

The bottom-left graph in Figure 5.11 shows that using *static PW* sharing between the virtual and the macro-cell yields to network-wide gains in the whole range of values of  $\delta_{Pv}$ , with the higher gains observed when  $\delta_{Pv}=90\%$ , a similar result as found for the bandwidth sharing scheme. This is because, as in the case with BW sharing, the neighboring cell users to the virtually sectorized cell experience less interference from the users in the macro-cell, because it is allocated with less power. At cell level a similar effect as to the case with static BW sharing happens. When the virtual cell is allocated most of the power, the macro cell users experience very low SINR values because the interference from neighboring cells is high and their RSS is very small. On the other hand, when the macro-cell is assigned with most of the transmit power, e.g.  $\delta_{Pv}=10\%$ , the majority of the users experience medium to high throughputs, boosting the cell's average throughput but the users with poor performance in the virtual cell impact the 10th user throughput percentile performance. However, when the virtual cell is allocated with  $\delta_{Pv}=30\%$  a better balance is achieved between virtual and macro-cell and gains are achieved for both KPI metrics.

Similar to what was done for the results presented in 5.1 and 5.2, the *best configuration* for each static resource allocation scheme is determined based on the 10th user throughput percentile results of the bottleneck cells for the simulations of the different BW and PW allocations at high load. For the case when only once cell (cell 52) in the network is virtually sectorized and the traffic hotspots are located close to the eNodeBs, the *best static BW* allocation is  $\delta_{Wv}=20\%$  and the *best static PW* allocation is  $\delta_{Pv}=40\%$ . As it was the case for the other two deployment scenarios presented, in both cases the bottleneck cell is cell 40. The impact of offered load in the network and in the bottleneck cell is simulated using the *best static resource configurations* for ViS with the offered loads shown in Table 5.2. The results from this study are presented in Figure 5.12, where the top graphs correspond to the BW sharing scheme and the bottom graphs to the bottleneck cell results.

From Figure 5.12 it is observed that both resource sharing schemes perform similarly when ViS is imple-

mented only in once cell in the network, showing moderate gains in the whole range of simulated offered loads. The gains in network-wide and cell-specific (bottleneck cell) throughputs is higher at high loads because in this scenario interference of concurrent users starts to play a bigger role. This is better observed in the behavior of cell 40, the bottleneck cell. This cell is a first tier neighbor to cell 52, the cell which is virtually sectorized. As the offered load increases, the bottleneck cell benefits more from the reduction of interference as a result of implementing ViS and achieves small throughput and capacity gains. The capacity when ViS is implemented using *static BW* sharing is  $44.14 \text{ Mbps/km}^2$  and  $44.32 \text{ Mbps/km}^2$  when *static PW* sharing is used which means that there are practically no gains in capacity over the No ViS case.

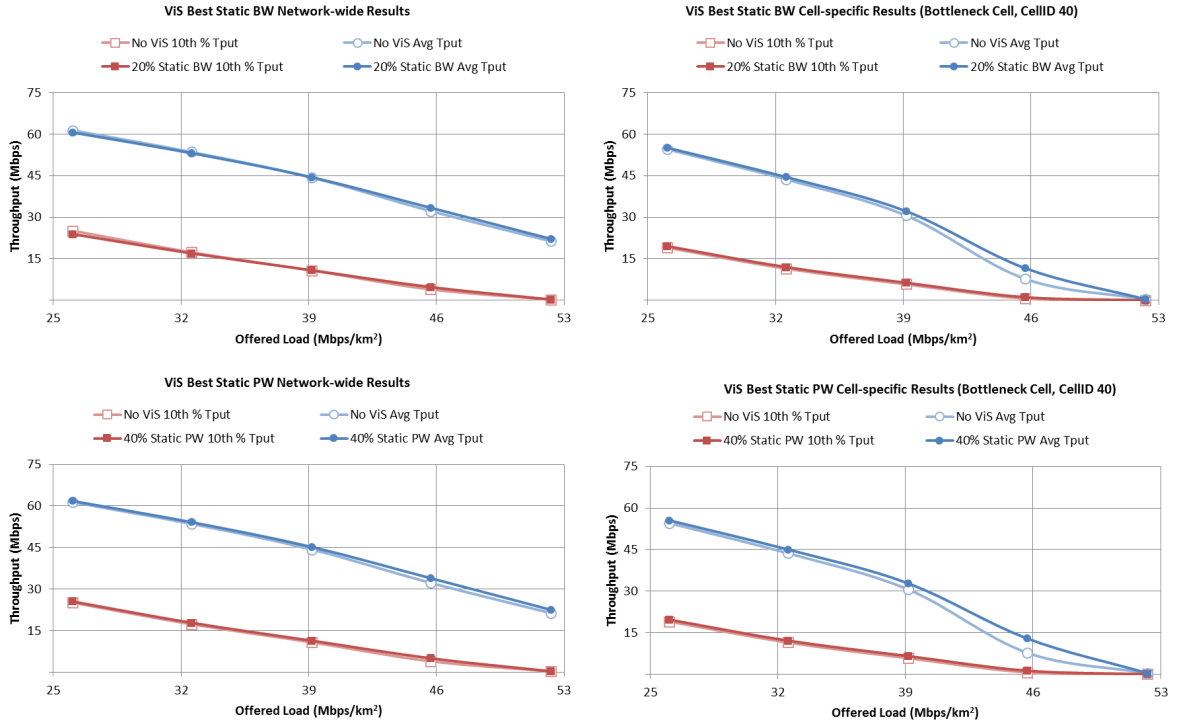


Figure 5.12: ViS in most loaded cell: Bottleneck cell results with hotspot close to the eNodeB

Since the results obtained for the traffic map with hotspots far from the eNodeB show the same behavior as the results already presented in this section and can be explained with the same arguments given for the previous scenarios, the throughput and capacity curves for these simulations are not presented in this section and can be found in Appendix B.

## 5.4. CONCLUDING REMARKS

From the results and analysis presented in this chapter, the following general observations are noted:

- Using a static transmit power sharing scheme always leads to higher performance improvement at network and cell-specific level when compared to static bandwidth sharing, especially in the cases when more than one cell is virtually sectorized. Both resource schemes have demonstrated that when all the virtually sectorized cells use the same static resource allocation the interference levels in the network are reduced and in most of the cases it results in improved SINR values. The main benefit from PW sharing is that on top of the slight improvement in SINR, it doubles the bandwidth resources and the users experience high gains. With BW sharing there is also an improvement in SINR because fewer users interfere in the same frequency band, however, when more bandwidth is allocated to the virtual cells the users in the macro cells don't have enough resources and show very poor performance because the macro-cell usually serves many more users than the virtual cell. For example, if the virtual cell is

given 60% of the BW ( $20 \text{ Mhz} \times 0.60 = 12 \text{ MHz}$ ) and it is serving only one user at a particular time in the simulation while the macro-cell serves 3 users, the user in the virtual cell will transmit using 12 MHz and each user in the macro-cell will be allocated with 2.6 MHz ( $12/3 \text{ MHz}$ ). This highlights the need for an adequate BW split scheme that accounts for the number of users in each cell.

- It is noted that in general, the static BW sharing performs better when smaller bandwidth is allocated to the virtual cell. Because the number of users in the virtual cell is usually smaller than the number of users in the macro-cell, a better fit of the bandwidth to the user distribution is achieved with this kind of allocation. Since the BW allocation is kept the same during the entire simulation time, there are moments in which the bandwidth assigned to the virtual cells and the number of users served by them doesn't fit, hence, limiting the performance of the network. This is an indication that with an intelligent SON bandwidth allocation algorithm the performance can be improved and the gains maximized.
- The location of the hotspot within the coverage area of the macro-cell impacts mainly the 10th user throughput percentile once ViS is implemented. This is explained by understanding the interference experienced by the users being served by the virtual and macro cells as well as the users being served by its neighbor cells. When the hotspots were located far from the eNodeB and ViS was implemented, the gains in 10th user throughput percentile were higher because the hotspot users are closer to the cell-edge and these users are the ones that benefit the most from the reduction of interference coming from the neighboring cells (cell-edge users are the ones that typically experience the worst transmission conditions). The explanation for the gains is the same as the for the case when the hotspots are closer to the eNodeB, the main difference is that interference levels are lower.
- Out of all the static resource deployment strategies for ViS, the one that yields higher capacity gain for the Hannover network when the hotspots were close to the eNodeBs is the case when ViS is implemented in all the cells in the network, as shown in Table 5.4. This strategy, used in combination with a fixed transmit power sharing scheme with  $\delta_{pv}=40\%$ , returned a 22% capacity gain over the No ViS reference scenario.

Table 5.4: Capacity gains summary for ViS with static resource allocation for the map with hotspots close to the eNodeB

Deployment Strategy	Static BW Split Capacity Gain	Static PW Split Capacity Gain
ViS in All Cells	3%	22%
ViS in Four Cells	9.40%	9.60%
ViS in One Cell	0%	0%



# 6

## VIS SON ALGORITHM DESCRIPTION

The generation of a highly focused beam supporting a virtual cell within an existing cell creates interference that can considerably impact performance. To fully benefit from ViS, adequate resource allocation is needed to mitigate interference and maximize performance. The solutions proposed in this thesis, based on available literature, are bandwidth sharing and transmit power sharing.

### 6.1. BANDWIDTH SHARING SON ALGORITHM

Bandwidth sharing is a frequency domain solution in which the virtual and corresponding macro-cells use different – non-overlapping – portions of the total available bandwidth. In the proposed implementation, the transmit power per Hertz remains unchanged after ViS activation (i.e. all Physical Resource Blocks (PRBs) are transmitted with the same power). The SON algorithm for ViS dynamically allocates the available bandwidth to the macro and virtual cells. If the virtual cell has no traffic under its coverage area, no bandwidth resources are allocated to it by the SON algorithm.

The SON algorithm splits the frequency bandwidth according to the Proportional Fair (PF) utility of the users throughputs which is a well-known and tested fair sharing criterion [29]. The PF sharing criteria is used because it provides a good trade-off between throughput optimization and fairness in resource sharing. Recalling that  $\delta_{Wv}$  denotes the proportion of bandwidth allocated to the virtual cell, the PF utility is written as follows:

$$U_{PF}(\delta_{Wv}) = \sum_{u \in virtual} \log(\delta_{Wv} \overline{R}_u) + \sum_{u \in macro} \log((1 - \delta_{Wv}) \overline{R}_u)$$

where  $\overline{R}_u$  is the data rate of user  $u$  when his serving cell is allocated the entire bandwidth so that the actual rate of a user in the virtual cell is  $R_u = \delta_{Wv} \overline{R}_u$  and of a user in the macro-cell is  $R_u = (1 - \delta_{Wv}) \overline{R}_u$ . The utility is concave in  $\delta_{Wv}$ , so the Karush-Kuhn-Tucker (K.K.T) conditions for optimality are equivalent to finding a  $\delta_{Wv}$  that satisfies the following equation

$$\frac{\partial U_{PF}(\delta_{Wv})}{\partial \delta_{Wv}} = 0$$

Which yields to a closed form expression of the sharing proportion  $\delta_{Wv}$  [21] given by

$$\delta_{Wv} = \frac{N_v}{N_v + N_m}$$

where  $N_v$  and  $N_m$  are respectively the number of users in the macro and virtual cells. This bandwidth proportion is updated at each call departure or arrival in the network. It is noted that the bandwidth allocation doesn't depend on  $\overline{R_u}$  because the optimization is done over  $\delta_{Wv}$ , i.e. to find the value where the utility function is maximum and, as a consequence, when the resources are shared fairly among the users in the virtual and the macro-cell.

This particular approach was chosen because it is a simple solution and does not depend on the particular channel quality of the users present in the virtual or macro-cells. Alternatively, one could think in other sharing alternatives that could take into consideration the SINR of each call to make a better decision, for instance, assigning more bandwidth to the users experiencing worse channel conditions. The downside of these alternatives is that the calculation of the bandwidth allocation is not so straight-forward because this represents the need of a mapping between SINR values to bandwidth allocation, while the PF approach results in a much simpler solution.

## 6.2. TRANSMIT POWER SHARING SON ALGORITHM

A similar approach is taken for the transmit power proportion allocated to the virtual cell, denoted by  $\delta_{Pv}$ , in the case of a transmit power sharing scheme. The heuristic expression for  $\delta_{Pv}$  is given by

$$\delta_{Pv} = \frac{N_v}{N_v + N_m}$$

where  $N_v$  and  $N_m$  are the number of users in the macro and virtual cells, respectively. As for the bandwidth sharing case, the value of  $\delta_{Pv}$  is updated every time a call arrives or departs from the system.

Since the power for the virtual and macro cells is reduced compared to the case where ViS is not implemented, a SINR degradation may be observed due to reduced useful signal and increased interference for all the users, however, the full reuse of the available bandwidth is expected to enhance the performance and maximize capacity. The optimization of the transmit power split between the virtual and macro cells is done with the simple approach of using a similar expression to calculate  $\delta_{Pv}$  at each call arrival or departure event as the one used for the BW sharing algorithm because this strategy proves to share the resources fairly among the users in the virtual and macro cells.

## 6.3. SON ALGORITHM SIMULATION SCENARIOS

In order to test the impact on performance of the SON frequency sharing algorithm and SON transmit power sharing algorithm the network is simulated when ViS is implemented in the same deployment scenarios as mentioned in 4.4. Additionally the impact of call arrival rate (the higher the call arrival rate the higher the load and vice versa) is addressed by testing the SON algorithms with different values of offered load  $\lambda$ , introduced in 4.2. The values of offered loads used in the simulations are presented in Table 6.1.

Table 6.1:  $\lambda$  values for simulations

Hotspot Location	Offered Load [Mbps/km <sup>2</sup> ]
Close	[26, 33, 39, 46, 52, 59]
Far	[27, 34, 41, 48, 55, 61]

The optimum tilt and azimuth configuration for each cell is used for all the simulations and for each traffic map with hotspots located close and far from the eNodeB. The combination of SON algorithms and hotspot locations yields to a total of four simulation scenarios, as shown in Table 6.2, per deployment strategy. This amounts to a total of twelve distinct scenarios, each of which contains six simulations (one for each load).

Chapter 7 will show the performance of these algorithms when applied to the realistic LTE network described in Chapter 4 for the aforementioned scenarios and compare it to the case when ViS is not imple-

Table 6.2: SON ViS simulation scenarios

<b>Hotspots Close to eNodeB</b>	<b>Hotspots Far from eNodeB</b>
SON BW Sharing	SON BW Sharing
SON Transmit Power Sharing	SON Transmit Power Sharing

mented and when fixed resource allocation is used.



# 7

## VIS SON ALGORITHM PERFORMANCE

In this chapter the performance of the SON ViS algorithms is evaluated when compared to the reference scenario when ViS is not active (No ViS) and to the case of static resource sharing. The results are divided in three main sections corresponding to the ViS deployment strategies mentioned in the scenarios description in 6.3. First the results of implementing ViS in all the cells in the network for both traffic maps and for both SON resource (bandwidth and transmit power) allocation algorithms are presented, followed by the results for the case when ViS is implemented in the four cells containing hotspots and moving on to the case when only the most loaded cell in the network uses ViS and this cell also contains a hotspot. The tilt and azimuth configuration for the virtual cells is kept the same as the one described in 4.4 and illustrated in the BSA maps from Figure 5.1. For consistency with the results presented in 5, the same KPIs are monitored to understand the impact on performance of implementing ViS and in the same cells, i.e. the most loaded cell in the network (cell 52) and the bottleneck cells in each scenario.

### 7.1. SON VIS DEPLOYED IN ALL CELLS IN THE NETWORK

The performance of ViS has been evaluated for the case when all the cells in the network are virtually sectorized with the optimum tilt and azimuth configuration corresponding to the traffic density map with hotspots close and far from the eNodeB. In the following figures, the graphs on the left hand side show the network-wide performance for each resource sharing scheme while the graphs on the right hand side present the cell-specific (most loaded cell in the network, cell 52) performance results for each resource scheme. The graphs on the top correspond to the results of using the SON BW algorithm while the graphs on the bottom present results of using the SON power algorithm. On the left hand side of the figure the network-wide results are presented and on the right the results for the most loaded cell in the network (cell 52). The  $x$  axes in each graph represents the offered traffic load in  $Mbps/km^2$  used for each simulation as mentioned in 6.3, while the  $y$  axes is used for throughput in Mbps.

The results for the baseline scenario without ViS, the scenario with the best static resource allocation and for the cases when SON ViS is active for the traffic map with hotspots close to the eNodeB are shown in Figure 7.1. The graphs in the top part of the figure show that when an intelligent *SON BW* algorithm is employed, ViS yields gains in both network-wide and cell-specific (most loaded cell, cell 52) results for the whole load range over the No ViS case and over the static BW scenario ( $\delta_{Wv}=20\%$ ), which supports the idea presented in 5 that when a good fit between the number of users in the virtual cells and the BW allocated to them is achieved, the gains from ViS with this resource scheme are maximized. As already discussed in 5, when BW sharing is used the interference in the network is reduced because there are less users interfering in the same frequency band, which leads to improved SINR values. The main problem with static BW sharing is that even though the users were experiencing higher SINR, they were also allocated with a portion of the BW that in most of the cases doesn't match with the user distribution and leads to poor performance. It was also found, especially when looking at the cell-specific results shown in Figure 5.2, that there was a BW allocation configuration that

led to small gains. In this case the distribution of the users between macro and virtual cell fits (on average) with the BW allocated, but this distribution is not constant during the whole simulation duration (calls arrive and depart from the cells). The SON BW algorithm, on the other hand, updates and matches the BW allocated to the virtual cells at each call arrival and departure event, which results in gains for the whole range of offered loads.

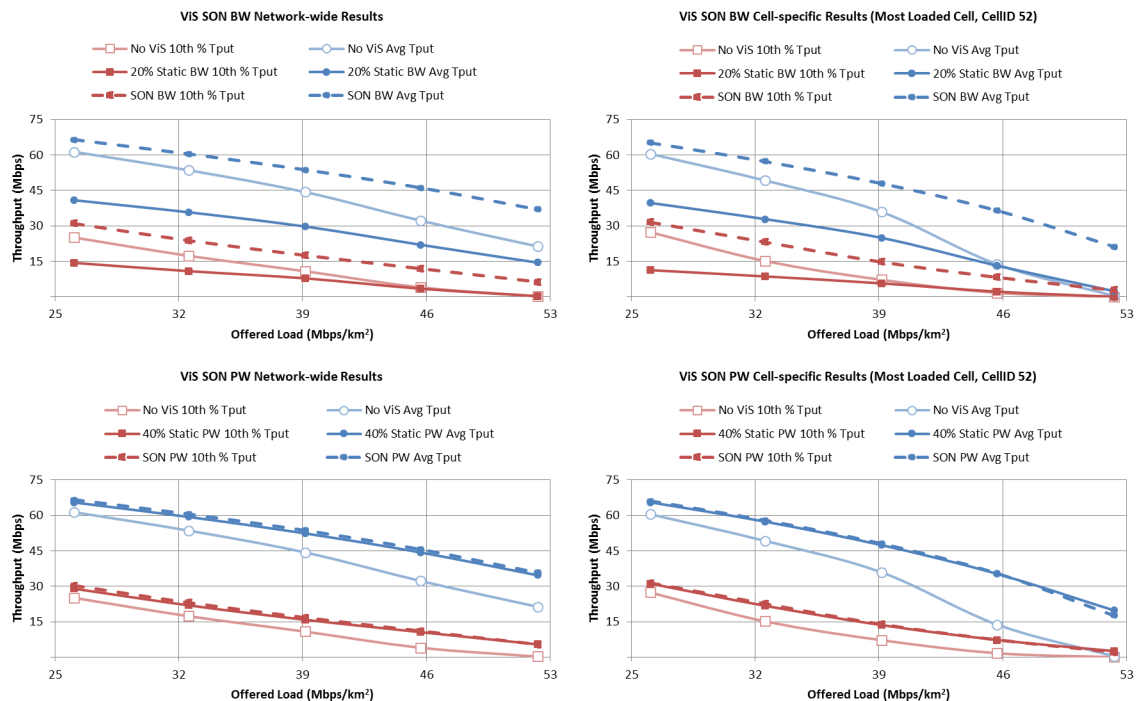


Figure 7.1: ViS in all cells: SON average throughput and 10th user throughput percentile results with hotspots close to the eNodeBs

The results for the *SON PW* algorithm, presented in the bottom part of Figure 7.1, show that the algorithm performs better than the reference scenario without ViS in the whole load range while it performs slightly better than the scenario with the static PW allocation ( $\delta_{PV}=40\%$ ) under lighter loading conditions. It is interesting to note that when the offered load increases the performance of the algorithm matches the performance of the static allocation. It has been explained in 5.1.1 that using PW sharing affects the interference levels among neighboring cells and the RSS experienced by the users, the combination of these effects leads to improved SINRs, a benefit which is then added to the benefit of doubling BW resources. When the offered load is lower, the interference between neighboring cells is low because of the reduced number of simultaneous users in the network and the power allocated by the SON PW algorithm (which fits the user distribution between macro and virtual cells) provides a better RSS to the users than in the case of static PW. At higher loads it is observed that the performance of the network is more limited by the interference from and to neighboring cells because the number of concurrent users increases. This means that even though the SON PW algorithm allocates the amount of power to the virtual and macro cells based on the number of current active users, it doesn't take into account the impact on interference towards neighboring cells, which at higher loads hurts the performance. Static PW allocation shows slightly higher gains at these loads because, even though the interference towards the neighboring cells is also not taken into account when deciding the static power allocation, all the virtual cells in the network are allocated the same amount of PW. This can be seen as a coordinated interference management strategy, which apparently slightly favors the performance of static PW allocation under high loading conditions. The fact that the SON PW algorithm doesn't consider interference is considered a weakness that will be approached as part of an already envisioned future work.

To investigate the capacity gains of the SON algorithms, a similar procedure as explained in 5 is used to compare the performance of the bottleneck cell, i.e. the cell with the lowest 10th user throughput percentile in the network, for the scenarios without ViS, with ViS using static resource sharing (BW and PW) and with ViS SON resource sharing algorithms. In all cases the bottleneck cell is cell 40, and its location is indicated in

the BSA map from Figure 5.1. The throughput results as a function of offered load for the bottleneck cell (cell 40) are shown in Figure 7.2. The SON BW results are presented on the left-hand side plot, while the SON PW results can be seen on the right.

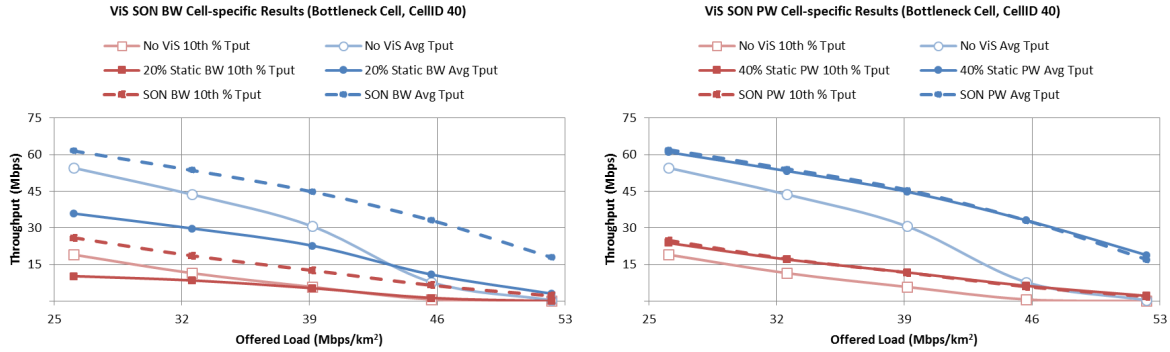


Figure 7.2: ViS in all cells: SON bottleneck cell results with hotspots close to the eNodeBs

The performance of both throughput curves for the bottleneck cell follows the same trend as the results presented in Figure 5.1. The *SON BW* algorithm shows the best performance for the whole range of offered loads when compared to the rest of the scenarios. The achieved capacity when using ViS with the *SON BW* algorithm, measured at the load its 10th user throughput percentile falls below the 2 Mbps threshold, is  $53.3 \text{ Mbps/km}^2$ . This represents a gain of 22.1% over the No ViS scenario and 18.2% over the case when ViS is implemented with static BW allocation of  $\delta_{Wv}=20\%$ . The *SON PW* algorithm again shows to perform the same as the static PW allocation scenario but still performs better than the No ViS case. The capacity in the scenario using a *SON PW* algorithm is  $50.7 \text{ Mbps/km}^2$ , which returns a gain of 16.2% over the No ViS scenario and an almost identical capacity to the case when ViS is implemented with static PW allocation of  $\delta_{Pv}=40\%$ .

By comparing all the presented results in this section, it is concluded that in this scenario the highest capacity and performance gains are achieved when the *SON BW* algorithm is implemented.

The results obtained for the traffic map with hotspots far from the eNodeBs show the same behavior as the results already presented for the traffic map with hotspots close to the eNodeBs and can be explained with the arguments already stated in this section. The results of these simulations are not presented here and can be found in Appendix C.

## 7.2. SON ViS DEPLOYED IN FOUR CELLS WITH HOTSPOTS

The results obtained when SON ViS was implemented in only the four cells with hotspots close to the eNodeBs are shown in Figure 7.3, along with the results for the No ViS and static resource sharing scenarios. Similar to the results in 7.1, the graphs on the top of the figure correspond to the results of using the *SON BW* algorithm while the graphs on the bottom present results of using the *SON power* algorithm. On the left hand side the network-wide results for both resource schemes are presented, on the right hand side the cell-specific results for the most loaded cell in the network (cell 52) are shown. The  $x$  axes in each graph represents the offered traffic load in  $\text{Mbps/km}^2$  used for each simulation as mentioned in 6.3, while the  $y$  axes is used for throughput in Mbps.

From the top part of Figure 7.3 it can be observed that using ViS in combination with the *SON BW* algorithm leads to the highest network-wide and cell-specific (most loaded cell) performance gains when compared to No ViS reference scenario and the case when ViS is implemented with static BW sharing ( $\delta_{Wv}=20\%$ ). The reasoning behind these results is the same as already presented in 7.1, although the impact on the network-wide results is smaller because in this scenario only four cells are virtually sectorized. In this case the impact on network-wide performance from ViS is weakened because only a small number of cells experience changes and the rest stay the same as in the reference scenario. In the bottom part of Figure 7.3, it can be seen that the network-wide performance for the case of ViS using the *SON PW* algorithm is the same as the static

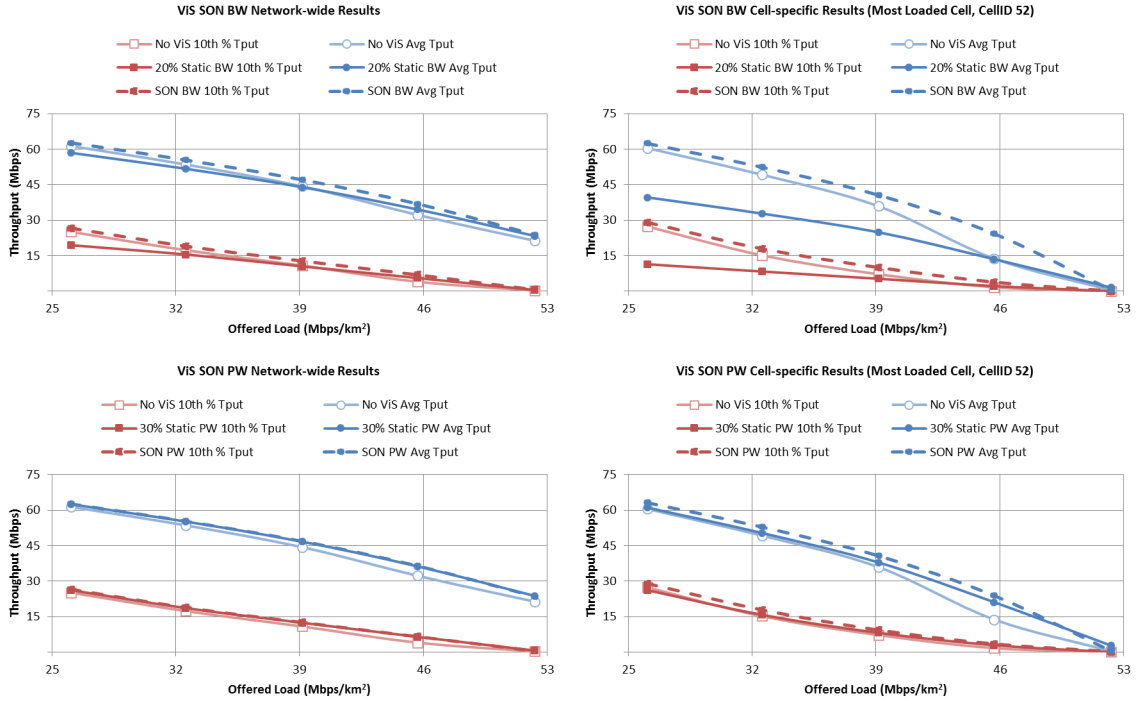


Figure 7.3: ViS in four cells: SON average throughput and 10th user throughput percentile results with hotspots close to the eNodeBs

PW allocation ( $\delta_{PV}=30\%$ ) in the whole load range. In the most loaded cell, it is seen that the SON algorithm performs somewhat better than the cases without ViS or static PW allocation because the effect of the power allocation to the virtual and macro-cells is stronger than the effect of the neighbor cell interferences. Since only three other cells (besides most loaded cell 52) are sectorized in the network, the effect of the interference reduction to the most loaded cell is not as large as it was for the scenario when all the cells are virtually sectorized. With the *SON PW* a better distribution of the power based on the number of users served by the virtual and macro-cells plays a more important role and the users benefit from a stronger RSS.

To investigate the capacity gains of the SON algorithms, a similar analysis as done in 7.1 is used to compare the performance of the bottleneck cell for the scenarios without ViS, with ViS using static resource sharing (BW and PW) and with ViS SON resource sharing algorithms. In all cases the bottleneck cell is again cell 40, and its location is indicated in the BSA map from Figure 5.1. The throughput results as a function of offered load for the bottleneck cell (cell 40) are shown in Figure 7.4. The SON BW results are presented on the left-hand side plot, while the SON PW results can be seen on the right-hand side.

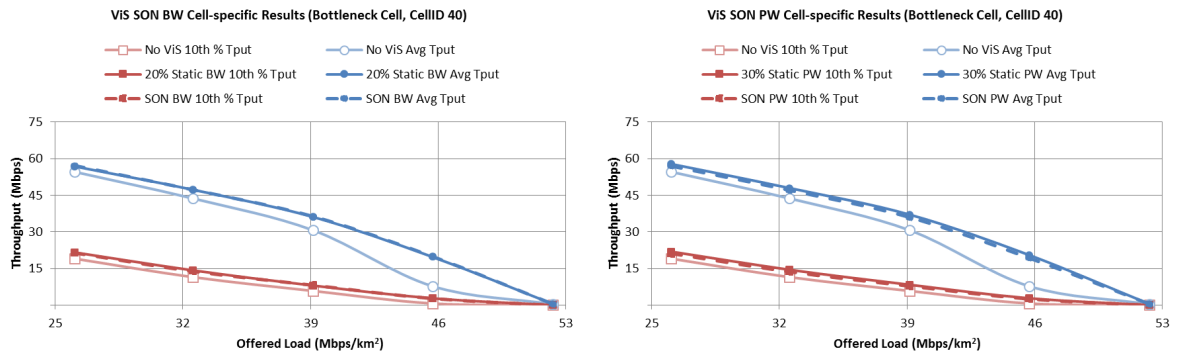


Figure 7.4: ViS in four cells: SON bottleneck cell results with hotspots close to the eNodeBs

From Figure 7.4 it can be seen that the bottleneck cell always benefits from using both SON algorithms when compared to the reference scenario without ViS. It is important to remark that the bottleneck cell (cell 40) is a 1st tier neighbor to the cells that are virtually sectorized, but ViS is not deployed in it because it was only used in the cells with artificially created hotspots and the hotspots were located in the more central cells from downtown Hannover. When compared to the static resource allocations, in the case of *SON BW* the performance of the bottleneck cell remains the same because the interference reduction towards cell 40 from the virtually sectorized cells is no longer improved since the number of virtually sectorized cells is small. The capacity achieved with the *SON BW* algorithm is  $47.7 \text{ Mbps/km}^2$  for a gain over the No ViS case of 9.4%, and no capacity gains over the static BW allocation of  $\delta_{Wv}=20\%$ . The *SON PW* algorithm also returns better performance in the bottleneck cell when compared to the No ViS case and performs almost identical as the static PW allocation scheme. In this scenario the decisions taken by the *SON PW* algorithm to boost the performance of the virtually sectorized cells affect the performance of the neighboring cells. This means that, while the algorithm gives better performance in the virtually sectorized cells, as seen in the bottom-right graph from Figure 7.3, it creates more interference towards the neighbor cells and their performance is lower when compared to the case with static allocation. In this scenario the capacity when using the *SON PW* algorithm is  $47.5 \text{ Mbps/km}^2$  with a gain over the NO ViS scenario of 9% and no significant gains over the static PW scheme. This indicates that the chosen static PW allocation is very good and robust and that the *SON PW* algorithm, as indicated in the previous section, needs to be updated in future work considering other factors such as the interference from and to the neighbor cells. On the other hand, even though the performance is practically identical between the static PW and *SON PW* implementation, the advantage of using a SON algorithm is that it will adapt automatically to changes in the traffic distribution in the network without the need of a calibration process to find the best static allocation. From the presented results in this section it has been observed that the higher network-wide gains in this scenario are obtained when ViS is used in combination with a *SON BW* algorithm. In terms of capacity, about the same capacity gains are achieved with the *SON BW* algorithm and with *both static and SON PW* allocation.

The results obtained for this scenario for the traffic map with hotspots far from the eNodeB, as it was the case in 7.1, are not presented here and can be found in C.

### 7.3. SON ViS DEPLOYED IN THE MOST LOADED CELL

The results obtained when SON ViS was implemented in only the most loaded cell in the network (which also contains a hotspot) using the traffic map with hotspots close to the eNodeBs, are shown in Figure 7.4.

The curve for both SON algorithms shows similar behavior as observed in the scenario presented in 7.2, with *SON BW* presenting a slightly better performance. This result is a consequence of the way the neighboring cells benefit from the reduction of interference, however the impact on network-wide performance is limited because ViS is only implemented in one cell. The cell-specific results show that the most loaded cell (cell 52), which in this scenario is the one which is virtually sectorized and contains a hotspot, achieves slightly better performance when using the SON resource sharing algorithms.

For this scenario both *SON BW* and *SON PW* have comparable results. This means that when deploying ViS in one cell, both SON algorithms will create benefits for the cell, but *SON BW* will have larger benefit for the neighboring cells, leading to higher network-wide throughput gains. Additionally, the effect of the neighboring cells is the same in both cases because the rest of the cells in the network remain the same as in the reference scenario without ViS. As it was explained in 5.3, BW static allocation is always the worst choice because the BW split doesn't match with the user distribution in the cells.

The performance of the bottleneck cell of the network is also investigated, as it was done for the scenarios studied in the previous two sections. The bottleneck cell is cell 40 and its performance results are shown in Figure 7.6 for the cases without ViS, ViS using static resource allocations and ViS using SON resource sharing algorithms.

The results presented in Figure 7.6 can be explained with the same arguments as provided for the analysis of the bottleneck cell performance in 7.2. Slight gains in the bottleneck cells are achieved when using the SON algorithms or the static resource allocation schemes (either PW or BW) over the No ViS reference

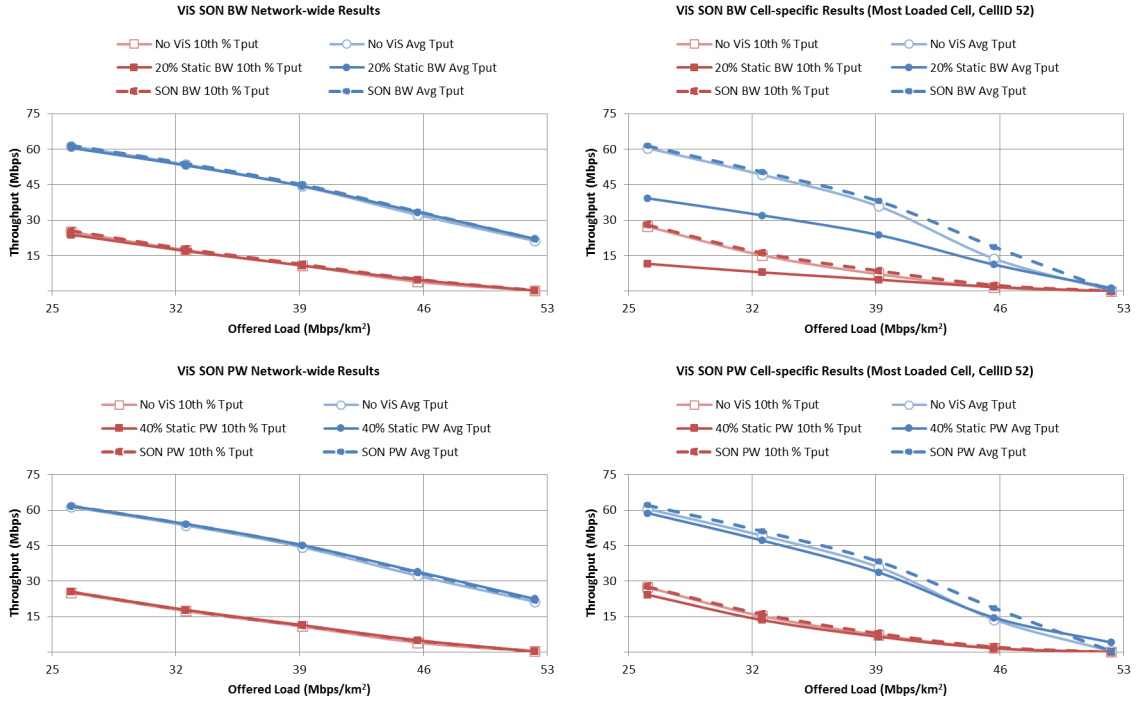


Figure 7.5: ViS in most loaded cell: average throughput and 10th user throughput percentile results with hotspots close to the eNodeBs

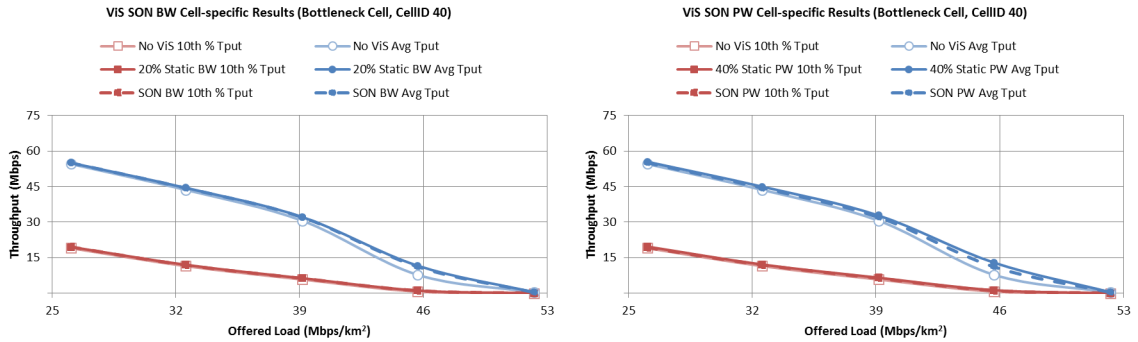


Figure 7.6: ViS in most loaded cells: SON bottleneck cell results with hotspots close to the eNodeBs

scenario, especially in average throughput at high loads. For all of these cases their performance is comparable because these schemes reduce more the interference from the ViS cell towards its neighbors, one of them being the bottleneck cell. The *SON PW* algorithm proved to enhance the performance of the virtually sectorized cell (bottom right graph in Figure 7.5), but this creates more interference to the bottleneck cell and hence the performance of this cell, as seen in the average throughput (blue dashed curve), is lower than the static PW allocation curve. In terms of capacity, both SON algorithms show a capacity of  $44 \text{ Mbps/km}^2$  for a 1% gain over the No ViS scenario and practically identical capacity results to the found for the static resource allocation schemes.

Even though using a *SON BW* sharing algorithm provides practically identical capacity as the No ViS scenario and the case when a static BW allocation is used, the network-wide and most loaded cell (in this case the virtually sectorized cell) performance gains are higher. Based on the presented analysis it is concluded that the *SON BW* algorithm is the best choice for deployment.

Once again, the results from the simulations using the traffic map with hotspots located far from the eNodeB are similar as the results already presented in this section and can be found in Appendix C.

## 7.4. CONCLUDING REMARKS

From the results analyzed in this chapter, the following general observations can be made:

- Using the SON algorithms presented in this thesis to dynamically share the available network resources always leads to performance and capacity improvements over the reference scenario when ViS is not used as shown in Table 7.1.

Table 7.1: Capacity gains summary for ViS with SON resource allocation for the map with hotspots close to the eNodeB

Deployment Strategy	SON BW Split Capacity Gains		SON PW Split Capacity Gains	
	Over No ViS	Over Static BW	Over No ViS	Over Static PW
ViS in All Cells	22.10%	18%	16.20%	0%
ViS in Four Cells	9.40%	0%	9%	0%
ViS in One Cell	0%	0%	0%	0%

- The SON BW algorithm presents the higher gains in performance for all the scenarios studied and the highest bottleneck cell capacity gains, except for the case when ViS is only implemented in one cell where the performance is practically identical to the reference scenarios. It is also observed that the gains in performance and capacity of using SON grow with the number of cells in which ViS it is implemented. When compared to the results obtained for static resource sharing schemes, SON BW always performs equal or better than any other configuration.
- The SON PW algorithm, on the other hand, has shown to have almost identical performance to the static PW allocation and only in selected cases shows higher gains. This is mainly due to the fact that using power sharing creates a more complicated interference scenario among neighboring cells, an effect not taken into account by the algorithm. This indicates that the chosen static PW allocation is very good and robust and that the SON PW algorithm needs to be updated in future work considering other factors such as the interference from and to the neighbor cells. Even though the performance is practically identical between the static PW and SON PW implementation, the advantage of using a SON algorithm is that it will adapt automatically to changes in the traffic distribution in the network without the need of a calibration process to find the best static allocation.
- Finally, as it was pointed out in Section 5.4, out of all the static resource deployment strategies for ViS, the one that yields higher capacity gain for the Hannover is the case when ViS is implemented in all the cells in the network. The highest capacity gain observed is 22.1% over the No ViS case when SON BW is used and ViS is deployed in all the cells. It is important to highlight that deploying ViS in all the cells in the network implies installing a new AAS in all the eNodeBs, which is costly to the operators and should be weighed against the expected capacity benefit. The case when ViS is deployed in four cells in the network, where some hotspots are located, yielded gains of around 9% in capacity from either SON algorithm over the reference case without ViS. These capacity gains could justify the investment on deploying four new antennas in the network, reducing the cost considerably when compared to the best deployment strategy and still achieving better network results.



# 8

## CONCLUSIONS AND FUTURE WORK

The research and results presented in this thesis, aim at showing whether and to what degree an AAS technique such as ViS, in combination with a static resource sharing scheme or SON resource sharing algorithm, is a suitable solution to improve the capacity and performance of a realistic LTE network and therefore can be chosen as a densification strategy for operators. In this chapter, some general conclusions are drawn about the use of ViS in an LTE network based on the results that were presented in Chapter 5 and Chapter 7. The final goal is to try to answer the research questions outlined in Chapter 3 of this thesis.

By looking at the results presented in this work, it can be generally concluded that ViS is indeed a suitable solution to improve the capacity and performance of a realistic LTE network using either static resource sharing schemes or SON resource sharing algorithms. The highest capacity gains (22.1%), over the No ViS case, are observed in the scenario when all the cells are virtually sectorized in combination with a *SON BW* sharing algorithm. Additionally to the capacity gain of 22.1

From the literature study done for ViS it was concluded since the beginning of this thesis that the virtual cell should be capable of capturing as many users as possible in order to achieve the highest possible performance. To do so, for this thesis an algorithm based on traffic intensity maps and BSA maps was developed to find the optimum tilt and azimuth configuration that would ensure that the virtual cell would capture as much traffic as possible from the original cell (the cell before implementing ViS).

It was observed that using *static transmit power sharing* yields to performance and capacity gains in all the deployment scenarios tested. Additionally it is concluded that *large changes in fixed power allocation leads to small variations in the gains (or losses)* and hence the performance of such scheme remains stable for a wide range of transmit power percentages, and a great benefit is obtained from the doubling of BW resources. On the other hand, using a *static bandwidth allocation* scheme leads to performance and capacity degradation in most of the cases even though the SINR in the virtually sectorized cells and the neighboring cells is improved. With static BW allocation the changes in bandwidth scale the performance linearly and the improvement in SINR is overpowered by the uneven proportions of BW allocated to virtual and macro-cells. Some gains were only observed in the case when a small fraction ( $\delta_{Wv}=[20-30\%]$ ) of the bandwidth is allocated to the virtual cell(s), which suggests that in these proportions the amount of users served by the macro and virtual cell is balanced.

The results indicate that using a fixed transmit power scheme always leads to higher performance improvement at network and cell-specific level when compared to fixed bandwidth sharing, but losses are also observed for some PW allocations, this was further studied in 5.1.1 by referring to the Shannon-Hartley capacity theorem. The results also show that for some bandwidth allocation percentages there are some performance gains, indicating the potential of using an intelligent bandwidth sharing. Hence the motivation for the development of SON resource sharing algorithms that work under the premise that the resources allocated to the virtual cell should be balanced with the amount of resources allocated to the macro-cell, based mainly on the traffic distribution in the cells (number of active users).

After implementing the SON algorithms it was shown that the SON BW sharing algorithm yielded the highest gains for the observed KPIs in all the scenarios, when compared to the reference case without ViS and to the best results from the static resource sharing schemes. This supported the idea that there was potential of using BW sharing if the bandwidth was shared dynamically and intelligently according to the number of users located in the virtual and macro cells. It is important to remark that even though SON bandwidth sharing turned out to be the most profitable solution, the gains achieved with SON power sharing were not so far behind but they were also comparable to the results of using static PW allocation, especially when looking at the impact of ViS in the neighboring cells.

Using the SON PW algorithm showed to have almost identical performance to the static PW allocation and only in selected cases shows higher gains. This is mainly due to the fact that the algorithm doesn't take into account the interference from neighboring cells and is left as an open issue for future work. The advantage of using the SON PW algorithm is that it will adapt automatically to changes in the traffic distribution in the network without the need of a calibration process to find the best static allocation.

By using different offered loads for the simulations it was observed that throughput gains using the SON algorithms grow as the network load increases. The highest gains are achieved when the network is heavily loaded. This result didn't come as a surprise since it is a recurrent statement in the literature related to VS and ViS and is mainly due to the fact that at higher loads the performance of the reference scenario is very poor and because ViS is a densification strategy aimed to improve performance under these loading conditions.

The location of traffic hotspots within the coverage area of the original cell (the cell before implementing ViS) impacts mainly the 10th user throughput percentile once ViS is implemented. This is explained by understanding the interference experienced by the users being served by the virtual and macro cells as well as the users being served by the neighbor cells. When a traffic hotspot is located near the eNodeB, the interference on users residing in the cell edge of neighboring cells is reduced, which translates into network-wide 10th user throughput percentile gains. On the contrary, a hotspot located near the cell edge of the original cell may lead to higher interference for neighboring cells and to performance degradation. The results presented in Chapter 5 and Chapter 7 indicate that using ViS with any of the resource sharing schemes affects the interference towards the neighboring cells and is the main responsible of the network-wide gains or losses observed in combination with the effect of doubling either BW or PW resources (according to each scheme tested).

The choice of ViS deployment strategy has a big impact on performance gains. In the scenario simulated for the Hannover network there were four hotspots located in the downtown area. When ViS was implemented in all the cells in the network large cell-specific and network performance and capacity gains were observed. As the number of virtually sectorized cells reduces, so are the gains. This is because the impact to neighboring cells is reduced given the fact that less cells are changing in the network. In the case in which only one cell is sectorized the network-wide gains are very small, but at cell-specific level high performance gains are observed.

Based on all the available results presented in this thesis, the recommendation for the Hannover network is to deploy ViS in combination with the proposed *SON BW* algorithm in all the cells in the network using an optimum tilt and azimuth configuration that will guarantee that virtual cell will capture as many users as possible in its reduced coverage area. Independently of the deployment strategy, using the proposed *SON BW* algorithm will lead to the best network-wide and cell-specific performance. Another advantage of using a SON algorithm to dynamically share the resources over a static resource allocation is that as the traffic distribution changes with time, the network is able to adapt automatically to the variations and maintain a high performance. Future work on ViS could focus on the development of a more complex SON algorithm capable of detecting a hotspot within a cell and dynamically adjust the tilt and azimuth of the virtual cell to target the problematic area and updating the SON PW algorithm to take into account the interference created by the virtually sectorized cells towards the neighboring cells and hence allocate a more appropriate power proportion.

# BIBLIOGRAPHY

- [1] *Ericsson Mobility Report*, Tech. Rep. (Ericsson, 2015).
- [2] *Cisco Visual Networking Index: Global Mobile Data Traffic Forecast Update*, Tech. Rep. (Cisco, 2015).
- [3] L. Jorgueski *et al.*, *Self-organizing networks in 3GPP: Standardization and future trends*, IEEE Communications Magazine, Communications Standards Supplement (2015).
- [4] *Evolved universal terrestrial radio access (e-utra) and evolved universal terrestrial radio access network (eutran) ts 36.300, v. 12.5.0, .*
- [5] S. Hahn *et al.*, *Final Report On A Unified Self-Management System For Heterogeneous Radio Access Networks*, Tech. Rep. (SEMAFOUR, 2015).
- [6] *LTE-Advanced Evolution in Releases 12-14: New services to pave the way to 5G*, Tech. Rep. (Nokia, 2015).
- [7] C. Cicconetti, *5G Network Architecture*, Tech. Rep. (EU FP7 RAS Cluster, 2014).
- [8] *Requirements related to technical performance for IMT-Advanced radio interface(s), ITU-R M.2134*, Tech. Rep. (ITU, 2008).
- [9] C. Cox, *An Introduction to LTE: LTE, LTE-Advanced, SAE, VoLTE and 4G Mobile Communications* (John Wiley & Sons, 2014).
- [10] G. de la Rouche *et al.*, *LTE-Advanced and Next Generation Wireless Networks* (John Wiley & Sons, 2013).
- [11] *5G Radio Access*, Tech. Rep. (Ericsson, 2015).
- [12] A. Osseiran *et al.*, *Scenarios for 5G mobile and wireless communications: The vision of the METIS project*, IEEE Communications Magazine (2014).
- [13] *5G Use Cases and Requirements*, Tech. Rep. (Nokia, 2014).
- [14] E. Hossain *et al.*, *5G cellular: Key enabling technologies and research challenges*, IEEE Instrumentation & Measurement Magazine (2015).
- [15] *Recommendation on SON and O&M Requirements*, Tech. Rep. (NGMN, 2008).
- [16] A. Imran *et al.*, *Challenges in 5G: How to empower SON with big data for enabling 5G*, IEEE Network (2014).
- [17] *Active Antenna Systems: A Step-change in Base Station Site Performance*, Tech. Rep. (Nokia, 2012).
- [18] K. Linehan and R. Chandrasekaran, *Active Antennas: The Next Step in Radio and Antenna Evolution*, Tech. Rep. (Commscope, 2011).
- [19] A. Tall, Z. Altman, and E. Altman, *Virtual sectorization: design and self-optimization*, Proceedings of IWSON 2015 (2015).
- [20] K. Trichias *et al.*, *Performance evaluation and SON aspects of vertical sectorisation in a realistic LTE network environment*, IEEE VTC 3rd International Workshop on Self-Organizing Networks (2014).
- [21] A. Tall *et al.*, *Self-optimizing strategies for dynamic vertical sectorization in LTE-Advanced networks*, IEEE Wireless Communications and networking Conference (2015).
- [22] O. Yilmaz *et al.*, *System level analysis of vertical sectorization for 3GPP LTE*, 6th International Symposium on Wireless Communication Systems (2009).

- [23] Y. Fu *et al.*, *Analysis of vertical sectorization for HSPA on a system level: Capacity and coverage*, IEEE Vehicular Technology Conference (2012).
- [24] F. W. Vook *et al.*, *Elevation beamforming with beamspace methods for LTE*, IEEE 24th International Symposium on Personal Indoor and Mobile Radio Communications (2013).
- [25] M. Ahn *et al.*, *Vertical sectorization techniques for active antenna systems*, International Conference on Information and Communication Technology Convergence (2014).
- [26] D. Kifle *et al.*, *Mathematical model for vertical sectorization (VS) in aas based LTE deployment*, 11th International Symposium on Wireless Communications Systems (2014).
- [27] M. Jiang *et al.*, *Enhancing LTE-Advanced network performance using active antenna systems*, International Conference on Computing (2015).
- [28] M. Heikkilä *et al.*, *Active antenna system (AAS) capabilities for 5G systems: A field study of performance*, International Conference on 5G for Ubiquitous Connectivity (2014).
- [29] K. Trichias *et al.*, *Self-optimization of vertical sectorization in a realistic LTE network*, European Conference on Networks and Communications .
- [30] C. Balanis, *Antenna theory: analysis and design* (John Wiley & Sons, 2012).
- [31] *Proposal to modelling active antennas*, Tech. Rep. (Kathrein, 2012).
- [32] Z. Altman *et al.*, *Efficient base station antenna models for dosimetric analysis*, IEEE Trans. Electromagnetic Compatibility (2002).
- [33] E. Tuomaala *et al.*, *Effective SINR approach of link to system mapping in OFDM/multi-carrier mobile network*, International Conference on Mobile Technology (2005).
- [34] T. Kürner *et al.*, *A run-time efficient 3D propagation model for urban areas including vegetation and terrain effects*, IEEE Vehicular Technology Conference (1999).
- [35] D. Rose *et al.*, *Outdoor-to-indoor propagation-accurate measuring and modelling of indoor environments at 900 and 1800 mhz*, European Conference on Antennas and Propagation (EUCAP) (2012).

# A

## VIRTUAL CELLS OPTIMUM CONFIGURATION

This appendix contains the tilt and azimuth configurations for the virtual cells according to the different traffic maps used in this thesis work.

Table A.1: Virtual cell configuration for the traffic map with hotspots close to the eNodeB

Macro Cell ID	Virtual Cell ID	Macro Cell ID	Virtual Cell ID	$\theta_{VIS}$	$\phi_{VIS}$	Macro Cell ID	Virtual Cell ID	Macro Cell ID	Virtual Cell ID	$\theta_{VIS}$	$\phi_{VIS}$	Macro Cell ID	Virtual Cell ID	Macro Cell ID	Virtual Cell ID	$\theta_{VIS}$	$\phi_{VIS}$
0	84	28	126	4	30	56	151	56	151	2	30	56	151	56	151	2	30
1	85	29	89	3	-5	57	152	57	152	3	15	57	152	57	152	3	15
2	88	30	127	10	0	58	153	58	153	3	-20	58	153	58	153	3	-20
3	91	31	130	6	5	59	115	59	115	1	0	59	115	59	115	1	0
4	92	32	99	4	25	60	154	60	154	5	25	60	154	60	154	5	25
5	95	33	131	3	10	61	120	61	120	4	-35	61	120	61	120	4	-35
6	96	34	132	10	0	62	155	62	155	4	30	62	155	62	155	4	30
7	97	35	123	3	15	63	124	63	124	5	-15	63	124	63	124	5	-15
8	98	36	135	3	30	64	156	64	156	5	-15	64	156	64	156	5	-15
9	100	37	136	3	20	65	104	65	104	4	-30	65	104	65	104	4	-30
10	101	38	137	3	15	66	157	66	157	3	20	66	157	66	157	3	20
11	102	39	93	3	10	67	90	67	90	3	0	67	90	67	90	3	0
12	105	40	138	4	-30	68	158	68	158	1	30	68	158	68	158	1	30
13	106	41	139	4	-30	69	159	69	159	4	-25	69	159	69	159	4	-25
14	107	42	140	4	-5	70	160	70	160	8	10	70	160	70	160	8	10
15	108	43	141	9	-25	71	161	71	161	4	0	71	161	71	161	4	0
16	103	44	128	4	0	72	118	72	118	3	-40	72	118	72	118	3	-40
17	109	45	142	3	-35	73	162	73	162	4	-15	73	162	73	162	4	-15
18	110	46	133	6	-10	74	129	74	129	9	-5	74	129	74	129	9	-5
19	111	47	143	3	15	75	163	75	163	4	-25	75	163	75	163	4	-25
20	112	48	144	10	0	76	164	76	164	3	-35	76	164	76	164	3	-35
21	113	49	145	4	40	77	86	77	86	5	35	77	86	77	86	5	35
22	116	50	146	4	-40	78	165	78	165	3	5	78	165	78	165	3	5
23	114	51	147	2	-15	79	166	79	166	4	25	79	166	79	166	4	25
24	117	52	148	5	10	80	87	80	87	4	30	80	87	80	87	4	30
25	119	53	149	1	-30	81	167	81	167	5	-5	81	167	81	167	5	-5
26	122	54	150	5	10	82	94	82	94	3	-10	82	94	82	94	3	-10
27	125	55	134	6	15	83	121	83	121	3	-20	83	121	83	121	3	-20

Table A.2: Virtual cell configuration for the traffic map with hotspots far from the eNodeB

Macro Cell ID	Virtual Cell ID	$\theta_{VIS}$	$\phi_{VIS}$	Macro Cell ID	Virtual Cell ID	$\theta_{VIS}$	$\phi_{VIS}$	Macro Cell ID	Virtual Cell ID	$\theta_{VIS}$	$\phi_{VIS}$
0	84	2	-5	28	126	4	30	56	151	2	30
1	85	3	-10	29	89	3	-5	57	152	3	15
2	88	3	0	30	127	10	0	58	153	3	-20
3	91	3	-25	31	130	6	5	59	115	1	0
4	92	3	-25	32	99	4	25	60	154	5	25
5	95	1	45	33	131	3	10	61	120	4	-35
6	96	5	30	34	132	10	0	62	155	4	30
7	97	5	5	35	123	3	15	63	124	5	-15
8	98	8	-15	36	135	3	30	64	156	5	-15
9	100	4	0	37	136	3	20	65	104	4	-30
10	101	5	40	38	137	3	15	66	157	3	20
11	102	4	30	39	93	3	10	67	90	3	0
12	105	6	30	40	138	4	-30	68	158	1	30
13	106	4	-25	41	139	4	-30	69	159	4	-25
14	107	10	0	42	140	4	-5	70	160	5	15
15	108	3	5	43	141	9	-25	71	161	4	0
16	103	4	-40	44	128	4	0	72	118	3	-40
17	109	3	0	45	142	3	-35	73	162	4	-15
18	110	10	0	46	133	6	-10	74	129	9	-5
19	111	3	-15	47	143	3	15	75	163	4	-25
20	112	3	-10	48	144	10	0	76	164	3	-35
21	113	2	-15	49	145	4	40	77	86	5	35
22	116	5	0	50	146	4	-40	78	165	3	5
23	114	2	5	51	147	2	-15	79	166	4	25
24	117	4	-10	52	148	5	-10	80	87	4	30
25	119	3	0	53	149	1	-30	81	167	5	-5
26	122	4	25	54	150	5	10	82	94	3	-10
27	125	4	0	55	134	6	15	83	121	3	-20



# B

## STATIC RESOURCE SHARING: ADDITIONAL RESULTS

This appendix contains the graphs with the results obtained when using ViS in combination with static resource sharing for the scenarios when ViS was deployed in four cells and one cell in the network.

### B.1. VIS IN FOUR CELLS

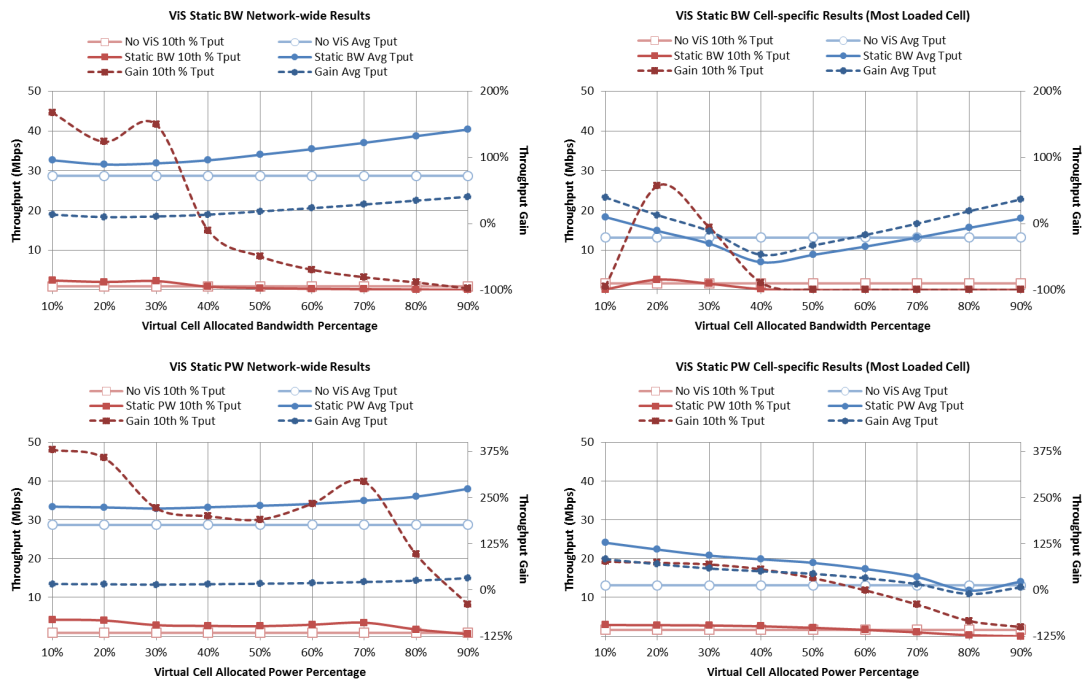


Figure B.1: ViS in four cells: average throughput and 10th user throughput percentile results with hotspots far from the eNodeBs

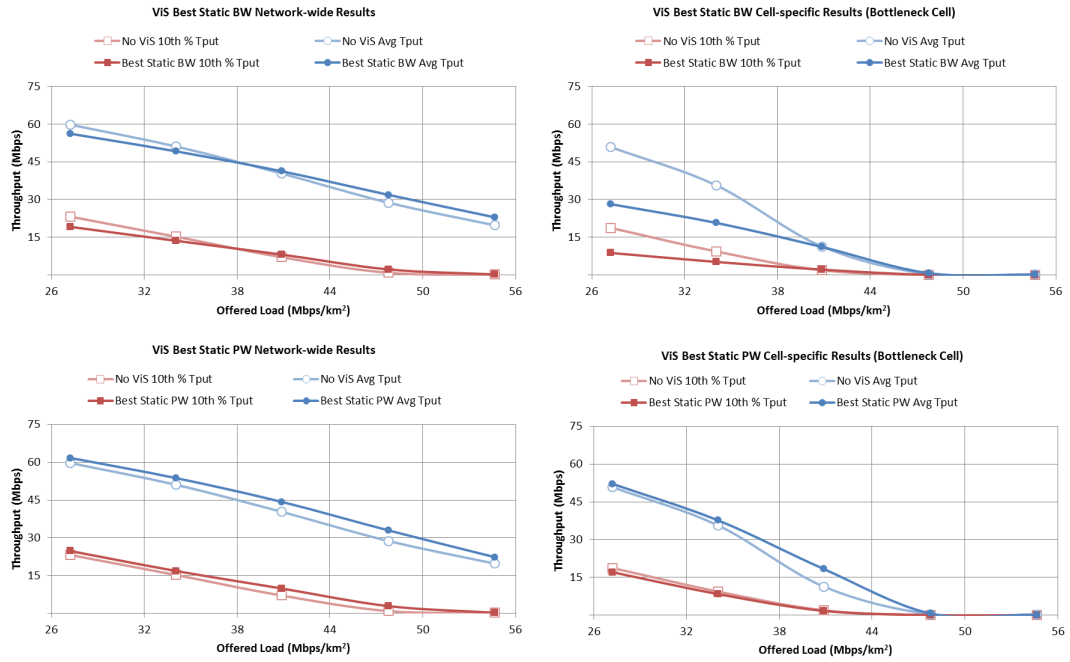


Figure B.2: ViS in four cells: Bottleneck cell results with hotspots far from the eNodeBs

## B.2. ViS IN ONE CELL

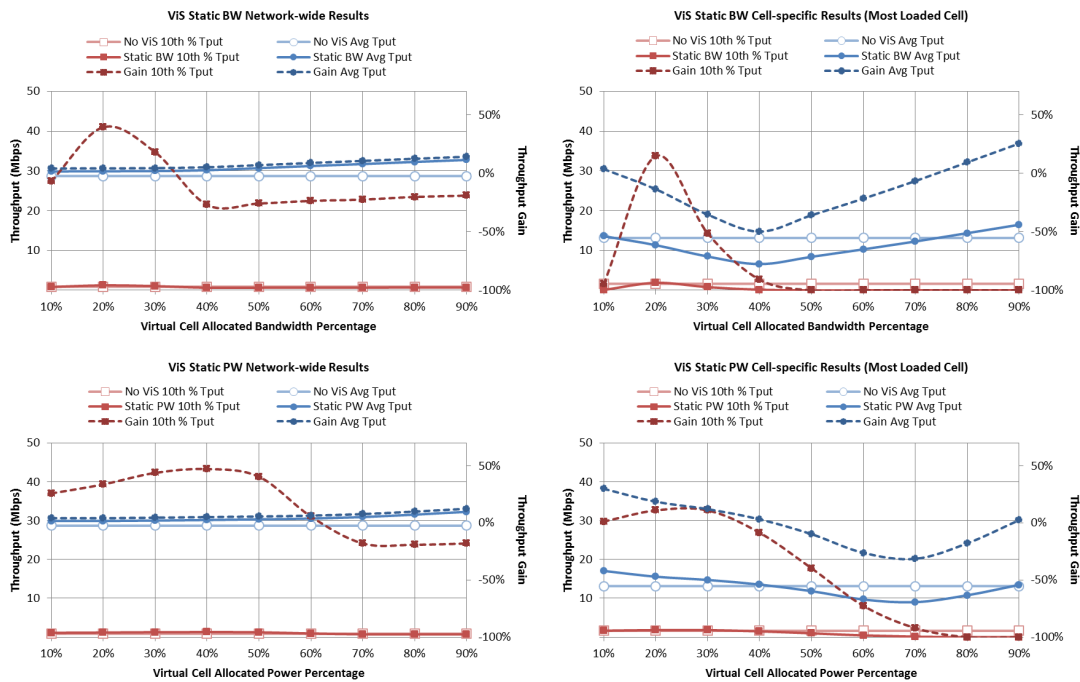


Figure B.3: ViS in one cell: average throughput and 10th user throughput percentile results with hotspots far from the eNodeBs

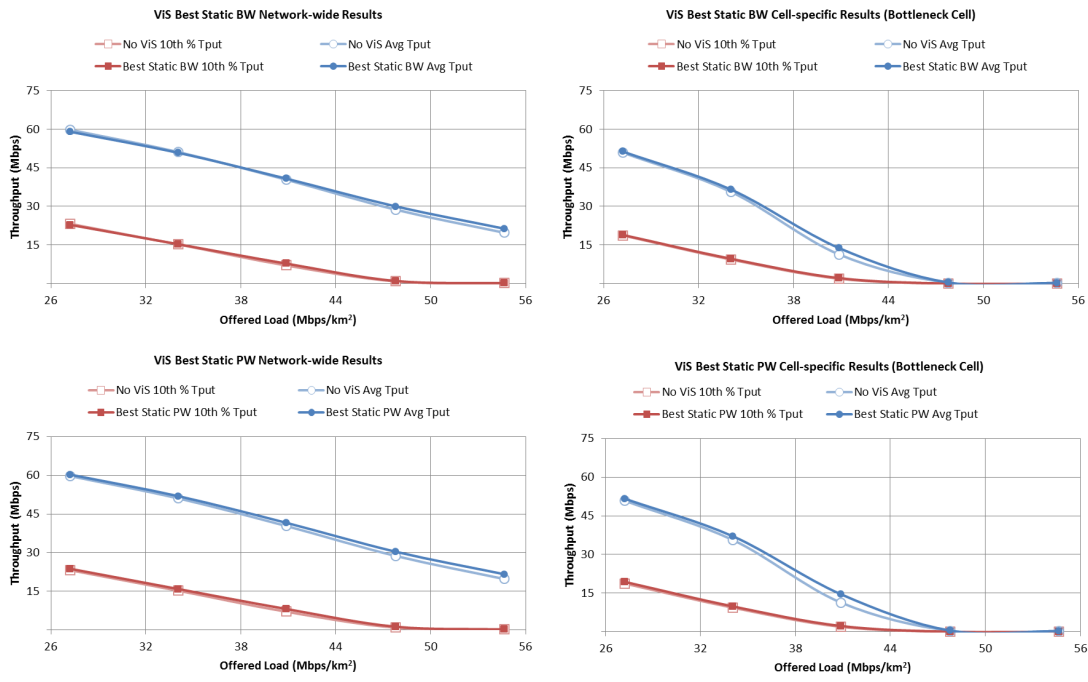


Figure B.4: ViS in one cell: Bottleneck cell results with hotspots far from the eNodeBs



# C

## SON RESOURCE SHARING: ADDITIONAL RESULTS

This appendix contains the graphs with the results obtained when using ViS in combination with the use of SON algorithms for the scenarios when ViS was deployed in all the cells, four cells and one cell in the network.

### C.1. VIS IN ALL CELLS

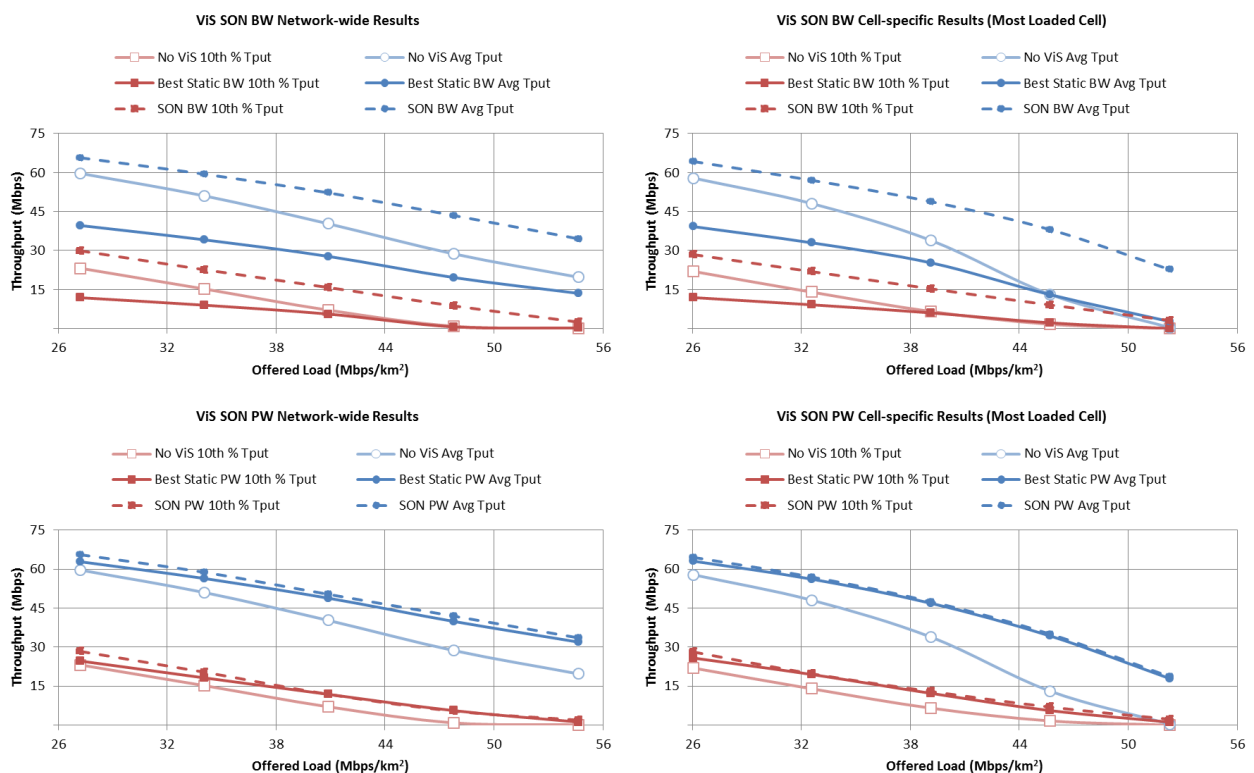


Figure C.1: SON ViS in all cells: average throughput and 10th user throughput percentile results with hotspots far from the eNodeBs

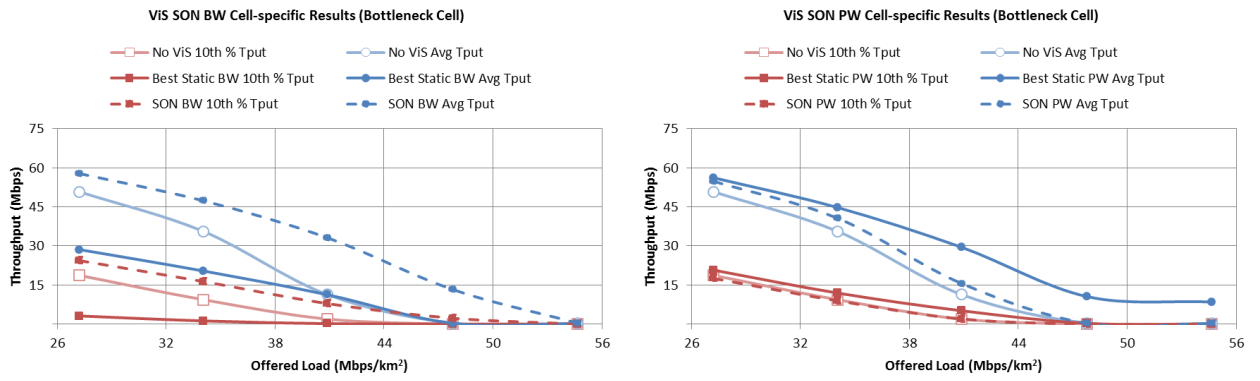


Figure C.2: SON ViS in all cells: Bottleneck cell results with hotspots far from the eNodeBs

### C.2. VIS IN FOUR CELLS

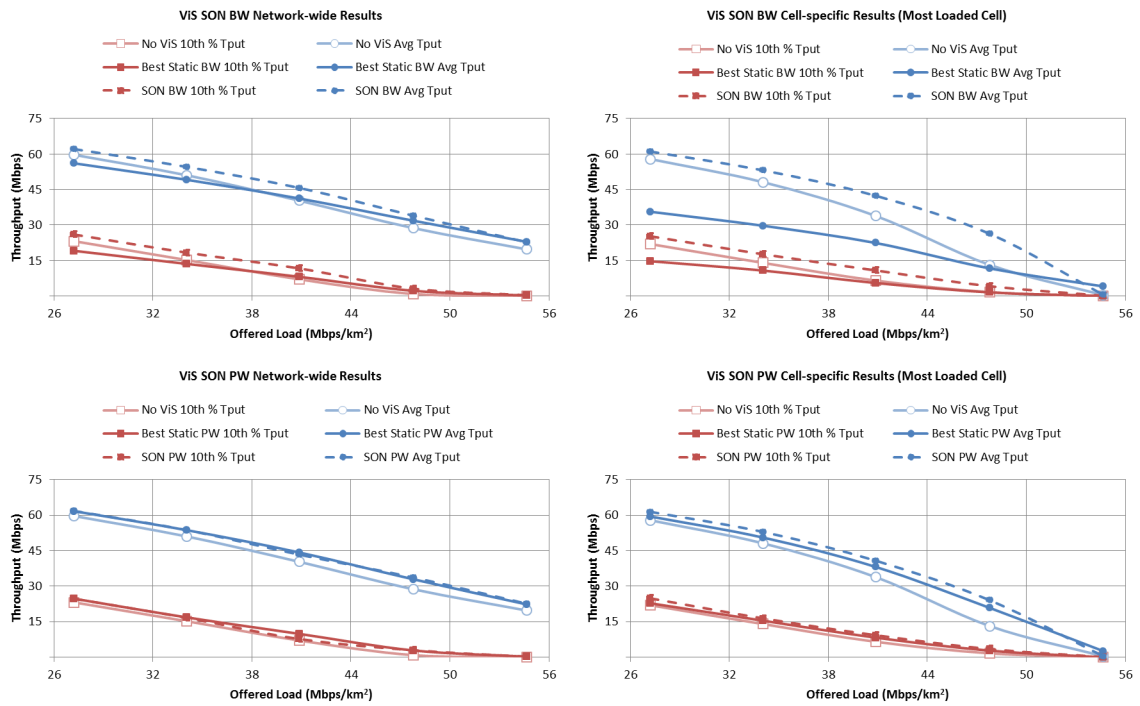


Figure C.3: SON ViS in four cells: average throughput and 10th user throughput percentile results with hotspots far from the eNodeBs

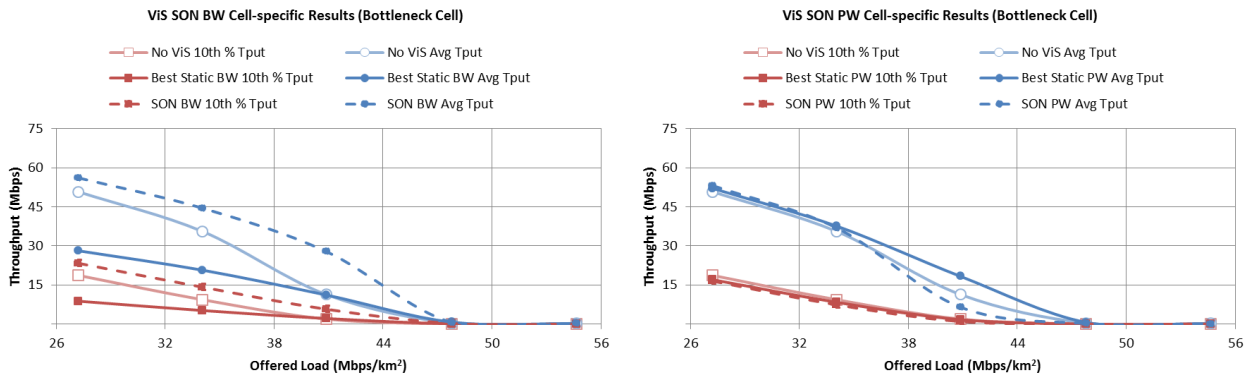


Figure C.4: SON VIS in four cells: Bottleneck cell results with hotspots far from the eNodeBs

### C.3. VIS IN ONE CELL

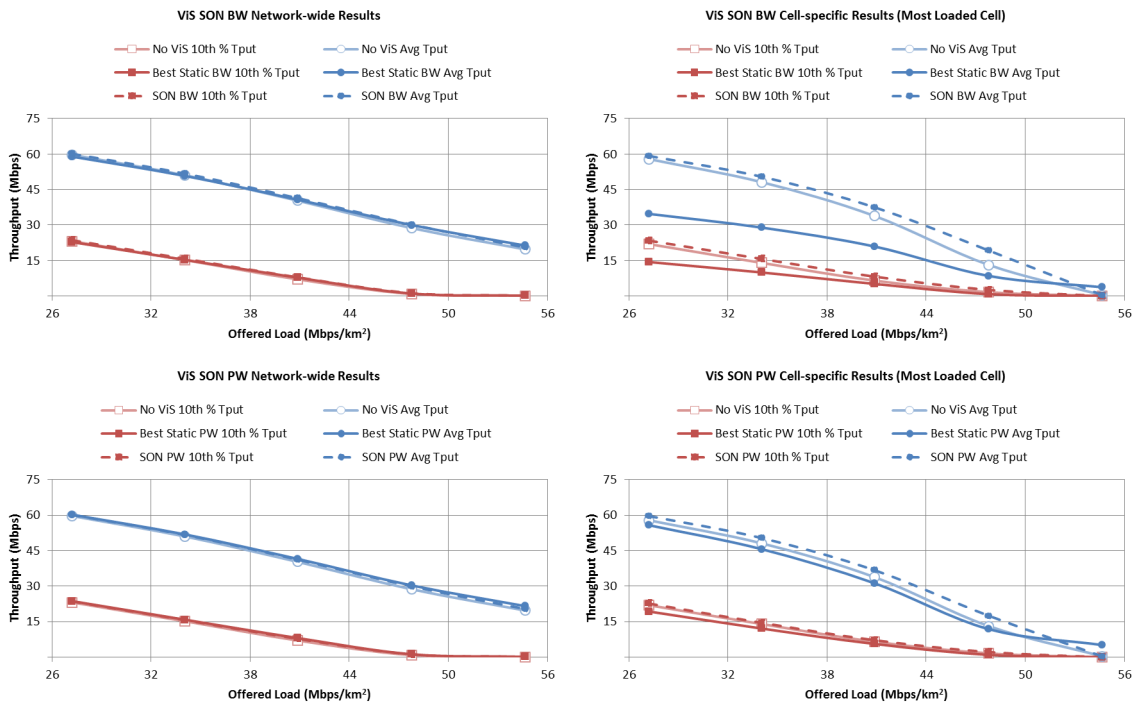


Figure C.5: SON VIS in one cell: average throughput and 10th user throughput percentile results with hotspots far from the eNodeB

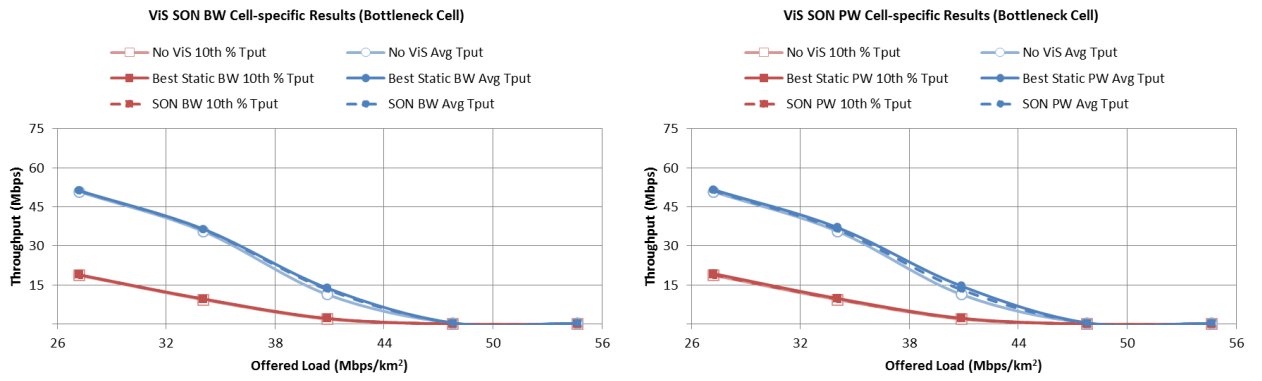


Figure C.6: ViS in one cell: Bottleneck cell results with hotspots far from the eNodeB

# LIST OF FIGURES

2.1	Small cell inter-cell interference problem. [9]	7
2.2	Key requirements for 5G and its typical applications. [12]	8
2.3	Evolution of SON features. [3]	10
2.4	Proposed SON system from SEMAFOUR. [5]	11
2.5	Active Antenna System. [17]	12
2.6	Cell Architecture Evolution. [18]	13
2.7	AAS Radiation Pattern Self-healing. [18]	13
2.8	AAS Advanced Tilt Features. [17]	14
2.9	VS and ViS Representation. [19][20]	15
2.10	Network-wide average user throughput and 10th user throughput percentile (VS in all cells) [20]	17
2.11	Network wide throughput using a SON controller (VS in all cells) [29]	17
2.12	VS Mean User Throughputs for Increasing Arrival Rates [21]	18
2.13	ViS Best Server Coverage Map [19]	19
2.14	ViS Mean and Cell-edge UE Throughput Over Time [19]	19
4.1	Hannover Realistic LTE Network Layout. (Background image: Google Maps)	23
4.2	ViS antenna design [19]	24
4.3	ViS antenna vertical plane (left) and horizontal plane (right) patterns	26
4.4	Effective SINR Mapping Schematic Flow-chart	27
4.5	Mutual information as a function of SINR for 64QAM modulation in LTE	28
4.6	Traffic intensity map generation [5]	29
4.7	Hannover BSA with hotspot locations	29
4.8	Traffic intensity maps with different hotspot locations	30
4.9	Propagation model representation [34]	31
4.10	Optimum ViS configuration for cell 148	33
5.1	Downtown Hannover BSA maps with ViS configuration optimized for each cell according to hotspot location	35

5.2	ViS in all cells: average throughput and 10th user throughput percentile results with hotspots close to the eNodeBs . . . . .	37
5.3	ViS in all cells: Bottleneck cell results with hotspots close to the eNodeBs . . . . .	39
5.4	ViS in all cells: average throughput and 10th user throughput percentile results with hotspots far from the eNodeBs . . . . .	40
5.5	ViS in all cells: Bottleneck cell results with hotspots far from the eNodeBs . . . . .	42
5.6	Static PW sharing, network-wide CDF of user experienced interference (left) and RSS (right) . . .	43
5.7	Static PW sharing, network-wide CDF of user experienced SINR (left) and average assigned BW (right) . . . . .	43
5.8	ViS in four cells: average throughput and 10th user throughput percentile results with hotspots close to the eNodeBs . . . . .	44
5.9	ViS in four cells: Bottleneck cell results with hotspots close to the eNodeBs . . . . .	45
5.10	Static BW sharing, network-wide (left) and neighboring cells (right) CDF of user experienced throughput . . . . .	46
5.11	ViS in most loaded cell: average throughput and 10th user throughput percentile results with hotspot close to the eNodeB . . . . .	47
5.12	ViS in most loaded cell: Bottleneck cell results with hotspot close to the eNodeB . . . . .	48
7.1	ViS in all cells: SON average throughput and 10th user throughput percentile results with hotspots close to the eNodeBs . . . . .	56
7.2	ViS in all cells: SON bottleneck cell results with hotspots close to the eNodeBs . . . . .	57
7.3	ViS in four cells: SON average throughput and 10th user throughput percentile results with hotspots close to the eNodeBs . . . . .	58
7.4	ViS in four cells: SON bottleneck cell results with hotspots close to the eNodeBs . . . . .	58
7.5	ViS in most loaded cell: average throughput and 10th user throughput percentile results with hotspots close to the eNodeBs . . . . .	60
7.6	ViS in most loaded cells: SON bottleneck cell results with hotspots close to the eNodeBs . . . . .	60
B.1	ViS in four cells: average throughput and 10th user throughput percentile results with hotspots far from the eNodeBs . . . . .	71
B.2	ViS in four cells: Bottleneck cell results with hotspots far from the eNodeBs . . . . .	72
B.3	ViS in one cell: average throughput and 10th user throughput percentile results with hotspots far from the eNodeBs . . . . .	72
B.4	ViS in one cell: Bottleneck cell results with hotspots far from the eNodeBs . . . . .	73
C.1	SON ViS in all cells: average throughput and 10th user throughput percentile results with hotspots far from the eNodeBs . . . . .	75
C.2	SON ViS in all cells: Bottleneck cell results with hotspots far from the eNodeBs . . . . .	76
C.3	SON ViS in four cells: average throughput and 10th user throughput percentile results with hotspots far from the eNodeBs . . . . .	76

---

C.4 SON ViS in four cells: Bottleneck cell results with hotspots far from the eNodeBs . . . . .	77
C.5 SON ViS in one cell: average throughput and 10th user throughput percentile results with hotspots far from the eNodeB . . . . .	77
C.6 ViS in one cell: Bottleneck cell results with hotspots far from the eNodeB . . . . .	78



# LIST OF TABLES

4.1	Hotspot traffic intensity factor $\alpha$ . . . . .	30
4.2	Cells with traffic hotspots . . . . .	32
4.3	Possible values for configuration parameters . . . . .	32
4.4	$\delta_{W\nu}$ and $\delta_{P\nu}$ fixed values for simulations . . . . .	33
4.5	ViS simulation scenarios . . . . .	33
5.1	ViS in All Cells: Bottleneck cells for each static resource allocation for the case with hotspots close to eNodeBs . . . . .	38
5.2	Load values for the case with hotspots close to the eNodeB . . . . .	38
5.3	Load values for the case with hotspots far from the eNodeB . . . . .	41
5.4	Capacity gains summary for ViS with static resource allocation for the map with hotspots close to the eNodeB . . . . .	49
6.1	$\lambda$ values for simulations . . . . .	52
6.2	SON ViS simulation scenarios . . . . .	53
7.1	Capacity gains summary for ViS with SON resource allocation for the map with hotspots close to the eNodeB . . . . .	61
A.1	Virtual cell configuration for the traffic map with hotspots close to the eNodeB . . . . .	68
A.2	Virtual cell configuration for the traffic map with hotspots far from the eNodeB . . . . .	69